Pacific Northwest
NATIONAL LABORATORY

PNNL-37699
LA-UR-20444

Using Separation-Enhanced Isotope Ratio Mass Spectrometry to Enable Increased Renewable Carbon Content in Transportation Fuels (CRADA 525)

September 2025

U.S. DEPARTMENT of ENERGY

Prepared for the U.S. Department of Energy
under Contract DE-AC05-76RL01830

DISCLAIMER

PACIFIC NORTHWEST NATIONAL LABORATORY
operated by
BATTELLE
for the
UNITED STATES DEPARTMENT OF ENERGY
under Contract DE-AC05-76RL01830

Printed in the United States of America

Available to DOE and DOE contractors from the Office of Scientific and Technical Information,
P.O. Box 62, Oak Ridge, TN 37831-0062
www.osti.gov
ph: (865) 576-8401
fax: (865) 576-5728
email: reports@osti.gov

Available to the public from the National Technical Information Service
5301 Shawnee Rd., Alexandria, VA 22312
ph: (800) 553-NTIS (6847)
or (703) 605-6000
email: info@ntis.gov
Online ordering: http://www.ntis.gov

PNNL-37699
LA-UR-20444

Using Separation-Enhanced Isotope Ratio Mass Spectrometry to Enable Increased Renewable Carbon Content in Transportation Fuels (CRADA 525)

September 2025

Russ Lewis
Michael B. Viola
Sophie B. Lehmann
Jim Moran
Holden M. Nelson
Alejandro Heredia-Langner
Rafal Gieleciak
Ajae Hall
Zhenghua Li
Marie Swita
J. Timothy Bays

Prepared for
the U.S. Department of Energy
under Contract DE-AC05-76RL01830

Pacific Northwest National Laboratory
Richland, Washington 99354

Cooperative Research and Development Agreement (CRADA) Final Report

Report Date: September 2025

In accordance with Requirements set forth in the terms of the CRADA, this document is the CRADA Final Report, including a list of Subject Inventions, to be provided to PNNL Information Release who will forward to the DOE Office of Scientific and Technical Information as part of the commitment to the public to demonstrate results of federally funded research.

Parties to the Agreement: Battelle Memorial Institute (Pacific Northwest National Laboratory (PNNL), TRIAD National Security, LLC (Los Alamos National Laboratory (LANL), Coordinating Research Council (CRC)

CRADA number: PNNL CRADA No. 525; LANL No. LA-21-C10826.000.000

CRADA Title: Using Separation-Enhanced Isotope Ratio Mass Spectrometry to Enable Increased Renewable Carbon Content in Transportation Fuels

Responsible Technical Contact at DOE Lab:

PNNL Technical POC:
Name: Dr. Tim Bays
Address: Pacific Northwest National Laboratory, 902 Battelle Blvd, Richland, WA 99352
Wk phone: (509) 375-6900
Cell phone: (509) 713-3705
E-mail: tim.bays@pnnl.gov

LANL Technical POC:
Name: Dr. Zhenghua Li
Address: Earth Systems Observations (EES-14), Earth and Environmental Sciences Division, Los Alamos National Laboratory, P.O. Box 1663, MS J966,
Los Alamos, NM 87545
Wk phone: (505) 667-1110
Cell phone: (505) 709-7080
E-mail: zhenghuali@lanl.gov

Name and Email Address of POC at Company:

Name: Amber Leland
Address: 5755 North Point Parkway, Suite 265, Alpharetta, GA 30022
Wk: (678) 795-0506 x106
Cell: (775) 225-1613
E-mail: aleland@crcao.org

DOE Program Office: Bioenergy Technologies Office

Joint Work Statement Funding Table showing DOE funding commitment:

Funding	Project Year 1	Project Year 2	TOTALS
Contractor #1, PNNL	135	65	200
Contractor #2, LANL	33.5	16.5	50
Participant, CRC			
In-Kind	63.6	31.8	95.4
Funds-In	-	27.7	27.7
Total Participant	63.6	59.5	123.1
TOTAL CRADA Value	232.1	141	373.1

Values are $K.

Abstract

Stable isotope ratio measurements of carbon atoms using isotope ratio mass spectrometry (IRMS) can be an effective tool for quantifying biogenic carbon in co-processed fuels, with results approaching the precision and accuracy of accelerator mass spectrometry (AMS). The lower cost of an IRMS may enable deployment to refineries, improving access and analysis hours), and, by extension, provide data that can allow process optimization to maximize renewable carbon in desired refinery products. This project explored the integration of chemical separation with IRMS analyses to enable highly detailed tracking of biogenic carbon into fuel product streams separated by boiling point range, chemical class, or specific compound. Forty-nine fuels and fuel components of fossil and biogenic origin, spanning gasoline and diesel boiling point ranges, were received from three refiners and were analyzed ^{13}C values via IRMS. Results spanned a ^{13}C range from ca. 10‰ to 44‰ and reflect materials derived from sustainable sources (e.g., C4 or C3 plants, animal-based pathways, syngas) or from fossil-derived fuels. Common ranges are approximately 18‰ to 9‰ and approximately 30‰ to 20‰ for C4 and C3 plants, respectively, and approximately 34‰ to 24‰ and approximately 70‰ to 33‰ for petroleum-derived fuels and methane, respectively. Fuel-like standards were developed and tested using direct-injection elemental analyzer (EA) IRMS for liquid fuels. This method was compared with the published methods, yielding statistically similar results. Four blend curve sets were produced ranging from 0% to 100% of a fuel containing biogenic carbon, focusing on 0% to 10% biogenic carbon. Linear fits were the most applicable for two of the four blend curve sets; however, two sets were found to exhibit slightly quadratic behavior, which was more pronounced in low biogenic blend samples, necessitating second-order fits. The origin of the slight quadratic behavior remains unclear; however, the discussion points to possible interpretations. CanmetENERGY thoroughly characterized a majority of the samples using one- and two-dimensional gas chromatography (GC and GC×GC, respectively) and other analyses. Selected samples were subjected to solid-phase extraction (SPE) for saturate, olefin, aromatic, and polar (SOAP) analysis, and the resulting solvent-diluted fractions containing saturates and aromatics were returned to Pacific Northwest National Laboratory (PNNL), where the solvent was removed via evaporation or physical separation using GC techniques. Characterization and separations provided an understanding of saturate and aromatic content, as well as boiling point ranges for each sample and sample fraction. Samples resulting from SPE were examined using EA-IRMS and gas chromatography combustion IRMS (GC-C-IRMS) analyses. Both approaches suggest that the range in values between end-members can be increased by selecting the paraffinic or aromatic fraction of the end-member or by selecting among individual compounds resulting from GC separation of the paraffinic fractions. Considerable work remains to put these approaches into practice and statistically validate the benefit for using a fraction or individual compound over bulk analysis of a sample. However, initial results suggest that separations provide advantages for samples having blend ratios of less than 10% biogenic blendstocks. ^{13}C results showed statistically similar biofuel blend results to those obtained at PNNL, although additional work is needed to obtain better reproducibility. Select samples were sent to Los Alamos National Laboratory (LANL) for IRMS measurements and Beta Analytics for AMS measurements. This work suggests that IRMS and AMS yield closely comparable results and in some circumstances, IRMS could serve as a surrogate for AMS. While additional work is needed to better resolve statistical advantages for separations and better show the comparable nature of IRMS and AMS in both the biogenic carbon analysis of bulk chemical classes, initial results from this study suggest that these should be pursued in order to proliferate this approach for quantifying biogenic carbon in transportation fuels to the refinery level, thereby potentially enabling process optimization in co-processing scenarios.

Executive Summary

Stable isotope ratio measurements using isotope ratio mass spectrometry (IRMS) have previously been shown by Los Alamos National Laboratory (LANL) to be effective for tracking co-processed biogenic carbon, with results approaching those of accelerator mass spectrometry (AMS). The lower cost of an IRMS may enable deployment to refineries, improving access and hours) and, by extension, generate data that can allow process optimization to maximize renewable carbon in desired refinery products. This work applied chemical separation approaches as part of the IRMS analyses, enabling biogenic carbon tracking in fuel product streams by boiling point range, chemical class, or molecular compound. This work shows that IRMS results can be comparable to AMS and that IRMS has the potential to improve precision and accuracy at low blend ratios, even below those typically reported by current AMS methods. The adoption and proliferation of IRMS has the potential, through lower instrumentation cost and rapid turnaround times, to optimize refinery processes through on-site analysis.

A major outcome of this work is the similarity of the percent biocarbon value determined from the ASTM D6866 B method using AMS with those from the ^{13}C values analyzed by IRMS for blended and co-processed samples. In the plots below, datapoints have statistical equivalence to the 1:1 line ($y = x$), indicating the percent biocarbon estimated from ^{13}C values can be a powerful tool for the refiners.

This report is arranged into subsections that describe results obtained for each project task. Task 1 was associated with sample receipt and organization. Task 2 developed or confirmed analytical methods and standards. Task 3 analyzed the samples as received from the refiners. Under Task 4, samples were characterized and separated into saturate and aromatic fractions at CanmetENERGY, and the fractions were analyzed using two approaches at PNNL. Under Task 5, samples were sent to LANL for ^{13}C measurements and to Beta Analytics for AMS measurements. This final report was undertaken as Task 6.

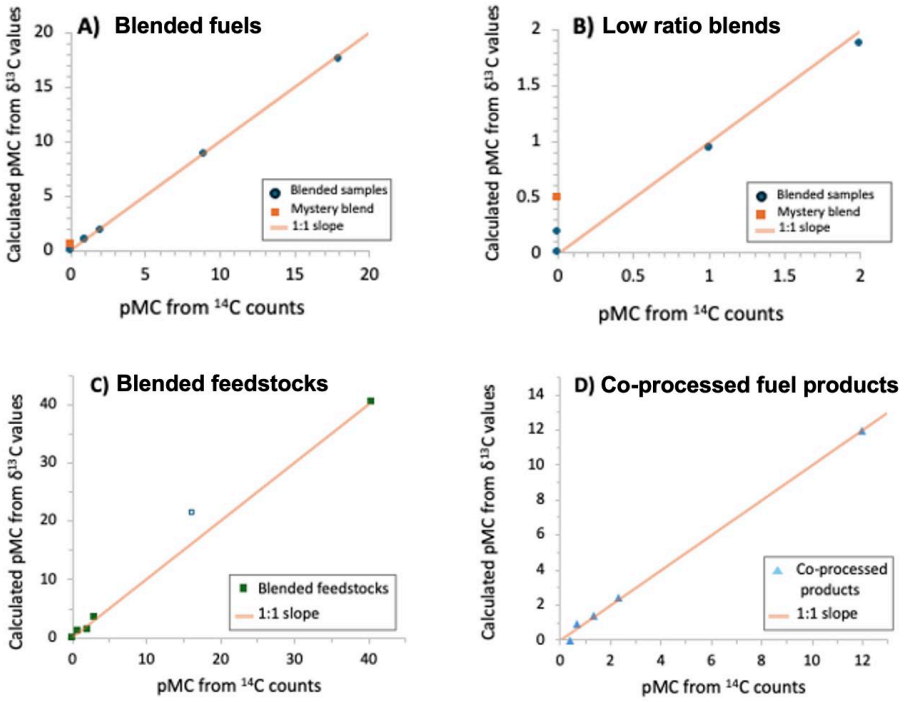

Figure ES.1. Percent modern carbon (pMC) data from ASTM D6866 B method using ^{14}C AMS ^{13}C values analyzed via IRMS for (A and B) blended fuels and (C and D) blended feedstocks and the corresponding co-processed fuels. The orange line is the 1:1 slope ($y = x$) along which all points would plot if the methods produced identical results, and the open square in panel C is an outlier point for which the sample needs reanalysis. Abbreviations: AMS = accelerator mass spectrometry; $^{13}C = ((R_{sample} / R_{standard}) - 1)) \times 1\,000$, in per mil (‰) where R = $^{13}C/^{12}C$ ratio; IRMS = isotope ratio mass spectrometry.

Task 1 resulted in the receipt of forty-nine samples over the course of the project from three refiners and their collaborators. These samples were organized by process, identifying the feedstocks, blendstocks, and products. Because of the complexity of the various sample relationships, a series of sample schematics were produced to provide a map for datasets for each task and to identify existing gaps in the datasets. These are shown in Appendix B. These schematics were referenced throughout this project to prioritize sample analysis for percent biocarbon determination.

Because of the complexity of the IRMS measurement and the desire to ensure measurement consistency across labs and within the lab at PNNL, the Project Team developed a series of analytical standards and agreed-upon sample handling and analysis methodologies under Task 2. Sample handling and analysis methodologies were agreed upon by the Project Team and are presented in Section 5.0, where bulk samples were introduced to the combustion unit by direct injection at PNNL and by sealing in a tin capsule under an argon environment for LANL. Bulk, combustible liquids that represented the behavior of the fuel and feedstock samples were identified at PNNL as in-house standards, supplied to LANL, and used at both locations to ensure continuity in data calibrations (Experimental Section, Section 5.0). In addition, standards with known isotopic compositions were obtained from external suppliers to correct and ^{13}C values of bulk and compound-specific samples.

In order to obtain comparative measurements for assessing any improvements in accuracy, precision, and detection limits when separations are introduced in Task 4, it was first necessary to perform analyses of the as-received samples. This is referred to as “bulk IRMS” and comprised the work under Task 3. Fuel and feedstock samples were received in three tranches, ^{13}C values via elemental-analyzer isotope ratio mass spectrometry (EA-IRMS) to provide bulk-IRMS measurements. Liquid samples were injected directly into the EA-IRMS instrument for combustion, and solid samples, such as tallow-based biofeeds, were weighed into smooth-sided tin capsules and sealed prior to being introduced into the EA-IRMS. Blend curves and assessments of linearity show that samples with small amounts of biofuel sometimes show a slightly quadratic relationship along the blending curve. When needed, quadratic models provide better precision of percent biocarbon in blind blends supplied by CanmetENERGY. The origin of the quadratic behavior is unknown; however, the nonlinearity is postulated to be related to fuel matrix effects or small variations arising during blending.

Task 4 was was conducted in two parts: the first at CanmetENERGY and the second at PNNL. Fuel samples were sent to CanmetENERGY for detailed characterization and solid-phase extractions (SPEs). Various analytical techniques including one- and two-dimensional gas chromatography (GC and GC×GC, respectively) were used to investigate the wide variation in sample hydrocarbon composition and boiling point distribution. GC with a flame ionization detector (FID) was employed to evaluate the fraction content for each sample after SPE. Normal-phase GC×GC and reverse-phase GC×GC were coupled with an FID to determine the hydrocarbon compositional fingerprint. Light naphtha samples were also resolved using paraffins, iso-paraffins, olefins, naphthenes, aromatics, oxygenates (PIONA) separation employing a GC coupled to a vacuum ultraviolet spectroscopy (VUV) detector. The three methods were compared for the more challenging, light samples and showed good agreement. ^{13}C values from different fractions from co-processed fuels and blended fuels with percent biocarbon values provided by GC-based separation methods for samples that span a small difference in percent biocarbon.

In the second part of Task 4, t ^{13}C values of product and feedstock fractions provide ^{13}C value of bulk samples alone. Instead of a single data point, incorporating a bulk analysis of fractions by compound class provides an ^{13}C values, with the resulting ^{13}C value of the bulk sample between that of ^{13}C value) and the saturate/paraffin fraction (less negative ^{13}C value). The range between the fuel fractions is larger for the product than they are for the fuel feedstock, potentially indicating the incorporation of biocarbon preferentially in the saturate fraction. However, this relationship requires additional analyses for fractions of co-processed fuels originating from the same feedstocks and experiencing the same processing parameters. Ideally, these measurements would be compared with percent biogenic carbon data provided by AMS measurements.

Initial compound-specific ^{13}C values of fuel and feedstock paraffin/saturate fractions for individual n-alkanes, suggesting a variable distribution of biocarbon for co-processed fuels across a range of compounds. Additional analyses of fuel fractions from feedstocks, blended fuels and, co-processed fuels are needed to better evaluate the distribution of biocarbon and estimate the percent biocarbon in different fractions. This analytical method could also be assessed for the potential to use a single compound to track percent biogenic carbon instead of the need to analyze each component. If so, the time needed for analysis could be decreased.

Due to limitations in time, resources, and sample availability, it was not possible to assess the biogenic carbon distribution by fraction under different conditions (e.g., processing method or renewable feedstock type). To fully assess the biogenic carbon distribution, sample sets must include all fractions for any single processing operation, including both feedstocks and the resulting products (e.g., gas, liquid, and solid products). Additional work on the biogenic carbon distribution will depend on the sample sets supplied by industrial partners.

Task 5 comprised interlaboratory comparisons, the results of which indicate that the LANL and ^{13}C values for the same fuel samples generally yielded similar values and therefore similar percent biocarbon estimates. Both labs noted slight quadratic curves across blend ratios, with a slightly stronger quadratic curve in the LANL data. To determine the influence(s) associated with the differences in ^{13}C values at low blend ratios, additional sample sets and sample blends need to be analyzed for each blend curve while using the sample, matrix-matched standards for correction. At this point, the influence of sample aging during the transport of samples to LANL from PNNL cannot be distinguished from blending errors or differences in blended fuel characteristics. In addition, small differences between sampling techniques, including a generally higher standard deviation (though slight) for the LANL technique, may influence fuels differently than oils, which were the sample type for which the ^{13}C values at low blend ratios.

Analytical techniques developed to distinguish neat ^{13}C proved effective, with the results obtained in hours and with the majority biogenic carbon content measurement aligning within 10% of the values determined by AMS. The blended feedstock set from landfill-derived material would benefit from additional analyses that account for the variation in the sample amount for the solid samples. A larger variation in the sample size can result in less- ^{13}C values from technical replicates and a higher variability from ^{13}C analyses, making a comparison of samples less precise. Some samples would have benefited from additional analyses; however, project timelines and, in some cases, later arrival of some samples precluded those analyses. However, the current data show strong proof-of-concept that good comparisons among techniques exist and that further analyses will improve the statistics for these measurements.

This study indicates that the method of direct injection of fuel into the EA-IRMS system produced reproducibility on replicate measurements comparable to the method in which samples were encased in tin capsules sealed under an argon environment. These methods are used to avoid potential isotope fractionation of low viscosity samples that could lead to nonrepresentative ^{13}C values. Direct injection also ^{13}C analysis, as fuel could be directly removed from a fuel stream, injected, and data provided within ca. 10 minutes. This method of sample introduction would allow for a streamlined analysis at the facility setting.

The approach was shown to be effective since the ^{13}C values of fuels can have high precision when measured in replicates and have been shown to provide precise estimates of the percent biocarbon. The new method of directly injecting fuel samples into the EA-IRMS system is comparable with the published method and may be more appropriate for liquid fuels as a ^{13}C values using direct-injection EA-IRMS provide statistically similar values for the biogenic carbon content to the approved ASTM D6866 B method using ^{14}C AMS measurements. However, in some cases, ^{13}C values depending on the source of carbon, meaning that the estimated percent biocarbon for a co-processed fuel will be less precise than for a co-processed fuel with a large range between feedstock/blendstock

of co-processed fuels even when the co-processed feedstocks are similar, providing the potential for increased accuracy and precision, as compared to direct analysis of the parent samples.

These results contribute to a deeper understanding of the applicability of IRMS for measuring the biogenic carbon in transportation fuels. In this study, a broad evaluation of several fuel separation methods, when combined with measuring the stable carbon isotope ratios of fuels and fuel fractions, suggests that this approach can quantify the biocarbon in fuels with greater precision than analyzing the neat sample, particularly at low blending ratios.

The findings from this project are likely to encourage refiners to co-process renewable feedstocks, even when only relatively small amounts of renewables are present in the fuel. This will increase the demand for renewable feedstocks, encourage the production of additional renewable feedstocks, increase domestic job opportunities, and ultimately increase renewable content in transportation fuels. Additionally, co-processed fuels deliver fuel properties compatible with today's engines, and future fuels will be adapted to meet the requirements of new engines. This project will benefit the U.S. taxpayer by ensuring that a transition to fuels having increased renewable content will be seamless, while reducing greenhouse gas emissions through the displacement of crude oil feedstocks.

IRMS has the potential to be deployed on-site at refinery locations to provide the rapid sample analysis needed to optimize refinery operations for the incorporation of biogenic carbon in the final transportation fuel product. In addition, lab requirements and the mastery of sample processing and instrumentation, the costs of instrumentation and lab setup, and the pool of individuals with expertise make stable carbon isotope analysis and IRMS-based measurements more approachable than ^{14}C measurements via AMS in a refinery setting. While not part of this study, ^{13}C measurements can also be made using optical spectroscopy, yielding results comparable to those obtained by IRMS, further reducing the costs for stable isotope ratio measurement, as well as instrument costs and stability over IRMS. This can only lead to an expansion of the use of ^{13}C at refinery locations, allowing further realization of the benefits of stable isotope measurement in the field.

Acknowledgments

The authors are grateful to Robert Natelson, Trevor Smith, and Alicia Lindauer, U.S. Department of Energy Technology Development Managers, and Kelly Nguyen, Project Monitor, for supporting this work. The Project Team is also grateful for the support received from Drs. Dan Gaspar, Corinne Fuller, and Huamin Wang for their help in navigating relationships with the Bioenergy Technologies Office. Additionally, we appreciate the valuable interactions and encouragement we have had with members of the Coordinating Research Council (CRC) Fuels for Advanced Combustion Engines Working Group, and support from the Advanced Vehicle/Fuel/Lubricants (AVFL) Committee, the Emissions Committee, and the Performance Committee, specifically Dr. Christopher Tenant, Amber Leland, and Betty Carter.

RG and AH would like to acknowledge Natural Resources Canada and the government of Canada's interdepartmental Program of Energy Research and Development for partial funding of the study. The authors are grateful to the analytical lab staff at CanmetENERGY in Devon, especially Mrs. Cecile Lay for her technical support. TB and SL would like to acknowledge contributions made by Marie Swita for the elemental and fuel analyses performed at PNNL and Karl Weitz for instrument troubleshooting and assistance.

This research was conducted as part of the Co-Optimization of Fuels & Engines (Co-Optima) initiative sponsored by the U.S. Department of Energy, Office of Energy Efficiency and Renewable Energy, Bioenergy Technologies, and Vehicle Technologies Offices. Co-Optima is a collaborative project between multiple national laboratories and was initiated to simultaneously accelerate the introduction of affordable, scalable, and sustainable biofuels and high-efficiency, low-emission vehicle engines. PNNL is a multi-program national laboratory operated by Battelle for the U.S. Department of Energy under Contract DE-AC05-76RL01830.

This work was also supported in part by the U.S. Department of Energy, Office of Science, Office of Workforce Development for Teachers and Scientists under the Science Undergraduate Laboratory Internships Program.

Acronyms and Abbreviations

AMS	accelerator mass spectrometry
API-D	American Petroleum Institute density measurement at 15 °C
ARO	aromatic sample
AVFL	Advanced Vehicle/Fuel/Lubricants
BioC	biocarbon
BP	boiling point
°C	degree(s) Celsius
C	combustion
ca.	circa
CARB	California Air Resources Board
CARBOB	California Air Resources blendstock for oxygenate blending
CD	canola diesel refiner
Co-Optima	Co-Optimization of Fuels & Engines initiative
CRADA	Cooperative Research and Development Agreement
CRC	Coordinating Research Council
CRU	circulating riser unit
cSt	centistoke(s)
^{13}C	$^{13}C = ((R_{sample} / R_{standard}) - 1)) \times 1000$, in per mil (‰) where R = $^{13}C/^{12}C$ ratio and $R_{standard}$ is the international reference value of Vienna Peedee Belemnite in per mil
DCO	distillers corn oil
DFO	Direct Funding Opportunity
DHDS	diesel hydrodesulfurization
DOE	U.S. Department of Energy
EA	elemental analyzer
EPA	U.S. Environmental Protection Agency
FAME	fatty acid methyl ester
FBP	final boiling point
FCC	fluid catalytic cracking
FID	flame ionization detector
FOG	fats, oils, greases
g/cm^3	gram(s) per cubic centimeter
GC	gas chromatography
GC×GC	two-dimensional gas chromatography
HEFA	hydroprocessed esters and fatty acids
HDS	hydrodesulfurization

HPR	High Performance Renewable
IBP	initial boiling point
ID	identification
IRMS	isotope ratio mass spectrometry
L	liter(s)
LANL	Los Alamos National Laboratory
LG	landfill gas refiner
min	minute(s)
mL	milliliter(s)
mV	milliVolt(s)
PCA	principal component analysis
Pet.	petroleum
PIONA	paraffins, iso-paraffins, olefins, naphthenes, aromatics, oxygenates
pMC	Percent Modern Carbon, where ‘Modern’ is defined as 1950 AD
PNNL	Pacific Northwest National Laboratory
R1, R2, R3	refiner(s) 1, 2, 3
R100	100% renewable fuel
RNW	renewable
s	second
SAK	synthetic aromatic kerosene
SAT	saturate sample
SI	spark ignition
SOAP	saturate, olefin, aromatic, and polar fractions
stdev	standard deviation
SPE	solid-phase extraction
T10, T50, T90	the temperatures at which 10%, 50%, and 90% of the sample has evaporated, respectively
ULSD	ultra-low sulfur diesel
U.S.	United States
USGS	United States Geological Survey
V%	volume percent
VPDB	International carbon isotope reference material Vienna Peedee Belemnite
VUV	vacuum ultraviolet spectroscopy
wt%	weight percent

Contents

Figures

Tables

1.0 Introduction

1.1 Motivation

The United States (U.S.) Department of Energy's Co-Optimization of Fuels & Engines (Co-Optima) initiative (DOE n.d.) examined simultaneous advances and developments in fuels and engines with the intention of improving vehicle fuel economy. The main period of the initiative ran for six years and included the participation of national laboratories, universities, and industry. This project within the Co-Optima initiative is the result of a cooperative research and development agreement (CRADA) between Pacific Northwest National Laboratory (PNNL), Los Alamos National Laboratory (LANL), and the Coordinating Research Council (CRC). This CRADA fits the Co-Optima goal of developing strategies that can shape the success of new fuels with industry and consumers by removing barriers related to the introduction of bio-derived feedstocks into transportation fuels. This project examines the use of isotope ratio mass spectrometry (IRMS) as an analytical tool for assessing the amount of biogenic material in a fuel sample.

1.2 Approach

Even seemingly small increases in incorporating renewable feedstocks into transportation fuels can have a strong impact on yearly CO_2 emission levels. The U.S. Energy Information Administration (EIA.gov) estimates total U.S. daily gasoline usage at 389.69 million gallons (in 2019) and distillate usage at 131.14 million gallons (in 2018) (EIA 2023). For every 1 percent increase in renewable feedstocks that are co-processed into the total gasoline/distillate pool as a result of economic incentives, an additional 1.9 billion gallons of low-carbon transportation fuels would displace traditional crude oil annually in the United States. With some assumptions, this equates to a potential reduction (per percentage increase in renewable usage) of between 10 and 25 million metric tons of CO_2 per year by displacing traditional crude oil with renewable feedstocks.

High-value renewables designed to impart specific fuel properties, like those developed under Co-Optima, can be directly blended as a fuel component. For some renewable fuel components this could be accomplished at the terminal, as is done with ethanol, where the amount of renewable feedstock being added to the fuel is directly traceable without needing complex analysis. However, not all biomass sources are suitable for producing high-value renewables. These lower-value renewable feedstocks are often blended with petroleum-derived feedstocks and co-processed to produce fuel blending components and finished fuels, while leveraging existing depreciated refinery infrastructure. Processing units may include fluid catalytic crackers, hydrotreaters, hydrocrackers, isomerizers, and reformers to produce gasoline, diesel, jet, heating oil components, and blendstocks. When the renewable feedstocks are co-processed, it is virtually impossible for traditional analytical approaches—focused on compound identifications alone—to distinguish between content produced from renewable feedstocks and content produced from fossil feedstocks (Mueller et al. 2016).

Recently, petroleum refiners have begun expanding their processing of renewable feedstocks to meet Renewable Fuel Standard requirements in response to state and federal incentives like California's Low Carbon Fuel Standard. Co-processing offers an additional option for refiners to increase renewable content in transportation fuels while obtaining tax credits to offset the increased costs associated with renewable feedstocks.

Presently, ^{14}C testing (Biogenic Carbon Content by ASTM D6866) is the only test method recognized by the federal government and state entities like the California Air Resources Board to validate renewable carbon content in fuels (ASTM 2020). Due to the stringent requirements established for this type of validation, only a few commercial analytical laboratories in the United States are qualified to conduct the testing, for example, Beta Analytics in Miami, FL and the Center for Applied Isotope Studies in Athens, GA. Further, routine turnaround times are ~2 weeks with results having an absolute uncertainty of ±3%, per ASTM D6866 (ASTM 2020), making accelerator mass spectrometry (AMS) an impractical approach for informing real-time process optimization in a refinery in terms of maximizing renewable feedstock conversion to fuel or to quantifying low blending levels. A recent report using this method for diesel fuels found an accuracy and precision of 0.26 weight percent (wt%) to be achievable (limit of detection = 0.44 wt%) with AMS, which are sufficient for refiners' needs (Haverly et al. 2019). Current AMS capabilities, however, do not produce rapid sample analysis turnaround, which would allow improved process control and optimization and thus enable a higher proportion of a biofeedstock to be captured in desirable process streams (e.g., blendstocks suitable for transportation fuels).

Widespread deployment of AMS instruments is presently not feasible because of the relative expense of the instrument, the sensitivity of the AMS to its environment, and the need for a dedicated, highly skilled operator to run the system. In contrast to AMS, IRMS is less expensive, has a much smaller instrument footprint, is much more common in research and commercial labs across the country, and requires less sample handling and preparation for operation. Together, these features give IRMS the potential to be located and operated at refineries. Historically, stable isotope content has proven to be a valuable tool for differentiating fossil fuel reservoirs as well as for understanding source materials and geologic history of these reserves (Schoell 1984; Sofer 1984). Extending IRMS analysis from naturally occurring petroleum stocks to include bio-derived feedstocks is a natural extension of previous work. Importantly, emerging work at LANL showed strong correlation between IRMS and AMS measurements (Li et al. 2020a, 2020b). While this work was encouraging, additional efforts are required to define the utility and broaden the scientific basis for using IRMS as an additional approach to measuring biogenic carbon content.

Providing an alternative analytical method for biogenic carbon in co-processed fuels (e.g., utilizing IRMS) has the potential to rapidly and accurately validate low levels of renewable material in final fuel products. Further, an IRMS method can be implemented in many commercial laboratories across the U.S., and potentially even in refineries, significantly reducing analysis times. On-site measurements and faster analysis provide refiners with the opportunity to track renewable carbon content throughout the refining process, offering the potential of adjusting processing parameters to optimize the renewable carbon content in transportation fuel streams. Optimized co-processing will ensure that an even higher percentage of the renewable feedstock is carried into their desired product streams, while ensuring quality fuels for today's engines. This will increase the value returned from the renewable feedstock to refiners, which is now offered as incentives, but can later be brokered into positive consumer sentiment, as the consumer sees value in fuels containing an increasing percentage of renewable feedstocks.

As refiners see an opportunity for increasing returns on their investment in renewable feedstocks, they will be inclined to obtain and co-process additional renewable feedstocks. This will in turn accelerate the introduction of renewables into transportation fuels, offsetting fossil-derived fuel components, leading to concomitant reductions in greenhouse gases.

By providing a more thorough scientific understanding of IRMS as a means of augmenting current measurements of biogenic carbon in fuels, this work will further educate stakeholders on the advantages and limitations of the IRMS approach.

This work shows integration of chemical separation approaches with IRMS analyses, enabling biogenic carbon tracking in fuel product streams by boiling point (BP) range, chemical class, and compound. Using a broader sample set than previously studied (Yan et al. 2019; Geeza et al. 2020; Li et al. 2020a, 2020b), this work demonstrates the potential for and future research directions needed for IRMS-based sample assessment to provide reliable biocarbon content estimates that can be comparable to those obtained by AMS analysis. Our initial results highlight the use of separations to improve sensitivity at low blend ratios and the use of rapid assessment strategies for enabling refinery process optimization through on-site analysis and biocarbon estimates.

2.0 Results and Discussion

Carbon has two stable isotopes, ^{12}C and ^{13}C, which can be foundational in analyzing carbon sources in various materials, including fuels. The lighter isotope, ^{12}C, is more abundant, while the heavier isotope, ^{13}C, occurs less frequently but provides a distinctive isotopic signature. The ^{13}C (see equation below), enables researchers to differentiate between carbon sources, such as fossil fuels and bio-derived materials, because these sources often have unique isotopic profiles.

$$\delta^{13}C = \left(\frac{R_{sample}}{R_{standard}} - 1\right) \times 1000$$

In the previous equation, *R* represents the ratio of the heavy to light isotopes ($^{13}C/^{12}C$) for the sample and standard, with values denoted in -notation as per mil values (‰). The excellent ^{13}C:

$$\delta^{13}C_{mixture} = f \times \delta^{13}C_{constituent\ 1} + (1 - f) \times \delta^{13}C_{constituent\ 2}$$

where f is the fraction of the added end-member in the mixed fuel product and ^{13}C values are related to the two fuels mixed together (i.e., constituent 1 and 2) and their product (i.e., mixture).

This project conducted ^{13}C to enhance co-processing procedures and estimate the biocarbon content of blended and co-processed fuels and fuel feedstocks, both fossil and renewable in origin. The materials, methods, results and discussion are summarized below. The research summary is structured to reflect the order of tasks and milestones laid out in the Scope of Work outlined within the Co-Optima DFO/CRADA Proposal for the collaborative work with PNNL, LANL, DOE Bioenergy Technologies Office (BETO), and CRC, Incorporated (CRC, AVFL-38) members.

2.1 Materials (Task 1)

Fossil fuels, biofuels, blended and co-processed fuels, and fossil and renewable biocarbon-based feedstocks (*n* = 45) were provided in three tranches by CRC members, from three main companies and their collaborators. See Table A.1, Appendix A for sample ID and origin, by refiner, but not broken down by delivery tranches. Refiners have been anonymized; however, fuels have been grouped by the contributing refiner, such that all fuels contributed by Refiner 1 have R1 associated with their sample ID.

Upon delivery, samples were kept chilled and subdivided into amber glass containers, then refrigerated. This process was performed to reduce the risk of sample aging and volatilization that could alter composition and allow isotopic fractionation. Isotopic fractionation could p ^{13}C values and chemical separation results. For every new analysis or task, samples were drawn from an unopened bottle containing a fresh sample.

Examples of samples include hydrotreated oils, distillation cuts from the given process, isomerization and reformate products of co-processed bio- and fossil feedstocks, diesel and gasoline samples of fossil origin, fuel blends, and biofuel feedstocks from plant and animal sources. Sample relationships were established based on descriptions provided by the CRC members and can be identified by refiner, biocarbon and fossil carbon blendstocks, and fossil

and renewable feedstocks used to produce co-processed fuel products. These relationships were utilized to select suites of "related" samples ^{13}C analysis of fuel fractions and then to prioritize the sample set for AMS analysis (discussed in following subsections), to best assess the incorporation of biocarbon in fuels by parallel AMS and IRMS methods. Appendix A identifies the samples provided from each refiner. Appendix B describes the sample interrelationships from each refiner.

An example of a co-processed sample set includes fossil feed and tallow-based biofeed, co-processed by Refiner 3 (R3) using a hydrotreater, and three resulting co-processed fuels (Figure 1). Sample relationships depicted include the hydrodesulfurization (HDS) biofeed (#3 HDS Bio-feed, Tallow-based biofeed) and the fossil feed (#3 HDS Feed Surge Drum) co-processed using hydrotreatment to form a fuel blendstock (#3 HDS Product). Additional co-processed fuels, including ultra-low sulfur diesel (ULSD; ULSD#2 Tank 37 Final, ULSD#2 Tank 30 Final) were presented as having been processed in the same manner but the ratios of biofeedstock to fossil feedstock are different from #3 HDS Product. It is also possible that the co-processing conditions were different for each of these three products. Samples from this dataset and other sample relationship sets were analyzed for bulk (entire sample) and fractional (subsets of the sample) ^{13}C values. Additionally, fractions were separated at CanmetENERGY and analyzed using GC×GC before being shipped to PNNL for ^{13}C analysis. Selected sample relationship sets were subsequently analyzed for percent biocarbon (i.e., percent modern carbon) using ASTM Method D6866 via AMS (ASTM 2020).

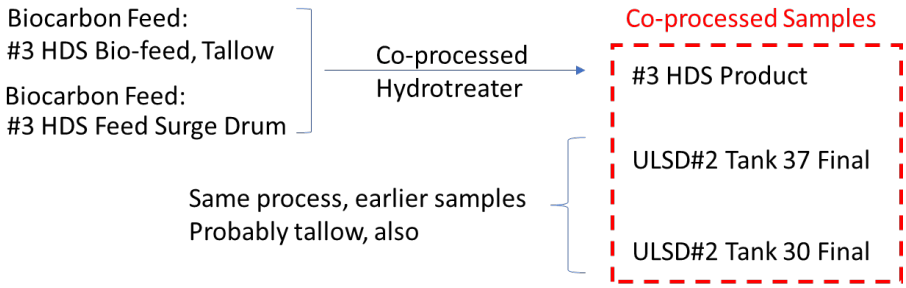

Figure 1. R3 Sample relationship for a set of feedstocks and the resulting co-processed products (dashed red box). Abbreviations: HDS = hydrodesulfurization; ULSD = ultra-low sulfur diesel.

Task 1 Outcome Assessment:

Proposed: Sample sets will be organized by process and renewable feedstock to assess gaps and assist in subsequent analyses.

Final: Forty-nine samples were received and organized by process, identifying the feedstocks and blendstocks. A series of sample schematics were produced to show sample relationships that provided a map for datasets for each task and to identify existing gaps in the datasets (e.g., Figure 1 and Appendix B). These schematics were referred to throughout this project to prioritize sample analysis for percent biocarbon determination.

2.2 Sample Preparation and Analytical Methods (Task 2)

This project included multiple methods, from wet chemistry methods used to separate fuels into saturates and aromatics, to analytical methods used to run instrumentation, and to statistical

methods used to determine values and uncertainty. These methods are described in detail in the Experimental Section (Section 5.0).

Analytical methods for IRMS were developed using compounds and ^{13}C-defined compounds that represented the behavior of liquid fuels and feedstocks. These methods were then applied to fuel samples to ^{13}C values of bulk fuels and feedstocks (Section 5.2—see Standards Development). ^{13}C values were also determined for saturate and aromatic fractions, analyzed as both bulk fractions (i.e., chemical class) and by separating fractions into individual compounds or chemical groups (i.e., compound specific) using ^{13}C-defined compounds and mixtures of compounds, as discussed in the subsections below. The development of analytical methods for different sample types allowed for multiple evaluations and set the stage for subsequent comparison of percent biocarbon estimates using bulk, chemical class, and compound-specific ^{13}C measurements in co-processed fuels. These data for the bulk fuel samples were then compared with results from AMS (using ASTM D6866) to evaluate efficacy (ASTM 2020). Additional work will be required to equate the IRMS results for chemical classes and compound-specific measurements to bulk IRMS results and AMS results.

Task 2 Outcome Assessment:

Proposed: Implementation of an analytical standard will ensure that results among institutions are comparable.

Final: Bulk, combustible liquids that represented the behavior of the fuel and feedstock samples were identified at PNNL as in-house standards, supplied to LANL, and used at both locations to ensure continuity in data calibrations (Experimental Section, Section 5.0). In addition, standards with known isotopic compositions were obtained from external suppliers to correct and normalize the $\delta^{13}C$ values of bulk and compound-specific samples. Sample handling and analysis methodologies were agreed upon by the Project Team and are also presented in Section 5.0, where bulk samples were introduced to the combustion unit by direct injection at PNNL and by sealing in a tin capsule under an argon environment for LANL.

2.3 ^{13}C Values of Bulk Samples and Blends (Task 3)

Ran e o ^{13}C Values of Bulk Samples: ^{13}C values from bulk bio/renewable fuel blend- or feedstocks, bulk fossil fuel blendstocks, blended fuel samples, and co-processed fuel samples (n = 49 samples) range from 43.79‰ ± 0.20‰ to 10.14‰ ± 0.01‰ (33.65‰ range) (Table A.3, Appendix A; Figure 2). Standard deviations (1) were calculated on technical replicates (n for the vast majority of samples) and range from ±0.03‰ to ±0.50‰. The greater standard deviations for some samples are attributed to slight inconsistencies in the manual, direct injection of liquid samples into an Elemental Analyzer (EA) IRMS and to sample volatility, where more volatile samples, such as naphtha-like samples, generally have a larger standard deviation. The ^{13}C values of samples often fit within the previously established empirical ^{13}C distribution of petroleum products, C3 plants, and C4 plants, as many biofuels in our dataset are derived from C3 plants, C4 plants, and animals that consume these plants (e.g., soy, canola, livestock). The less negative ^{13}C values correspond to fuels and feedstocks originating from C4 plants, and more negative ^{13}C values generally correspond to C3-derived samples. ^{13}C values of biofuel samples are generally less negative than those of fossil fuel samples, this is not always the case (Mook et al. 2000; Kohn 2010; Vieth and Wilkes 2010). For example, t ^{13}C value (43.79‰) corresponds to a biocarbon product produced from landfill waste containing methane and points to a microbial process (i.e.,

methanogenesis). This process is not directly related to C3 or C4. The potential for small differences between fossil- and bio-derived samples (when used as end-members of a blend or co-processing curve) highlights the need for methods to accentuate these differences to improve accuracy and precision at low blend levels. Additionally, the potential for fossil-derived samples to have less negative ^{13}C values than bio-derived samples calls out the need for knowledge of the ^{13}C values for each feedstock to accurately assess the ^{13}C value of the final blend or product. Both of these requirements are unique to using stable isotopes as a measure of biogenic carbon content and not experienced to such a degree using radiocarbon methods.

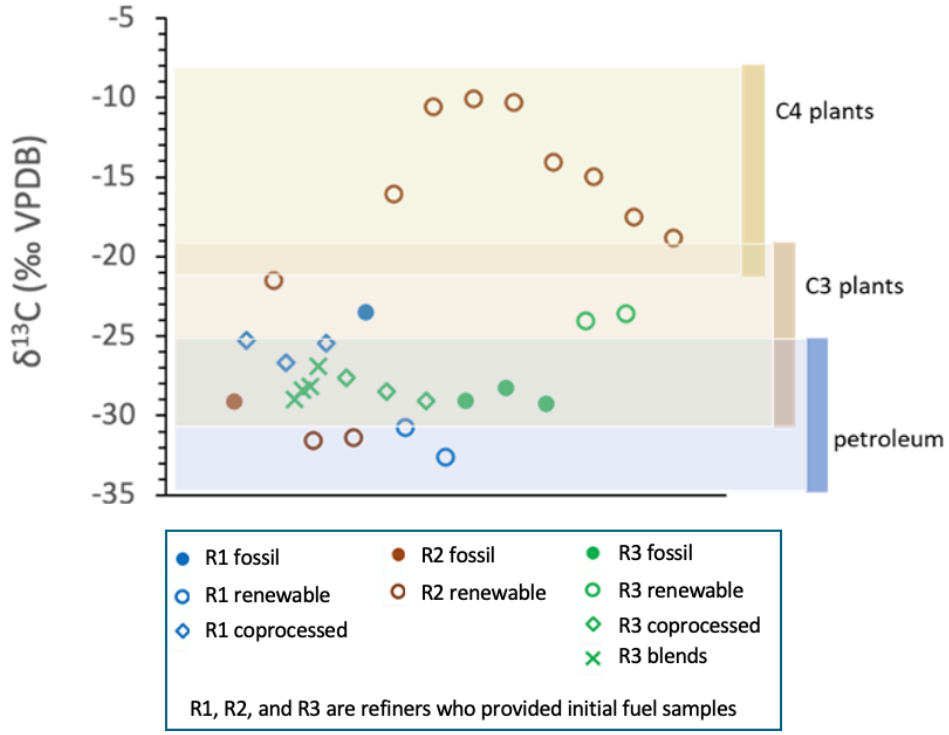

Figure 2. Bulk fuel and feedstock ranges: Representative ^{13}C values from biofuel feedstocks, fossil fuels, blends, and co-processed samples from CRC member refiners, R1, R2, and R3. Samples are binned by fuel type for each refiner within the legend below the plot. Not included in the figure are the 17 samples sent in delivery Tranches 2 and 3, where two samples lay outside the plot (LG CRU 50% F at 37.25‰ ± 0.03‰, a fossil-derived sample and LG CRU 100% F at 43.79‰ ± 0.20‰, a biogenic feed stock). Abbreviations: CRU = circulating riser unit; $^{13}C = ((R_{sample} / R_{standard}) - 1))$ x1000, in per mil (‰) where R = $^{13}C/^{12}C$ ratio; LG = landfill gas refiner; VPDB = Vienna Peedee Belemnite.

Blend Curves/Linear Blending Response: Samples blended at PNNL were analyzed for bulk ^{13}C values to evaluate the linearity of the blending response and to assess the utility of using ^{13}C values to estimate the percent biocarbon at low ratios. The fossil-derived samples, bio-derived samples, and co-processed samples used to create four blends are presented in Table 1, representing a ^{13}C range spanning from 1.70‰ to 18.43‰ between end-members. Results for blend curves are shown in Figure 3, with green triangles representing “blind blends” of each of the two end-members. Blind blends are sample mixtures prepared by

CanmetENERGY team members allowing PNNL team members to test the analytical accuracy, precision, or bias without prior knowledge of the exact contents.

Table 1. Range of blend isotope data. Renewable, co-processed, and fossil samples used for in-house ^{13}C data related to the range between end-member fuels, and the 95% calibration intervals for unknown samples (blind-blend analyses).

Sample ID	End-member type	^{13}C Value (VPDB ‰)	^{13}C End-member range (‰)	0%–10% biocarbon range ^{13}C (‰)	Width of 95% calibration interval unknown sample		^{13}C Avg. stdev (‰) from IRMS measurements
					0%–100% biocarbon range model	0%–10% biocarbon range model	
R2 Renewable Diesel from Sugar Mixture	Renewable	10.85	18.43	1.84	0.29	0.29	0.05
R2 Renewable HEFA-FOG	Renewable	21.29	7.97	0.8	0.51	0.68	0.05
R1 MP-30 D535	Co-processed	26.12	3	0.3	5.1	2.3	0.11**
R3 #3 HDS Product	Co-processed	27.68	1.7	0.17	1.53	0.22	0.04
R2 Pet. No. 2 Diesel	Fossil derived	29.28*	-	-	-	-	-

* Fossil end- ^{13}C values differ by ±0.11‰ for blend curves. A 1 L bottle of the fossil fuel was used over a two-day period during blending sessions. The bottle was refrigerated between each blend session to reduce the potential for isotopic fractionation related to volatilization. However, it is possible that the increased headspace-to-liquid fuel ratio in the bottle over time and ~1.5 hours without refrigeration may have resulted in isotopic fractionation.

** Note blends with a higher average standard deviation comprised light, volatile compounds.

Abbreviations: $^{13}C = ((R_{sample} / R_{standard}) - 1)) \times 1000$, in per mil (‰) where R = $^{13}C/^{12}C$ ratio; FOG = fats, oils, greases; HEFA = hydroprocessed esters and fatty acids; HDS = hydrodesulfurization; IRMS = isotope ratio mass spectrometry; Pet. = petroleum; R1, R2, R3 = refiner 1, 2, 3; stdev = standard deviation; VPDB = Vienna Peedee Belemnite.

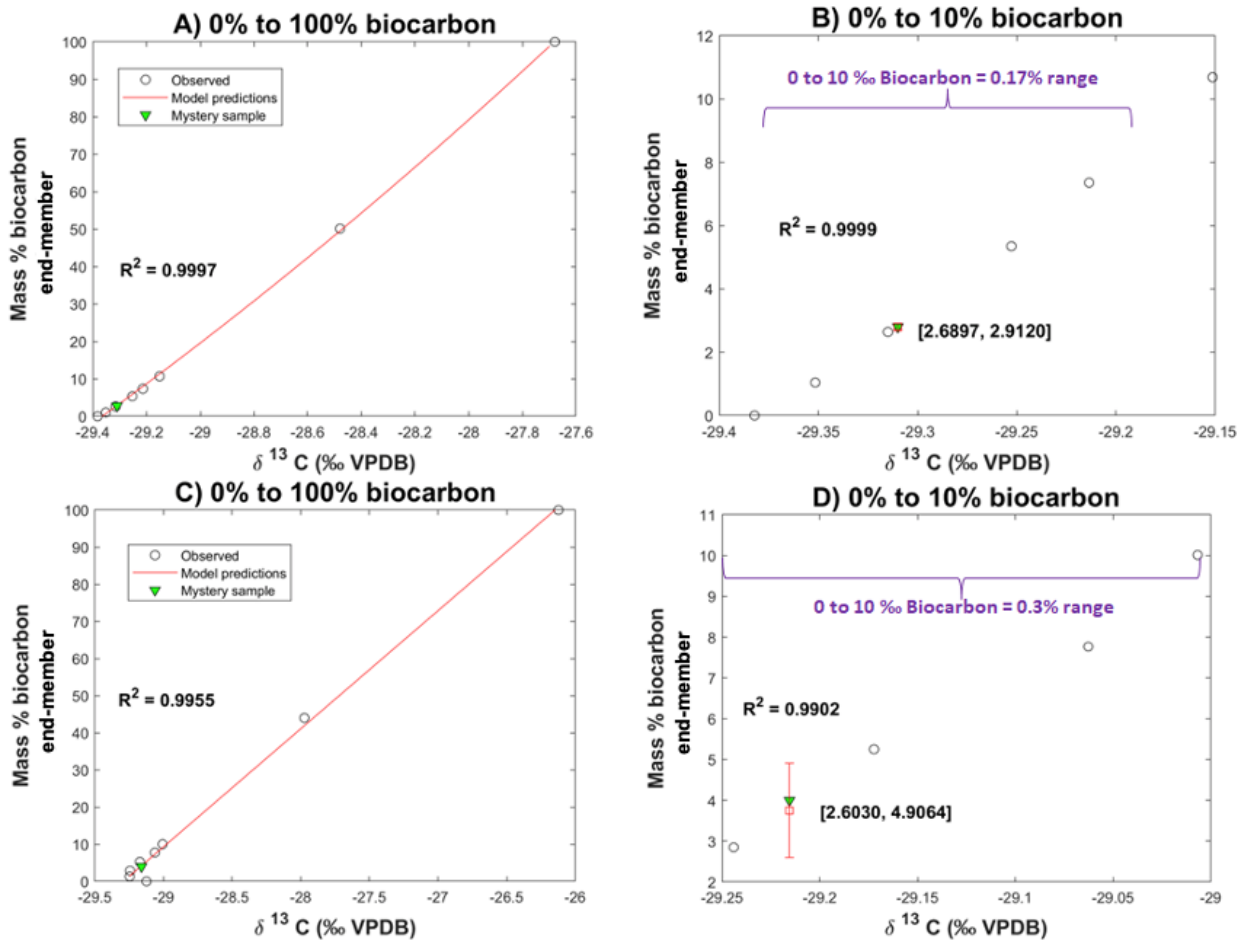

Figure 3. Blends with co-processed end-members. A) and B) Blends of a fossil end-member (R2 Petroleum #2 Diesel) and co-processed end-member (R3 HDS #3 Product) for a blend range of 0% to 100% co-processed sample and 0% to 10% co-processed sample, respectively. C) and D) Blends of a fossil end-member (R2 Petroleum #2 Diesel) and renewable end-member (R1 MP-30 D535) for a blend range of 0% to 100% renewable and 0% to 10% renewable, respectively. Blind-blend samples from CanmetENERGY are shown as green triangles. B) and D) provide estimated percent biocarbon range bars for blind-blend samples (denoted as mystery sample in the legend). Boxes and whiskers indicate 95% confidence intervals, with the minimum and maximum percent blended biocarbon end-member in brackets. The purple horizontal braces denote the low blend ratio range (0% to 10%) for percent biocarbon and the corresponding per mil range based on the ^{13}C values of blended samples. The red lines represent the best fit curves for the blends: a purely linear model for MP-30 D535 blends and a quadratic model for HDS #3 Product blends. Additional details for these fits and other fits can be found in Appendix D. Abbreviations: ^{13}C = $((R_{sample} / R_{standard}) - 1)) \times 1000$, in per mil (‰) where R = $^{13}C/^{12}C$ ratio; HDS = hydrodesulfurization; R1, R2, R3 = refiner 1, 2, 3; VPDB = Vienna Peedee Belemnite.

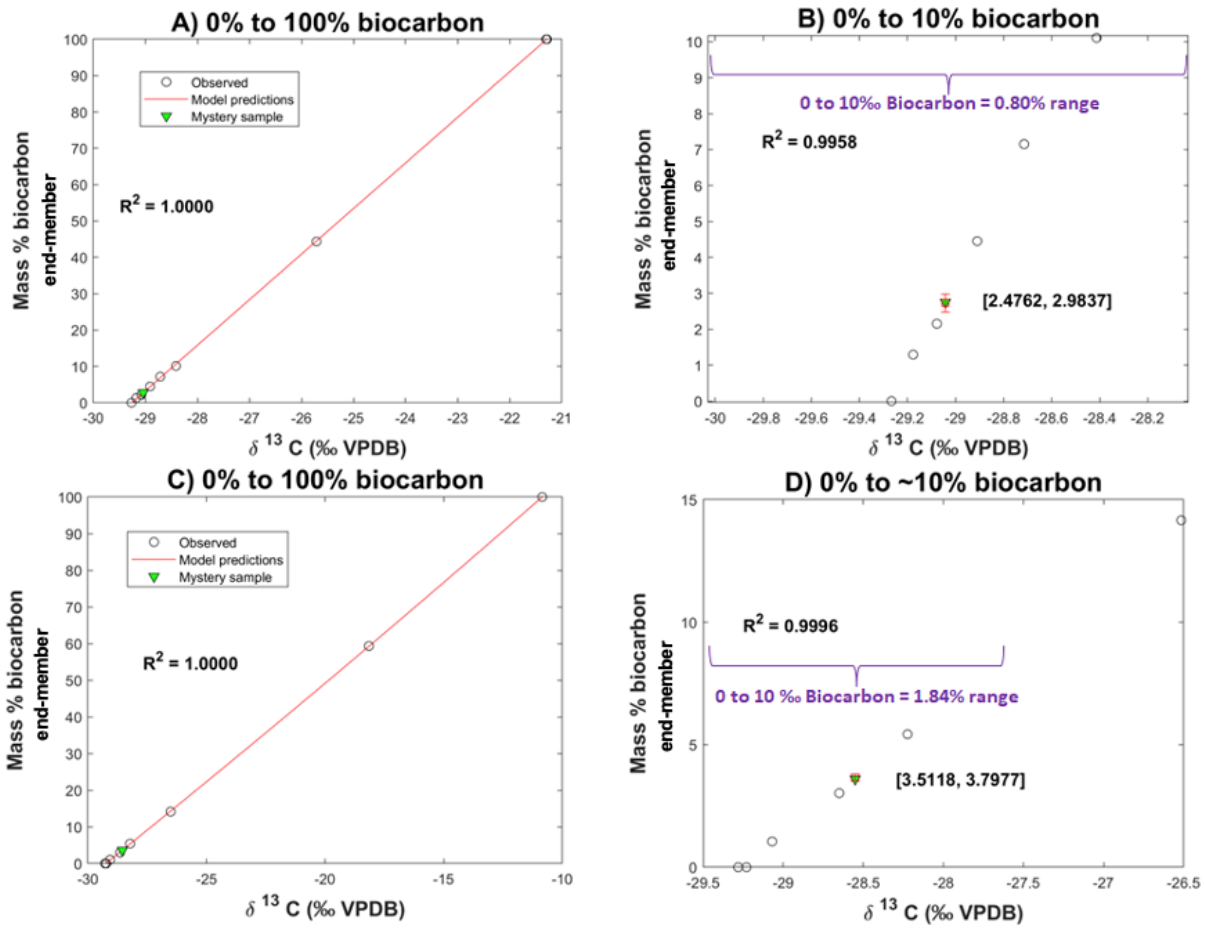

Figure 4. Blends with renewable end-members. A) and B) Blends of a fossil end-member (R2 Petroleum #2 Diesel) and renewable end-member (R2 Renewable HEFA-FOG) for a blend range of 0% to 100% renewable and 0% to 10% renewable, respectively. C) and D) Blends of a fossil end-member (R2 Petroleum #2 Diesel) and renewable end-member (R2 Biodiesel from Sugar Mixture) for a blend range of 0% to 100% renewable and 0% to 10% renewable, respectively. Blind-blend samples blended at CanmetENERGY are shown as green triangles. B) and D) provide estimated percent biocarbon range bars for blind-blend samples (denoted as mystery sample in the legend). Boxes and whiskers for the blind-blend samples indicate 95% confidence intervals, with the minimum and maximum percent blended biocarbon end-member in brackets. The purple horizontal braces denote the low blend ratio range (0% to 10%) for percent biocarbon and the corresponding per mil range based on the ^{13}C values of blended samples. The red lines represent the best fit quadratic curves for the blends: HEFA-FOG blends fit a linear curve and Biodiesel from Sugar Mixture blends fit a quadratic curve. Additional details for these fits and other fits can be found in Appendix D. Abbreviations: $^{13}C = ((R_{sample} / R_{standard}) - 1)) \times 1000$, in per mil (‰) where R = $^{13}C/^{12}C$ ratio; FOG = fats, oils, greases; HEFA = hydroprocessed esters and fatty acids; VPDB = Vienna Peedee Belemnite.

Figure 3A, Figure 3C, Figure 4A, and Figure 4C show the relationship of wt ^{13}C values of blended fuels that have the same fossil fuel end-member, R2 Petroleum #2 Diesel. While the blend curves can have a linear fit with high R^2 values (>0.9900), a slight quadratic

curve provides an improved fit, especially at low blend ratios. The quadratic curve is in contradiction to the linear relationship observed for blended oils from Li et al. (2020a; 2020b) and may be an artifact of the sample handling process during blending, but also could be related to differences in the properties of the fuels themselves. Fuels used for blending have different chemical compositions, which may lead to differences in combustibility during IRMS and differences in volatility, both of which can cause isotopic fractionation and consequently, a nonlinear response. Fuel matrix effects can arise from wide boiling ranges, high fused-ring aromatic content, or other aspects of the fuels that are known to make analyzing fuels/petroleum difficult, potentially leading to a nonlinear response in the percent biocarbon versus ^{13}C values from blendstocks and co-processed feedstocks and fuels. Additional testing would be necessary to clearly identify the source of this slightly nonlinear behavior. In contrast, the blend curve for R2 Renewable hydroprocessed esters and fatty acids (HEFA) and fats, oils, greases (FOG; or HEFA-FOG) blended with R2 Petroleum #2 Diesel is linear (Figure 4A, Figure 4B), which may be related to the compositional similarity of the two fuels.

The quadratic curves were used to estimate the percent biocarbon content for blind samples provided by CanmetENERGY (e.g., Figure 3B and Figure 3D, and Figure 4B and Figure 4D). The 95% confidence intervals were determined based on the analytical variability, as discussed in Appendix D, Statistical Analyses. The range of estimated percent biocarbon for each unknown blend is also related to the range between of the blend end-member ^{13}C values. In general, sample blends with a larger range of ^{13}C values between end-members have a narrow 95% confidence interval compared with end-members with a ^{13}C range (Figure 3B and Figure 3D, respectively); see Figures in Appendix D for Blend Curves with model information). The estimated range of percent biocarbon is also related to the standard deviation of technical replicates, where the larger the standard deviation, the wider the 95% confidence intervals, suggesting that additional replicates can be expected to narrow these ranges further.

The mass percent values of the biocarbon-containing fuels were supplied by CanmetENERGY and were compared with the ^{13}C-predicted mass percent values for the blind blends. Our results, Table 2, showed that in three of four cases, the biocarbon range predicted by the ^{13}C analysis encompassed the “accepted” values supplied by CanmetENERGY.

Table 2. Blind blends from CanmetENERGY as mass percent biocarbon fuel in blend and estimates for stable carbon isotopes from IRMS at PNNL.

Fossil-based blendstock	Biomass-based blendstock	Mass percent biocarbon fuel in blend	Estimated range from ^{13}C value (mass % biocarbon)
R2 Petroleum #2 Diesel	R3 #3 HDS Product	2.13	2.69 to 2.91
R2 Petroleum #2 Diesel	R1 MP-30 D535	4.02	2.60 to 4.91
R2 Petroleum #2 Diesel	R2 Renewable Diesel from Sugar Mixture	3.59	3.51 to 3.80
R2 Petroleum #2 Diesel	R2 Renewable HEFA-FOG	2.45	2.48 to 2.98

Abbreviations: $^{13}C = ((R_{sample} / R_{standard}) - 1)) \times 1000$, in per mil (‰) where $R = {}^{13}C/{}^{12}C$ ratio; FOG = fats, oils, greases; HDS = hydrodesulfurization; HEFA = hydroprocessed esters and fatty acids; IRMS = isotope ratio mass spectrometry; PNNL = Pacific Northwest National Laboratory; R1, R2, R3 = refiner 1, 2, 3.

Task 3 Outcome Assessment:

Proposed: Bulk IRMS measurements for each sample will provide comparative measurements for assessing any improvements in accuracy, precision, and detection limits when separations are introduced in Task 4.

*Final: Fuel and feedstock samples were provided in three tranches, and the bulk materials were analyzed for their $\delta^{13}C$ values via EA-IRMS (**Figure 2**) to provide bulk IRMS measurements. Liquid samples were injected directly into the EA-IRMS for combustion, and solid samples, such as tallow-based biofeed, were weighed into smooth-sided tin capsules and sealed prior to being introduced into the EA. Blend curves and assessments of linearity show that samples with small amounts of biofuel sometimes show a slightly quadratic relationship with each other along the blending curve. When needed, quadratic curves/models give better precision of percent biocarbon from blind blends supplied by CanmetENERGY. The origin of the quadratic behavior is unknown; however, the nonlinearity is postulated to be related to fuel matrix effects or small variations arising during blending.*

2.4 Separation and IRMS Analyses of Fractions (Task 4)

2.4.1 Analysis and Separation of Fuel Samples (Task 4a)

Several approaches are possible when considering separations in fuels. Due to project scope and timeline, as well as sample characteristics and complexity, not all approaches were undertaken for each sample. GC methods can be applied directly to spark-ignition (SI) fuels with a high likelihood of achieving baseline separations for many of the individual chemical components (ASTM 2014). This is not the case for compression-ignition fuels where the chemical composition is far more complex. Instead of isolating each component, GC methods, such as ASTM D2887 (ASTM 2016), are commonly used to represent compression-ignition fuels in the boiling point (BP) domain. Additional approaches, such as solid-phase extractions performed by CanmetENERGY, can separate the sample into chemical classes, such as saturate, olefin, aromatic, and polar (SOAP) fractions. These separations assist in understanding sample relationships for blended and co-processed fuels and provide the fractions that will be analyzed for the ^{13}C composition.

2.4.1.1 Sample BP Distributions

The BP distribution, derived from “normal-phase” two dimensional GC×GC flame ionization detection (FID) analyses, where “normal” refers to a nonpolar mobile phase followed by a polar chromatographic column configuration, presented in Figure 5 is expressed in terms of several key parameters:

1. initial boiling point (IBP): This represents the temperature at which the first component of the sample begins to boil. It provides insight into the volatility of the lightest fraction within the sample.
2. T10/T50/T90: These are the temperatures at which 10%, 50%, and 90% of the sample has evaporated, respectively.
3. final boiling point (FBP): The temperature at which the last component of the sample evaporates. It represents the BP of the heaviest fraction and provides insight into the sample’s high-end volatility range.

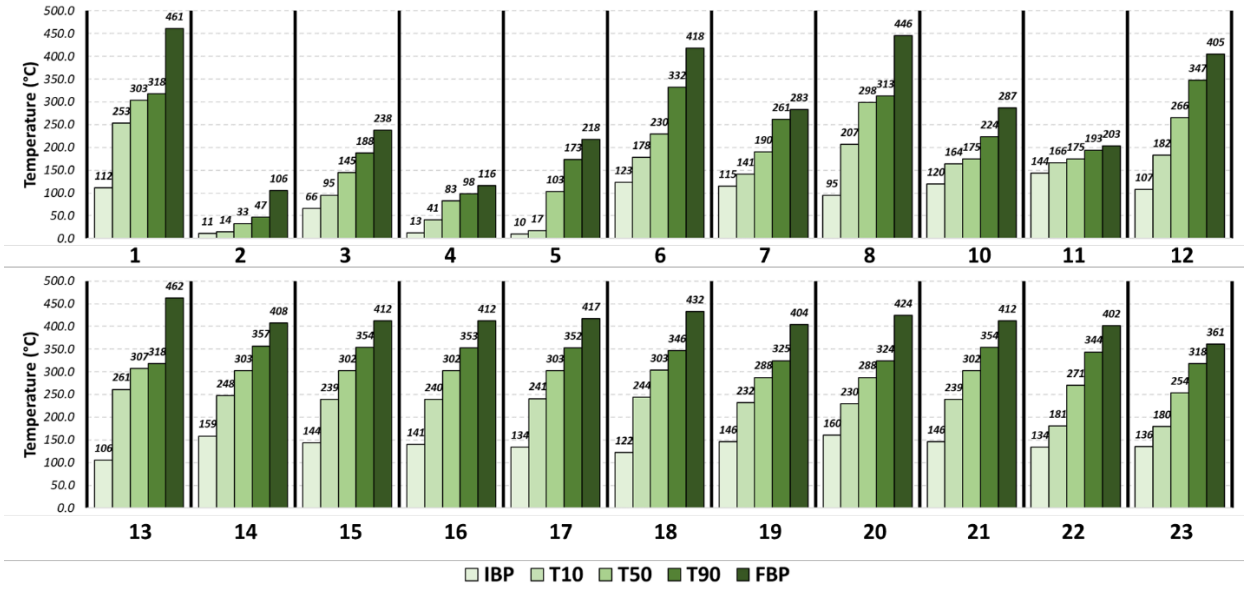

Figure 5. Boiling point distribution, based on "normal" GC×GC-FID, expressed as the temperatures at which we observe the boiling of components in the respective cuts. Sample identification numbers can be found in Section 5.1, Table 5. Abbreviations: FBP = final boiling point; IBP = initial boiling point; T10, T50, T90 = the temperatures at which 10%, 50%, and 90% of the sample has evaporated, respectively.

As shown in Figure 5, the IBPs and FBPs of samples 2, 3, 4, 5, 7, 10, and 11 are lower than those of the other samples, indicating that these samples are naphtha type or even lighter fraction than naphtha. Consequently, our team decided to further analyze all the light samples (i.e., 2, 3, 4, 5, 7, 10, and 11) using paraffins, iso-paraffins, olefins, naphthenes, aromatics, oxygenates (PIONA) analysis (ASTM D8071) by GC equipped with a vacuum ultraviolet spectroscopy (VUV) detector, as detailed in the next section.

2.4.1.2 PIONA Analysis of Fuel Samples

As mentioned in the previous section, the light naphtha samples were subjected to PIONA (Paraffins, Iso-paraffins, Olefins, Naphthenes, Aromatics) separation using a GC system equipped with a VUV detector. This method allows for the precise identification and quantification of the different hydrocarbon classes within the samples. This analysis achieved high-resolution separation and accurate quantification of paraffins, iso-paraffins, olefins, naphthenes, and aromatics in the light naphtha samples. The composition distributions are presented in Table 3.

Table 3. PIONA analysis (ASTM D8071) by GC-VUV for light naphtha samples showing the mass percent compositions of P – Paraffins, I – Iso-paraffins, O - Olefins, N – Naphthenes, and A – Aromatics. Sample identification numbers can be found in Section 5.1, Table 5.

No	Origin	Sample info	P (%)	I (%)	O (%)	N (%)	A (%)
2	R1	MP-30, D-535	2.5	86.5	0.0	11.0	0.0
3	R1	MP-30, D-140	6.4	26.7	0.4	3.2	63.4
4	R1	Renewable Naphtha	52.9	36.7	0.1	10.2	0.1

No	Origin	Sample info	P (%)	I (%)	O (%)	N (%)	A (%)
5	R1	CARBOB, 1005	11.1	37.7	0.3	22.6	28.3
7	R2	Renewable HEFA - Mixture of FOG	17.5	72.8	0.1	9.6	0.0
10	R2	Renewable Diesel from Sugar Mixture	0.3	2.9	3.5	14.0	79.3
11	R2	Renewable SAK - Mixture of Sugars	0.0	0.0	0.0	0.0	100.0

Abbreviations: CARBOB = California Air Resources blendstock for oxygenate blending; GC-VUV = gas chromatography–vacuum ultraviolet spectroscopy; FOG = fats, oils, greases; HEFA = hydroprocessed esters and fatty acids; R1, R2 = refiner 1, 2; SAK = synthetic aromatic kerosene.

Figure 6 compares the aromatic and saturate compositions (paraffins and iso-paraffins) of the light naphtha samples, expressed as weight percents (wt%), obtained using three different techniques described in this report. Interestingly, there is a surprisingly good agreement between the methods. The only sample that deviates is the very light naphtha, listed as Sample 2. SOAP analysis results indicated both aromatic and saturate content, whereas GC-VUV and GC×GC analyses showed that the sample is purely composed of saturated species.

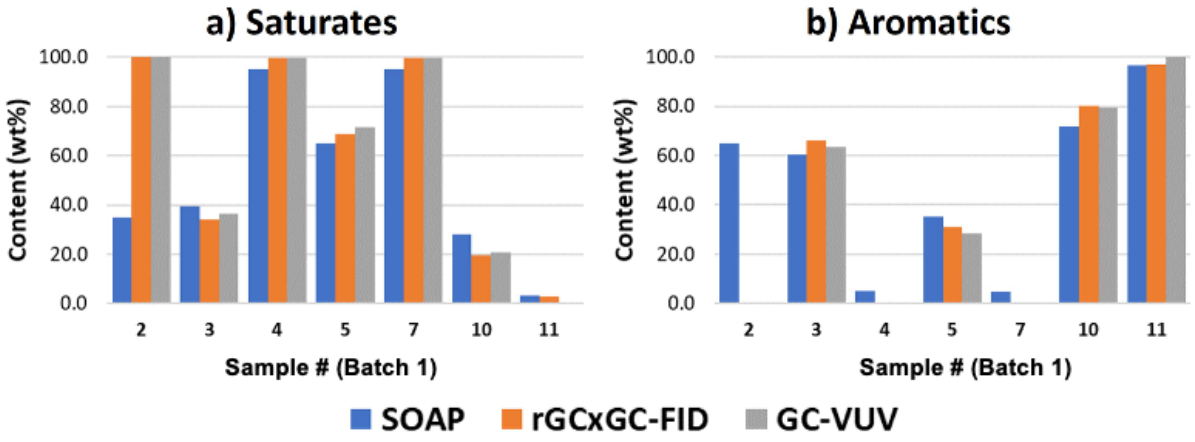

Figure 6. Comparison of aromatic and saturate content in light naphtha samples (wt%) obtained using three different techniques. Sample identification numbers can be found in Section 5.1, Table 5. Abbreviations: FID = flame ionization detector; GC = gas chromatography; rGC×GC = reversed phase two-dimensional gas chromatography; SOAP = saturate, olefin, aromatic, and polar fractions; VUV = vacuum ultraviolet spectroscopy; wt% = weight percent.

2.4.1.3 GC-FID Analysis of Fuel Samples Separated Using SOAP Analysis

Figure 7 shows the GC-FID results of the SOAP analysis conducted on Batch 1 samples (Table 5). The SOAP analysis separates the fuel components into saturates, olefins, aromatics, and polar compounds. For most samples, saturates are present in much higher concentrations than aromatics. Only a few samples contain polar compounds. Sample 9 is a pure renewable biodiesel from soy feedstock, so all its components are fatty acid methyl esters (FAMEs), which are considered polar compounds. The other samples containing noticeable amounts of polar compounds are the blends of Petroleum #2 Diesel with Biofuel high performance renewable (HPR). It is important to note that the SOAP analysis was designed to be effective for samples containing minimal polar content and starting to boil at temperatures greater than 150 °C. The

second condition is not fulfilled for several very light samples in Batch 1, such as samples 2, 3, 4, 5, 7, 10, and 11.

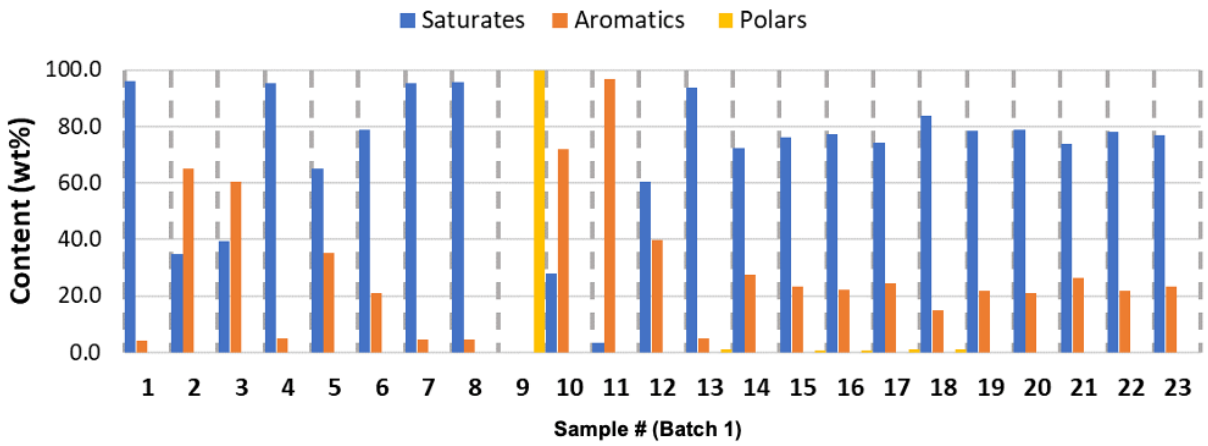

Figure 7. GC-FID results of the SOAP analysis conducted on Batch 1 samples. Sample identification numbers can be found in Section 5.1, Table 5. Abbreviations: FID = flame ionization detector; GC = gas chromatography; SOAP = saturate, olefin, aromatic, and polar fractions; wt% = weight percent.

2.4.1.4 GC×GC-FID Analysis of Fuel Samples Separated Using SOAP Analysis

The selected saturate and aromatic fractions were analyzed further using GC×GC to identify and quantify individual hydrocarbon components, as discussed in the following section.

Figure 8 presents the compositional information limited to hydrocarbon types reported by SOAP analysis (i.e., saturates and aromatics) for comparison purposes with Figure 7. We find relatively good agreement between the hydrocarbon compositions reported by SOAP and GC×GC-FID—with an exception for very light naphtha samples (such as sample 2, which is MP-30, D-535), for which the SOAP analysis is not as accurate as GC methods.

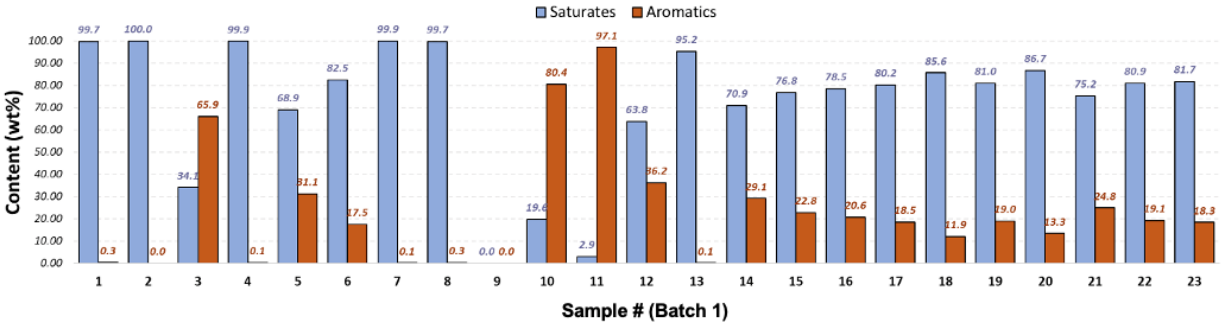

Figure 8. GC×GC-FID results for Batch 1 samples. Only the saturate and aromatic contents are plotted. Sample 9 contains 100% FAMEs. Abbreviations: FAME = fatty acid methyl ester; FID = flame ionization detector; GC×GC = two-dimensional gas chromatography; wt% = weight percent.

Figure 9 presents GC×GC-FID chromatograms for Batch 1 samples (Table 5). Similar chromatograms were obtained for Batch 2 samples (Table 6) but are not included in this report for the sake of brevity.

Figure 10A exclusively shows the content of polar compounds, specifically FAMEs, in blends of Petroleum #2 Diesel with Biofuel HPR. This allows for a clear observation of the trend between the amount of Biofuel HPR and the FAMEs content in the blends (Figure 10B), which can be used as a calibration curve for determining the renewable content in these or similar blends.

The quality of the SOAP separation into saturates and aromatics was further validated using “reverse-phase” GC×GC-FID analysis. Figure 11 presents the GC×GC-FID chromatograms of the saturate and aromatic fractions of two selected samples. It is evident from Figure 11 that the separation was successful, as there is no indication of cross-contamination between fractions; aromatics do not appear in the saturates, and vice versa.

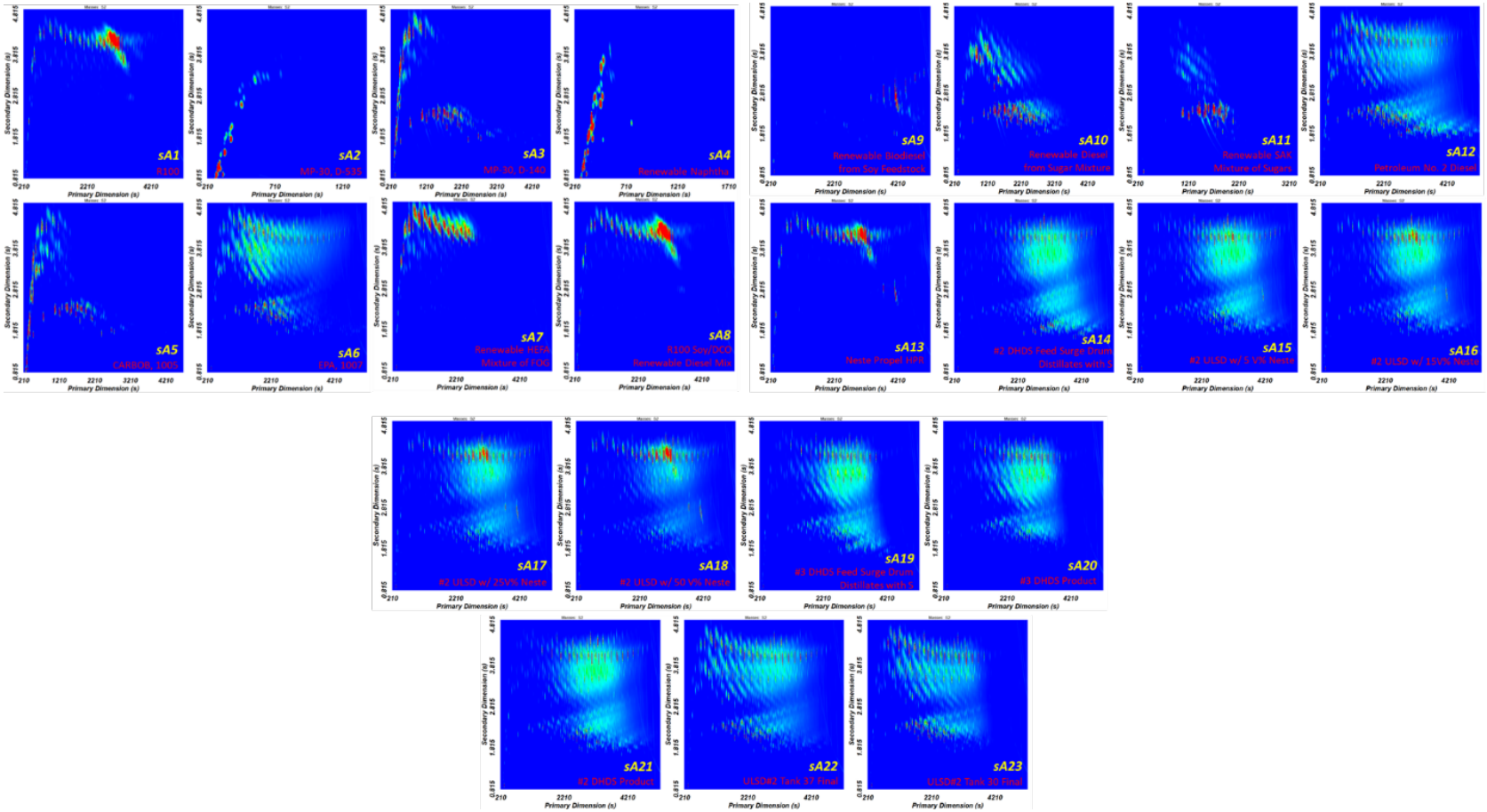

Figure 9. A “reversed phase” GC×GC-FID contour plot of Batch 1 samples. The number in yellow represents the sample number. The *x*-axis represents the retention time on the primary column (in seconds), while the *y*-axis shows the retention time on the secondary column (in seconds). The color intensity illustrates the signal intensity, with blue representing the baseline and red representing the most intense peaks in the chromatogram. Sample identification numbers can be found in Section 5.1, Table 5. Abbreviations: CARBOB = California Air Resources blendstock for oxygenate blending; DCO = distillers corn oil; DHDS = diesel hydrodesulfurization; EPA = U.S. Environmental Protection Agency; FID = flame ionization detector; FOG = fats, oils, greases; GC×GC = two-dimensional gas chromatography; HEFA = hydroprocessed esters and fatty acids; HPR = high performance renewable; R100 = 100% renewable fuel; SAK = synthetic aromatic kerosene; ULSD = ultra-low sulfur diesel; V% = volume percent.

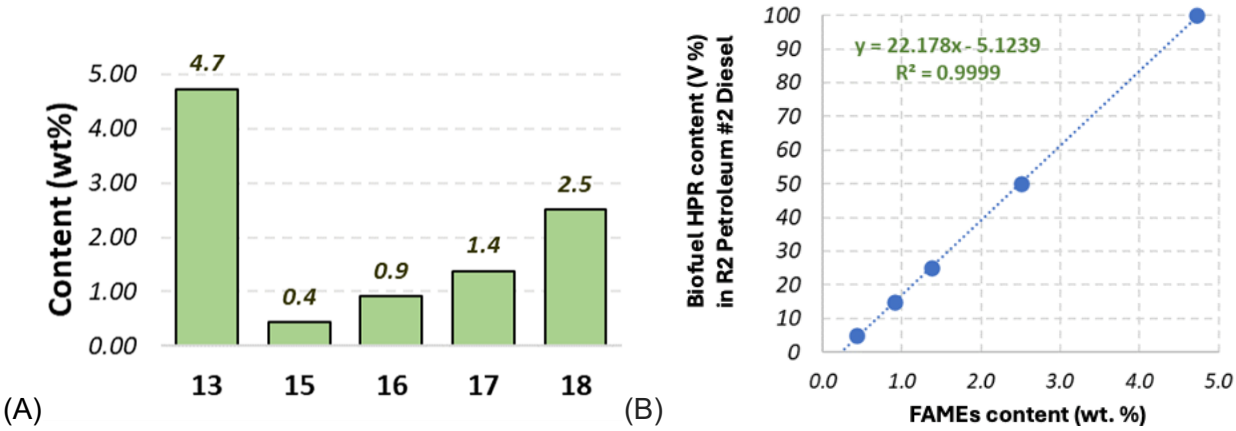

Figure 10. A) FAMEs content in selected Batch 1 samples analyzed by GC×GC-FID, B) correlation between FAMEs content and Biofuel HPR content (R3) in Petroleum #2 Diesel (R2). Abbreviations: FAME = fatty acid methyl ester; FID = flame ionization detector; GC×GC = two-dimensional gas chromatography; HPR = high performance renewable; R2, R3 = refiner 2, 3; V% = volume percent; wt. %, wt% = weight percent.

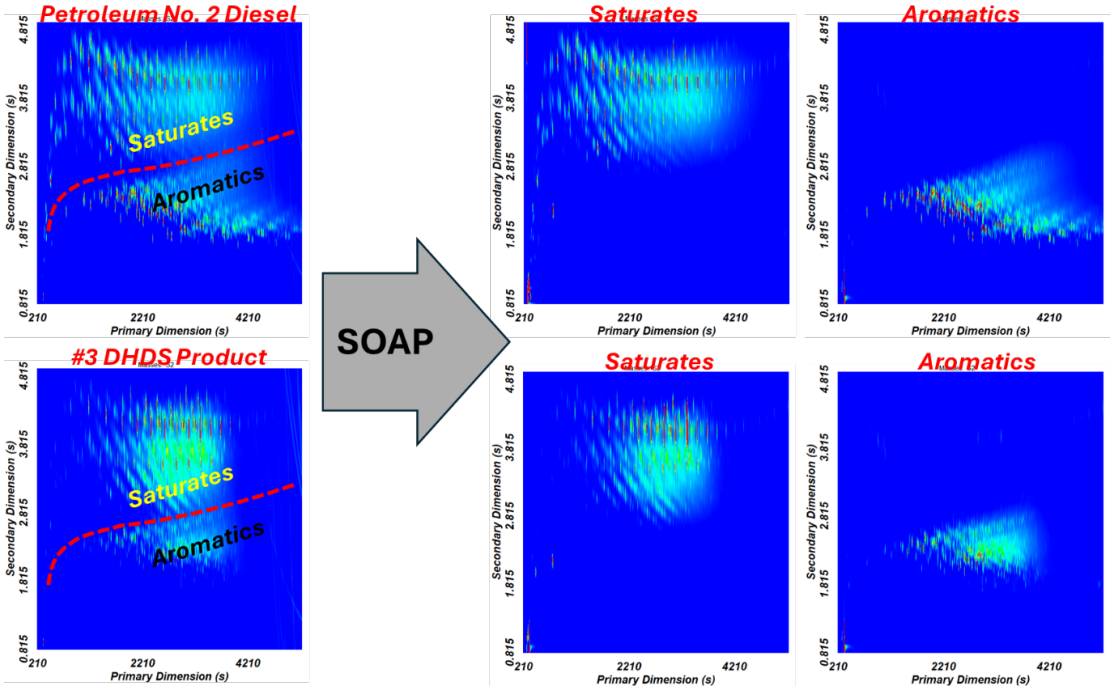

Figure 11. GC×GC-FID chromatograms of selected samples Petroleum # 2 Diesel (upper panel) and HDS #3 Product (lower panel) before and after SOAP analysis. Abbreviations: DHDS = diesel hydrodesulfurization; FID = flame ionization detector; GC×GC = two-dimensional gas chromatography; HDS = hydrodesulfurization; s = second(s); SOAP = saturate, olefin, aromatic, and polar fractions.

Task 4a Outcome Assessment:

Proposed: Sample sets separated into fractions based on a separation approach.

Final: Fuel samples were sent to CanmetENERGY, and solid-phase extractions were performed. Sample characteristics vary widely in terms of hydrocarbon composition and volatility, and different analytical techniques were used to separate fuels into BP ranges, chemical classes, and fractions. GC-FID provided an evaluation of the bulk fraction content for each sample (Figure 11, GC-FID results for SOAP). Samples were also analyzed by normal-phase GC×GC and reverse-phase GC×GC coupled with FID to quantify hydrocarbons, fraction content, and BP distribution. Light naphtha samples were also separated by PIONA separation using a GC-VUV detector. The three methods were compared for the more challenging, light samples and are in good agreement. Further work includes comparing the $\delta^{13}C$ values from different fractions from co-processed fuels and blended fuels with percent biocarbon values provided by GC-used separation methods for samples that span a small difference in percent biocarbon.

2.4.2 Bulk and Compound-Specific IRMS Analyses of Saturates and Aromatics (Task 4b)

Sample fractions were analyzed for bulk ^{13}C and compound-specific ^{13}C to evaluate how separations can aid in estimating the percent biogenic carbon of co-processed fuels. Example analyses for a set of co-processed fuels from R3 are used to illustrate the resulting observations (Appendix B, Figure B.3).

2.4.2.1 EA-IRMS Analysis of Select Fuel Samples

Figure 12 shows the variation in the ^{13}C values for bulk samples and the corresponding bulk aromatic and saturate fractions of those samples (Appendix B, Figure B.3). Samples include the fossil feed (#3 HDS Feed Surge Drum), biofeed (#3 HDS Bio-Feed, Tallow-based biofeed), and co-processed fuels (Products 1, 2, and 3). For Product 1, the isotopic separation between the aromatic and saturate fractions of the fossil feed (ca. 1.2‰) is slightly smaller than that of the resulting co- ^{13}C value of each whole sample falls between that of the fractions. The tallow-based biofeedstock was assumed not to ^{13}C range found in Product 1 (versus that in its corresponding fossil feedstock) most likely results from the incorporation of carbon from the tallow-based biofeed into the product, as can be observed by ^{13}C value for the Product ^{13}C value ^{13}C value for the aromatic fraction would require additional analyses not undertaken here. This trend is observed for the fossil feed and Product 3 fractions. Product 2 did not appear to represent the same trend and was reanalyzed to rule out instrument performance errors. ^{13}C values of Product 2 still did not follow the same pattern as the other sample sets.

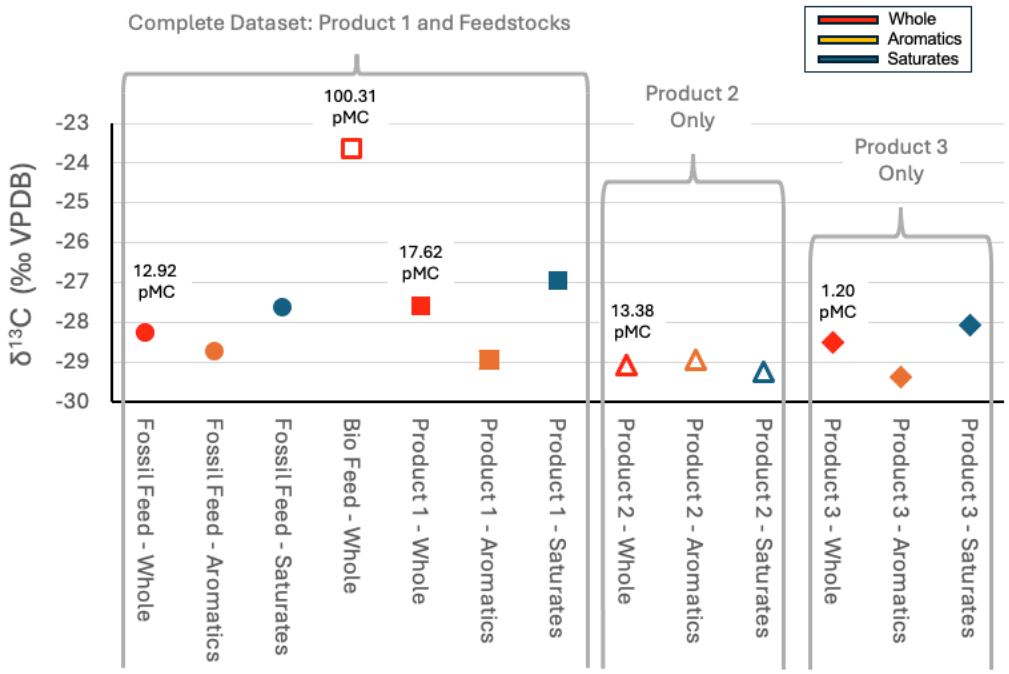

Figure 12. EA-IRMS analyses of select R3 samples described in Appendix B, Figure B.3. Marker shapes are the same for datapoints derived from a single fuel or feedstock. When available, the pMC values for whole feedstocks and fuel products are noted above the respective markers. The estimated percent biocarbon for products were supplied by the refiner and are as follows: Product 1, unknown; Product 2, ~15%; Product 3, ~1.5%. Note that the sample assigned as "fossil feed" has a renewable carbon component as determined by AMS analysis (12.92 pMC), indicating a clear biogenic component in this end-member. Abbreviations: AMS = accelerator mass spectrometry; $^{13}C = ((R_{sample} / R_{standard}) - 1)) \times 1000$, in per mil (‰) where R = $^{13}C/^{12}C$ ratio; EA = elemental analyzer; IRMS = isotope ratio mass spectrometry; pMC = percent modern carbon; R3 = refiner 3; VPDB = Vienna Peedee Belemnite.

In general, replicate measurements of fractions tended to have a larger standard deviation (0.41‰ ± 0.17‰, range from ±0.20‰ to ±0.66‰) than that of whole fuels (0.11‰ ± 0.13‰, range from ±0.04‰ to ±0.38‰). Potential reasons for why the standard deviations of these samples were higher could be the sample preparation methodology (i.e., a smooth-sided tin capsule sealed in atmosphere and evaporation of solvent), poor combustibility of aromatics, and high instrument pressure resulting in reduced peak stability.

Products 2 and 3 were processed with what were purported by the refiner to be different ratios of tallow-based feed to fossil feeds, as well as potentially different tallow-based biofeedstocks, but represent similar co-processing parameters. Both products have a lower percent modern carbon (pMC) than estimated from the blend ratio supplied by R3. AMS-determined pMC values for the products are listed in Figure 12, and the pMC values for the biofeed and fossil feed are 100.31% and 12.92%, respectively. AMS values for each of the three whole products are listed above each product.

While the ^{13}C value of the biofeed is only ca. 5‰ less negative than the fossil feed ^{13}C value, the biogenic carbon blend ratios are known to be low; therefore, the products are more similar to

the fossil feed. This is confirmed by the AMS results with Product 1 (17.62 pMC) being close to the fossil feedstock value of 12.92 pMC.

2.4.2.2 GC-C-IRMS Analysis of a Fuel Sample Separated Using SOAP

Sample fractions of Product 1 presented in Figure 13, Figure 14, and Figure 15 were analyzed via gas chromatography–combustion isotope ratio mass spectrometry (GC-C-IRMS) to further ^{13}C values between a co-processed fuel and the fossil and biogenic feedstocks.

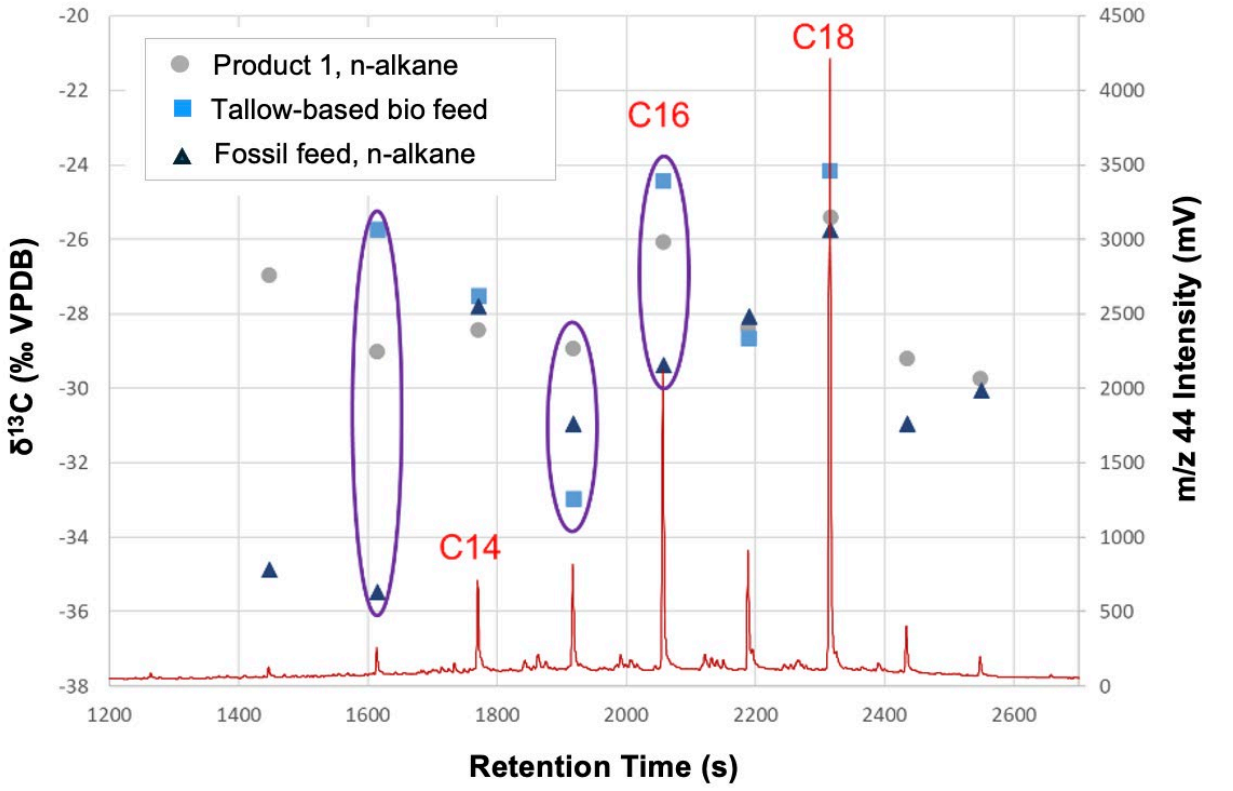

Figure 13. Peak-specific ^{13}C values of n-alkanes from feedstocks and the resultant co-processed fuel product alongside a representative GC trace. GC-C-IRMS analyses of a select sample separated by SOAP, showing the differences in stable isotope ratios for select n-paraffin peaks. Purple ovals highlight examples of larger variations (i.e., ranges in ‰) between the fossil feed and biofeed used to produce Product 1 (e.g., R3, #3 HDS Product). Carbon numbers are listed over n-paraffin carbon chains of lengths C14, C16, and C18 to provide a visual reference. The GC trace of Product 1 is displayed as a red line as the m/z 44 output (m/z representing CO_2 of isotopic composition $^{16}O^{12}C^{16}O$) from the IRMS in milliVolts (mV; right *y*-axis). Abbreviations: C = combustion; $^{13}C = ((R_{sample} / R_{standard}) - 1)) \times 1000$, in per mil (‰) where R = $^{13}C/^{12}C$ ratio; GC = gas chromatography; HDS = hydrodesulfurization; IRMS = isotope ratio mass spectrometry; R3 = refiner 3; s = second(s); SOAP = saturate, olefin, aromatic, and polar fractions; VPDB = Vienna Peedee Belemnite.

Figure 13 ^{13}C values of individual n-alkane peaks from the paraffin/saturate fraction. The GC trace of Product 1 (i.e., R3 HDS #3 Product) is displayed as a red line with a signal intensity reported in units of milliVolt(s) (mV) from the IRMS. N-alkanes with even carbon numbers (C14, C16, C18) and a peak intensity >500 mV are labeled for visual reference, while n-alkanes with odd carbon numbers are not labeled. The n-alkane peaks are separated by the retention time—the time it takes a molecule to travel through the GC, the combustion reactor, and into the IRMS— ^{13}C values of the bio and fossil feedstocks and the co-processed fuel as a whole are overlaid on the corresponding n- ^{13}C values for the feedstocks and co-processed fuel are found to be different for the different n-alkanes. In addition, the range between the ^{13}C values of these samples (e.g., the difference in ^{13}C values between bio and fossil feedstocks, as well as the whole product) varies with each n-alkane. Notably, these compound-specific differences can have a greater or smaller range than those presented in the previous section. For example, where the bulk analysis of each component Product 1, Product 1 Aromatics, and Product 1 Saturates was found to have a range of ca. 2‰ ^{13}C values of whole end-member feedstocks vary by ca. 4‰ (Figure 12), and individual n- ^{13}C values that can range up to 10‰. Interestingly, the Product 1 value for C15 is not within the ^{13}C range bound by the end-members. This may reflect a difference in how the hydrotreating process changes the carbon makeup of the sample.

Immediate next steps to further define the use of n-alkane isotopic content would be the evaluation of compound- ^{13}C values for feedstocks and co-processed products across a range of blend ratios using the same co-processing parameters. Additionally, a more robust statistical study for the compound-specific values returned by the GC-C-IRMS method would permit a better understanding of the significance of these results.

Figure 14 is the same chromatogram as presented in Figure 13 but specifically highlights the ^{13}C values of the iso/cyclo-paraffin peaks, generally found to elute between n-alkane peaks. Due to their low abundance/small peak size and lack of baseline resolution between individual iso/cyclo-paraffins, we report the ^{13}C values of a combined integration encompassing the suite of co-eluting peaks. The refinement of sample preparation methods combined with the optimization of GC separation methods would likely improve the signal-to-noise ratio, peak separation, etc., removing the necessity of grouping the peaks. ^{13}C values of the feedstocks and the co-processed fuel are overlaid on the corresponding iso/cyclo-paraffin series of peaks between the larger n-alkane peaks, and data points compare similar series of iso/cyclo-paraffin peaks across the run.

While it might be expected that the ^{13}C values of the products would fall between the end-members, much as a blended sample, this may not be the case for a co-processed sample, depending upon the nature of the co-processing step. During co-processing, changes to the molecular structure can occur that result from portions of more than one molecule combining to form the product. These changes depend upon the co-processing process, the catalyst, and process conditions, as well as the identity of the underlying feedstocks. Compound-specific IRMS may shed some light on altering these process variables to favorably include biogenic carbon in the desirable fractions of a product stream. Strong conclusions for the iso/cyclo-paraffin peaks cannot be made without further work to understand whether these small signals can be reliably grouped or a better method developed to enhance the intensity of these peaks. However, the more intense peaks of the n-paraffins, shown in Figure 13, suggest that the ^{13}C value of the product does not necessarily fall between those of the feedstocks, although additional work is needed to show this conclusively.

As with the n- ^{13}C values of the iso/cyclo-paraffins series for the feedstocks and co-processed fuel indicate that there is variation across compounds, both for an individual sample and between samples. The ranges ^{13}C values of these samples appear to span as great as ca. 10‰ — a larger range than when considering the bulk, whole samples and bulk fractions, as was observed in Figure 12. However, caution needs to be exercised when evaluating these results as the samples pushed the IRMS capabilities to or below their operational windows. Many of the individual compounds identified were below the linear range of the instrument, which may introduce analytical errors and add to uncertainty in the results. For example, the iso/cyclo-paraffin peaks were all below the amplitude needed for accurate isotope measurement, had indications of co-elution between peaks, and (in large part owing to their small size) had a very low signal-to-noise ratio in comparison to backgrounds. Still, many of the n-alkane peaks fell within a reasonable size window for analysis with results indicating a degree of complexity beyond the simple mixing of two sample types and that the co-processing methods employed may induce carbon exchange between compounds. Future method development is needed in this area to improve the signal intensity and help more thoroughly evaluate the complex carbon dynamics at play. As for the n-paraffin analysis, additional work is needed to understand whether there is statistical significance for results related to these groupings of peaks.

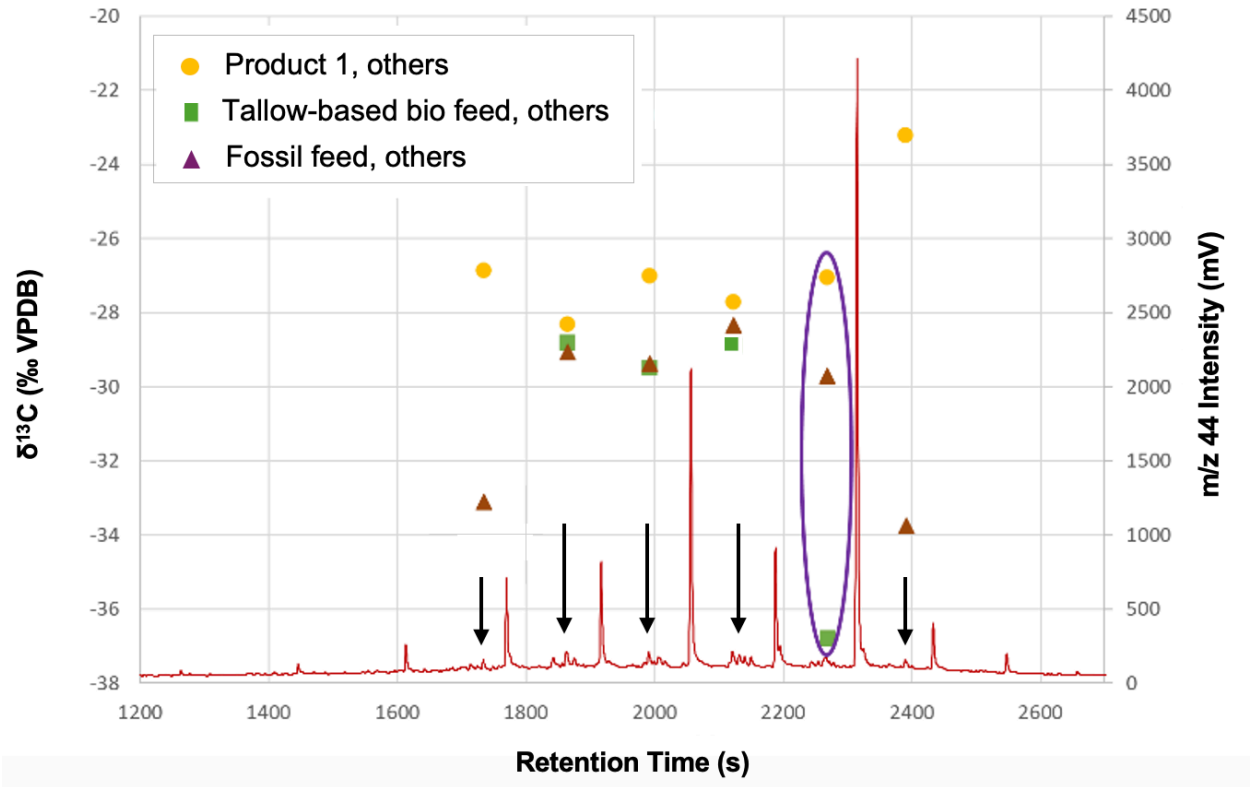

Figure 14. ^{13}C of combined iso/cyclo-paraffins for feedstocks and the resultant co-processed fuel product alongside a representative GC trace. GC-C-IRMS analyses of a select sample separated by SOAP, showing the differences in stable isotope ratios for select iso/cyclo-paraffin peaks. The purple oval highlights an example of larger variation (i.e., range in ‰) between the fossil feed and biofeed used to produce Product 1 (i.e., R3, #3 HDS Product) within the iso/cyclo-paraffin component. The GC trace of Product 1 is displayed as a red line as the m/z 44 output from the IRMS

in milliVolts (mV; right *y*-axis). The black arrows indicate the series of peaks between n-alkanes that were combined to provide $\delta^{13}C$ values represented by the symbols in the legend. Abbreviations: C = combustion; $\delta^{13}C = ((R_{sample} / R_{standard}) - 1)) \times 1000$, in per mil (‰) where R = $^{13}C/^{12}C$ ratio; GC = gas chromatography; HDS = hydrodesulfurization; IRMS = isotope ratio mass spectrometry; R3 = refiner 3; s = second(s); SOAP = saturate, olefin, aromatic, and polar fractions; VPDB = Vienna Peedee Belemnite.

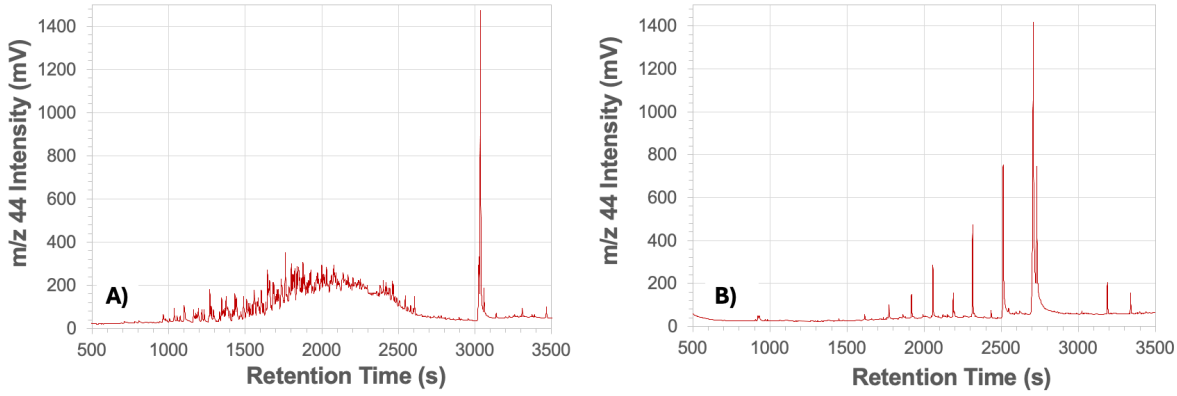

Figure 15. GC traces from the GC-C-IRMS system for A) the aromatic fraction of Product 1 (i.e., R3, #3 HDS Product) and B) saturates from a tallow-based biofeed. The GC traces are displayed as red lines, and the peak intensity is denoted as the m/z 44 output from the IRMS in milliVolts (mV; *y*-axes). The aromatic fraction is representative of other aromatic fractions from fuel samples, where numerous compound peaks are not easily separated and sit upon an elevated background "hump" (A). In comparison, the peaks of individual compounds from n-paraffins from saturate fractions are more easily distinguishable, as peaks are separated and there is a lower background signal (B). Abbreviations: C = combustion; GC = gas chromatography; HDS = hydrodesulfurization; IRMS = isotope ratio mass spectrometry; R3 = refiner 3; s = second(s).

Compound-specific data from aromatic fuel fractions show the variation between feedstocks and the resulting co-processed fuel (Figure 15). These samples were run via GC-C-IRMS utilizing the same analytical method as that for the paraffin fraction. While this method separated saturate fraction compounds well, aromatic fractions were more complex and incorporated a background "hump," similar to what is seen in GC traces from diesel fuel. Aromatic fractions were analyzed for $\delta^{13}C$ values; however, further detailed investigation is needed to evaluate the potential utility for biocarbon quantification to determine the possibility of removing the "hump" from the aromatic compound peaks or to leverage information contained in the "hump" to provide additional sample information. As part of this investigation, an alternative GC-C-IRMS method may need to be developed to better separate peaks and enhance the intensity of the m/z 44 signal to accurately and reproducibly determine $\delta^{13}C$ values and identify specific compounds for comparison between samples.

N-alkanes from saturate fractions were evaluated for compound-specific $\delta^{13}C$ values for blends of a co-processed diesel (R3, #3 HDS Product) and fossil diesel (R2, Petroleum #2 Diesel). The range in $\delta^{13}C$ values for the bulk $\delta^{13}C$ values of the two end-members is ca. 1.7‰. The initial evaluation of individual n- $\delta^{13}C$ values indicates that additional work is needed to assess the differences between fuels and blends. An unaccepted analytical result is that the $\delta^{13}C$

values of the blends did not fall between the ^{13}C values of the end-members. Much like the aromatic fractions and iso/cyclo-paraffins discussed above, compound peaks from blended samples were below the amplitude (mV) needed for accurate isotope measurement. Enhanced analytical error likely added to the uncertainty in the results. Factors influencing the uncertainty can result in largely obscuring data trends when the range of ^{13}C values is small, such as for these samples, meaning substandard analytical conditions. An additional consideration is that the samples may have been subjected to aging due to being held at the Canada–U.S. border for several months in ill-suited vials. These sample sets require additional analyses with peak amplitudes within the instrument's linear range and with a low background to assess compound-specific trends from these blends.

Task 4b Outcome Assessment:

Proposed: (1) Comparison of each fraction and the sum of sample fractions with the results from Task 3. (2) Assessment of the biogenic carbon distribution by fraction based on process conditions, renewable feedstock, etc.

*Final: The $\delta^{13}C$ values of product and feedstock fractions provide additional information that cannot be obtained from the $\delta^{13}C$ values of bulk samples alone (**Figure 12**). Instead of a single data point, incorporating a bulk analysis of fractions by compound class provides an increased range of $\delta^{13}C$ values, with the $\delta^{13}C$ value of the bulk sample laying between that of the aromatic fraction (more negative $\delta^{13}C$ value) and the saturate/paraffin fraction (more negative $\delta^{13}C$ value). The range between the fuel fractions is larger for the product than they are for the fuel feedstock, potentially indicating the incorporation of biocarbon preferentially in the saturate fraction. However, this relationship requires additional analyses for fractions of co-processed fuels originating from the same feedstocks and experiencing the same processing parameters. Ideally, these measurements would be compared with percent biogenic carbon data provided by AMS measurements.*

Initial analyses (GC-C-IRMS) demonstrate variations among the $\delta^{13}C$ values of fuel and feedstock paraffin/saturate fractions for individual n-alkanes, suggesting a variable distribution of biocarbon for co-processed fuels across a range of compounds. Additional analyses of fuel fractions from feedstocks and blended and co-processed fuels are needed to better evaluate the distribution of biocarbon and estimate the percent biocarbon in different fractions. This analytical method could also be assessed for the potential to use a single compound to track precent biogenic carbon instead of the need to analyze each component. If so, the time needed for analysis could be decreased.

Time, resources, and sample variety/availability did not allow an assessment of the biogenic carbon distribution by fraction based on different factors (e.g., processing conditions, renewable feedstock type). To assess the biogenic carbon distribution, sample sets must include all fractions for any single processing operation, including feedstocks going in and products produced (i.e., all gas, liquid, and products). Additional work on the biogenic carbon distribution is reliant upon sample sets supplied by industrial partners.

2.5 Comparative Calculations and Analysis, and Consultation (Task 5)

PNNL and LANL coordinated to analyze the same samples, a subset of the total sample set. In Section 2.5.1, data are compared to evaluate approaches for ^{13}C values for liquid fuel samples. In Section 2.5.2, the percent biocarbon values from ^{14}C radiocarbon counting via

AMS were compared with estimates of percent biocarbon values calculated from the ^{13}C values measured at PNNL. These sets of comparison provide the foundation to assess which methods are appropriate for preparing and analyzing liquid fuel samples for the ^{13}C composition, provide an accurate estimate of the percent biocarbon, and allow the evaluation of ^{13}C values to help enhance the inclusion of biocarbon in co-processed fuels.

2.5.1 Interlaboratory Comparison of Isotopic Values from the Same Samples (Task 5)

^{13}C analyses for two sets of blend samples to compare sample analyses and data processing methodologies. The liquid fuel samples analyzed at LANL were loaded in tin capsules, which were then sealed within an argon environment before analysis via EA-IRMS. In contrast, samples analyzed at PNNL were directly injected into the EA-IRMS system. Samples at both LANL and PNNL were analyzed using a Delta V IRMS (i.e., equivalent precision) via continuous flow sample introduction. ^{13}C values provided by PNNL and LANL are listed in Table 4 and plotted in Figure 16. The larger variability observed around LANL replicates may be related to sample properties or preparation, along with potential sample aging, since LANL analyses were not carried out until later in the project. An analysis was conducted to check for statistically significant differences in the intercept (offset) or slope between the linear models used to describe the data from both laboratories. No differences were found between the two datasets (intercept or slope) at the 95% significance level, indicating that no statistically significant differences exist between the PNNL and LANL results.

Table 4. Com ^{13}C values from PNNL and LANL for R3 #3 Product blends and R2 Renewable Sugar Mixture Diesel (Renew Sugar) blends. Both fuels were blended with Petroleum #2 Diesel fossil fuel from R2.

Sample ID	Weight percent biocarbon-based fuel	PNNL Avg. ^{13}C (‰ VPDB)*	PNNL ^{13}C ±1σ stdev	# Repli-cates	LANL Avg. ^{13}C (‰ VPDB)	LANL ^{13}C ±1σ stdev	# Repli-cates
R2 Petroleum #2 Diesel for HDS R3 #3 Product blends	0.00	29.38	0.03	3	29.51	0.07	3
R3 7.5% HDS #3 Product	7.36	29.21	0.04	4	29.28	0.04	3
R3 50% HDS #3 Product	50.12	28.48	0.05	3	28.54	0.06	2
R3 100% HDS #3 Product	100.00	27.68	0.03	3	27.66	0.01	3
R2 1% Renew Sugar	1.05	29.07	0.08	2	29.10	0.02	3
R2 2.5% Renew Sugar	3.02	28.65	0.04	4	28.56	0.20	3
R2 3a Blind Blend Renew Sugar	3.60	28.55	0.06	3	29.28	0.07	3
R2 5% Renew Sugar	5.43	28.22	0.08	3	28.10	-	1

Sample ID	Weight percent biocarbon-based fuel	PNNL Avg. ^{13}C (‰ VPDB)*	PNNL ^{13}C ±1σ stdev	# Repli-cates	LANL Avg. ^{13}C (‰ VPDB)	LANL ^{13}C ±1σ stdev	# Repli-cates
R2 14% Renew Sugar	14.16	26.51	0.05	3	26.68	0.06	3
R2 60% Renew Sugar	59.34	18.15	0.02	3	18.25	0.17	2
R2 100% Renew Sugar	100.00	10.85	0.06	3	10.68	0.07	3

* Fuel-like standards were used to normalize data. The typical repeatability of standards ranges from ±0.05‰ to 0.09‰ with 5 to 9 replicates per run session.

Abbreviations: $^{13}C = ((R_{sample} / R_{standard}) - 1)) \times 1000$, in per mil (‰) where R = $^{13}C/^{12}C$ ratio; HDS = hydrodesulfurization; LANL = Los Alamos National Laboratory; PNNL = Pacific Northwest National Laboratory; R2, R3 = refiner 2, 3; stdev = standard deviation; VPDB = Vienna Peedee Belemnite.

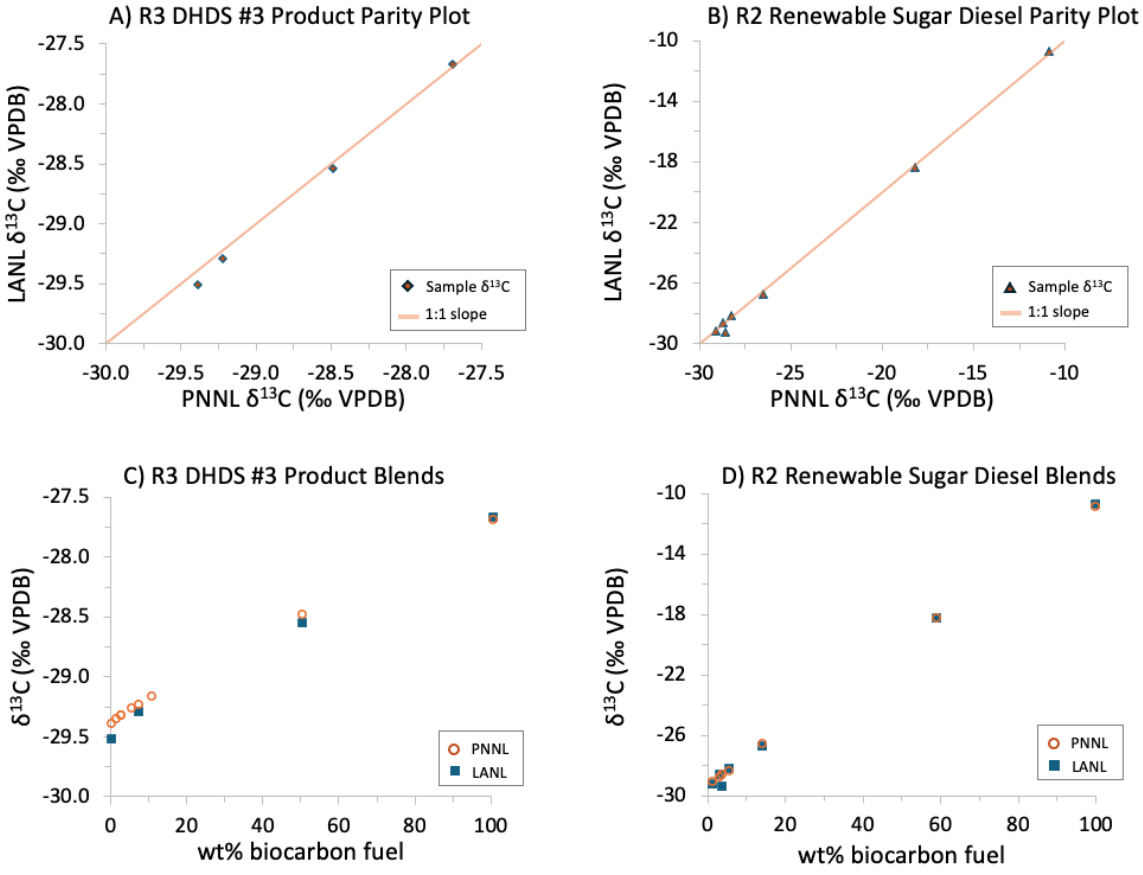

Figure 16. A) ^{13}C values from PNNL and LANL. Blended fuels represent weight percent (wt%) biocarbon-containing fuel with respect to a fossil fuel for blends from 0% to 100%, focusing on the range from 0% to 10%. The ^{13}C values are compared and plotted alongside a red line having a 1:1 slope ($y = x$). Perfect agreement between the results would fall on this line. C) and D) directly compare the ^{13}C values from PNNL and LANL. Data points are plotted against blend levels for PNNL and LANL. Note that only select data have been analyzed at LANL due to

timing constraints. Abbreviations: $^{13}C = ((R_{sample} / R_{standard}) - 1)) \times 1000$, in per mil (‰) where $R = {}^{13}C/{}^{12}C$ ratio; DHDS = diesel hydrodesulfurization; LANL = Los Alamos National Laboratory; PNNL = Pacific Northwest National Laboratory; R2, R3 = refiner 2, 3; VPDB = Vienna Peedee Belemnite.

The samples measured at PNNL and LANL are blends and represent end-member fuels that ^{13}C values across the blended fuels. The blend curve sample sets analyzed at both PNNL and LANL revealed a slight quadratic curve across the sample sets. The strongest nonlinear trend is observed for samples with low biocarbon fuel blend ratios, as is observed in Figure 16 as data points falling further off the 1:1 slope, $y = x$ (Figure 16A and Figure 16B), ^{13}C values (Figure 16C and Figure 16D). Both sets of blends require further analysis. Differences between the LANL and PNNL results may reflect challenges with sample handling and the potential for aging resulting from the widely different vapor pressures of the end-members and the resulting mixtures. Sample property differences may contribute to an elevated analytical uncertainty for some samples, which would be reflected, sometimes, in numerical differences between the two laboratories. Further sample exchanges and an increased number of replicates may relieve these differences or provide an indication of interlaboratory reproducibility of these complex measurements. A more detailed description of the blend curves and associated nonlinearities is provided in Appendix D.

The results from both labs indicate a stronger, though still slight, quadratic curve at low blend ratios for samples analyzed at LANL. While LANL samples had a slightly larger quadratic curve at low blend ratios, no sample loss was observed due to evaporation, as the recovery rate of carbon content (%) remained consistent (85% C); however, more analyses must be done to determine the origin and influence of the quadratic curve. The differences ^{13}C values between the labs could be related to sample preparation and sample aging. Samples at PNNL were directly injected into an EA-IRMS system from a septum-capped GC vial to avoid any vapor release. Samples at LANL were taken from an uncapped GC vial, potentially releasing volatile components. While samples were analyzed soon after blending at PNNL, samples analyzed at LANL were analyzed only after shipment, which may have resulted in aging. In addition, samples analyzed at PNNL were corrected using matrix-matched standards developed at PNNL; however, there were insufficient time and resources to make use of these standards during analyses performed at LANL.

Analyzed samples were targeted to 0%–10% biocarbon fuel blends but also covered the full range from 0%–100%. An overall comparison of the results obtained at PNNL and LANL suggests that both laboratories were able to produce strikingly similar values ^{13}C for each sample. Both labs produced replicate data from samples with a relatively high reproducibility using Thermo Delta V IRMS. Volatile and semi-volatile fuels would likely have a higher reproducibility if analyzed on higher resolution instrumentation (e.g., Thermo MAT 253), as indicated in (Geeza et al., 2020). However, the ability to produce replicates with the highest reproducibility is also reliant on the volatility. Samples with greater volatility, such as naphtha and naphtha blends, were not analyzed for ^{13}C values at both labs due to the timing and the need for further assessment to determine if direct-injection and argon purging methods are equivalent for volatile samples.

The argon purging method applied at LANL is an effective technique for oils and semi-volatile samples (e.g., co-processed products) and allows for accurate quantification of carbon content (Geeza et al., 2020). As a future consideration, the direct-injection method removes the sample preparation time that is needed to flush the tin capsules with argon, weigh liquid samples into

the tin capsules, and seal the capsules before opening an autosampler, loading the tin capsules, and pumping the atmosphere out of the EA-IRMS system before running. Within a refinery setting, a fuel sample could be analyzed immediately via direct injection. While PNNL utilized a manual injection method, a more automated method could quickly be developed using an automated injection system that injects samples and cleans the syringe and needle for the next sample. Further investigation is needed to assess whether the argon procedure used at LANL is also applicable for these sample types.

Additional work from several laboratories will be necessary to determine the repeatability and reproducibility statistics for analyzing liquid fuels using an EA-IRMS.

2.5.2 Percent Biocarbon Comparison Between ^{14} an ^{13}C for Co-processed and Blended Fuels and Feedstocks (Task 5)

The percent biocarbon of blended samples based on radiocarbon (^{14}C) measurements using the industry standard ASTM D6686-24 via AMS was acquired for select samples. The percent biocarbon was also ^{13}C values analyzed via direct-injection EA-IRMS. Figure 17A shows that across the series of blends, percent biocarbon estimates are similar and fall on or near the parity line ($y = x$) ^{13}C values determined from the direct-injection EA-IRMS method estimate the percent biocarbon in a manner that is comparable to those acquired by the ASTM-D6866 method using ^{14}C counting via AMS (ASTM 2020). Figure 17B highlights the variations in the estimates for blends with ca. 2% biocarbon. Samples with <0.44 pMC (%) are reported as having 0% biocarbon using AMS, in accordance with the methods applied by Beta Analytics. Percent biocarbon estimates calculated ^{13}C values are not so constrained, which is why two points have “zero” values for the *x*-axis, percent biocarbon from the ^{14}C measurements ^{13}C values can be used to evaluate the differences in the percent biocarbon for a small variation within a range that is not currently reportable using AMS.

The data presented in Figure 18 consider the percent biogenic carbon (as pMC) for feedstock blends and the co-processed products produced from these blend stocks. Feedstock blends were subjected to the same co-processing parameters to produce the fuel products. The biofeed component is landfill derived. The pMC and percent biocarbon data based on ^{14}C counting via AMS were supplied by the refiner for the feedstock blends and co-processed products. In addition, the pMC and percent biocarbon estimates were calculated from ^{13}C measurements.

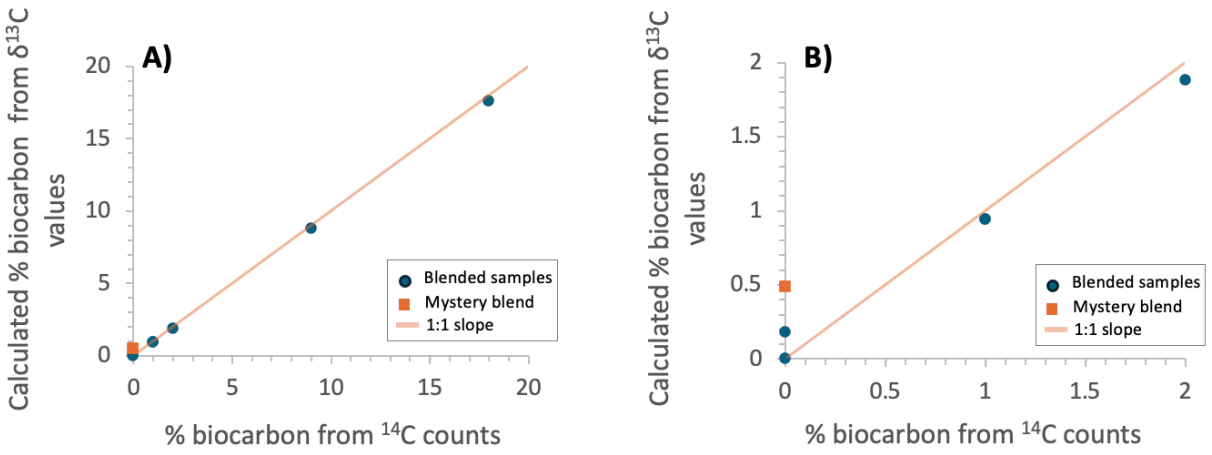

Figure 17. Comparison plots of the percent biocarbon determined from ^{14}C measurements and ^{13}C values. Blends are from co-processed R3 HDS #3 Product and R2 Petroleum #2 Diesel Blend samples and show data A) from the entire range of blends and B) focused on the lowest blend ratios. The orange line represents where data points would fall if the values from each method provided the same values. The biocarbon content of the blind blend (denoted as mystery blend) is <0.44 pMC as determined by the ^{14}C content via AMS and 0.49% as estimated by its ^{13}C value via IRMS. ^{13}C values range from 29.31‰ ± 0.02‰ to 27.68‰ ± 0.03‰, with the standard deviation of technical replicates of 0.08‰ (n = 3 to 4). Abbreviations: AMS = accelerator mass spectrometry; $^{13}C = ((R_{sample} / R_{standard}) - 1)) \times 1000$, in per mil (‰) where R = $^{13}C/^{12}C$ ratio; HDS = hydrodesulfurization; IRMS = isotope ratio mass spectrometry; pMC = percent modern carbon; R2, R3 = refiner 2, 3.

Parity data for both feedstocks (Figure 18A) and the co-processed products (Figure 18B) are plotted alongside a line having a slope of one, representing a 1:1 relationship ($y = x$) between the pMC provided by ASTM D6686 Method B and the pMC calculated from the ^{13}C values. Data points fall along the 1:1 slope, where feedstocks have a slope of 0.9993 and an intercept of 0.0046 and products have a slope of 1.0000 and an intercept of 0.0014. This suggests that the ^{13}C values can provide the estimated percent biocarbon at low blend ratios for feedstocks and co-processed products. Both the ^{14}C data and ^{13}C data provide percent carbon values that are greater in the feed blends than the corresponding fuels, indicating biocarbon was lost during processing.

The datapoint representing 16.05 pMC in Figure 18A (open square data point) is offset from the trendline and needs additional analysis as the offset is unexpected and could have been a result of a handling error, but is left in the dataset for completeness. Data for the 16.05 pMC sample were not used to define the model used to calculate the pMC from the ^{13}C values.

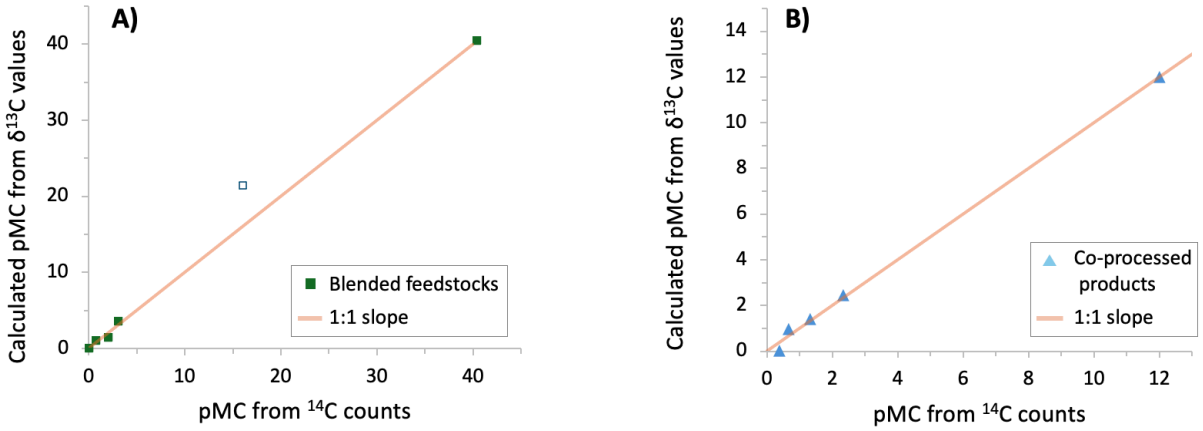

Figure 18. Parity plots comparing the ^{13}C with pMC data from ^{14}C data for A) different levels of biofeed blended with fossil feed and B) the co-processed fuel products from these blends. The parity data are plotted alongside a line having a 1:1 slope ($y = x$) for comparison. ^{13}C values from technical replicates of samples (n = 2 to 3) have a standard deviation of 0.25‰ ± 0.16‰ (±0.03‰ to ±0.50‰) for blended feedstocks and 0.17‰ ± 0.16‰ (±0.04‰ to ±0.41‰) for co-processed products. Abbreviations: $^{13}C = ((R_{sample} / R_{standard}) - 1)) \times 1000$, in per mil (‰) where $R = {}^{13}C/{}^{12}C$ ratio; pMC = percent modern carbon.

For the three datasets discussed above, there are no statistically significant differences between the values of percent biogenic carbon determined using IRMS and AMS (at the 0.05 level of significance). There is no offset, or constant difference, between the values obtained by the two approaches and no difference in the slope of each sample set. While samples were measured in replicates, additional samples and statistical analyses will help to better constrain the estimated biocarbon from these datasets. This will provide a more rigorous evaluation of the range of estimated percent biocarbon values compared with the standard ^{14}C dataset.

Task 5 Outcome Assessment:

Proposed: (1) Compare the variability of results based on lab, method, instrumentation, sample information, etc. (2) Corroborate results with provided or purchased AMS analyses. (3) Assess the accuracy, precision, and limit of detection of the IRMS method. (4) Assess the extensibility of LANL's biogenic carbon quantification approach to these widely different fuel sets, adapting as needed.

*Final: Interlaboratory comparisons indicate that the $\delta^{13}C$ values obtained by LANL and PNNL from the same fuel samples generally yielded similar values and therefore similar percent biocarbon estimates (**Figure 16**). Both labs noted slight quadratic curves across blend ratios, with a slightly stronger quadratic curve in the LANL data. To determine the influence(s) associated with the differences in the $\delta^{13}C$ values at low blend ratios, additional sample sets and sample blends need to be analyzed for each blend curve while using the sample, matrix-matched standards for correction. At this point, the influence of sample aging during the transport of samples to LANL from PNNL cannot be distinguished from blending errors or differences in the blended fuel characteristics. In addition, small differences between sample techniques, including a generally higher standard deviation (though slight) for the LANL technique, may influence fuels differently than oils, which were the sample type*

for which the technique was developed. All of these effects may influence the $\delta^{13}C$ values at low blend ratios.

Analytical techniques developed for distinguishing bulk fuels and fractions using $\delta^{13}C$ performed favorably in terms of length of time for a data point (≤2 hours), with the majority biogenic carbon content within 10% of the AMS-determined biocarbon composition. The blended feedstock set from landfill-derived material would benefit from additional analyses that account for the variation in the sample amount for the solid samples. A larger variation in sample size can result in less-precise average $\delta^{13}C$ values from technical replicates and a higher variability from $\delta^{13}C$ analyses, making a comparison of samples less precise. Some samples would have benefited from additional analyses, but project timelines and, in some cases, the later arrival of some samples precluded those analyses. However, the current data show strong proof-of-concept that good comparisons among techniques exist and that further analyses will improve the statistics for these measurements.

This study indicates that the direct injection of fuel into the EA-IRMS system produced similar reproducibility for replicate measurements as tin capsules sealed within an argon environment. Direct injection reduces the time needed for $\delta^{13}C$ analysis, as a fuel could be directly removed from a fuel stream, injected, and data provided within ca. 10 minutes. This method of sample introduction would allow for a streamlined analysis at the facility setting.

2.6 Reporting (Task 6)

Tasks and milestones were reported in quarterly reports, CRC AVFL-38 presentations, bi-weekly project meetings, and the American Chemical Society National Conference (2023). Outcomes are discussed in relation to the reported data within this report and outlined below.

Task 6 Outcomes Assessment:

Proposed: (1) The final deliverable from both parties is a report addressing the objectives and deliverables. (2) Distinguish samples and methods attaining favorable metrics (accuracy and precision within 10% of AMS in ≤2 hours). (3) Validate the LANL approach or an adapted approach for biogenic carbon quantification in renewable fuels.

Final: This report outlines the outcomes of the overall project by addressing the objectives and deliverables. Data indicate that the modified $\delta^{13}C$ technique for fuel samples developed at PNNL provides values that are comparable with the $\delta^{13}C$ technique developed at LANL. Estimates of the percent biocarbon calculated from the $\delta^{13}C$ values are well within 10% of the value from AMS, ASTM D6866. Samples analyzed by PNNL and LANL analytical methods both require less than 2 hours to analyze. Analytical improvements using fuel-like standards and additional analyses that provide better control of the sample amount could further improve the results for solid samples, such as LG blend stocks. The demonstration of direct-liquid injection into the IRMS port may further offer improvements in speed and reduce sample handling.

3.0 Next Steps

This project has explored the utility of evaluating the ^{13}C values from transportation fuels to track renewable carbon in products. In this report, we have discussed the successful quantification of low levels of renewable feedstock in blended and co-processed fuels by IRMS methods. We have demonstrated how these methods could help incentivize increased incorporation of renewable feedstocks into transportation fuels in a seamless manner that also enables scaling.

Initial r ^{13}C analysis to track the distribution of biogenic carbon across different/specific compounds, chemical class, or BP classification while obtaining a biogenic carbon balance for representative refinery conditions. However, the biogenic compositions of blended and co-processed fuel samples were not always known for the samples in this report. Additional work is necessary to quantify the biogenic carbon balance in fuel fractions of blended and co-processed fuels for samples and blend stocks with known origin and to provide data to complete a peer-reviewed publication.

The next steps needed to go beyond proof-of-concept include the following:

1. ^{13}C data from *class fractions* to provide additional data solidifying ^{13}C analysis in biogenic carbon quantification.
2. ^{13}C data of *specific compounds* from class fractions to provide additional data solidifying ^{13}C analysis in biogenic carbon quantification.
3. Analysis of the percent biocarbon via AMS (Beta Analytics) for analytical comparison and ^{13}C-derived calculations of the percent biocarbon from fractions.
4. ^{13}C data and AMS datasets to determine the variation and uncertainty for samples from focused studies to quantify the capability and limitation of the methods.
5. An interlaboratory comparison of the direct-injection EA-IRMS technique using manual and automated sample injection to evaluate the potential for the method to produce comparable data in other settings.
6. Further investigation of why some fuel blends have quadratic fits to determine if these fits are related to aging, volatility, sample handling, and/or the sample analytical technique.

^{13}C to assess the biogenic carbon content requires knowledge of the biogenic and fossil ^{13}C values to define the isotope range covered by the analysis. This is particularly ^{13}C ^{13}C values could be very small (e.g., <5‰ between fossil and C3 end-members).

Samples of known blend stocks and AMS biogenic quantification would be ideal to assess the use of fuel fractions to quantify the total carbon balance. Recently obtained samples are currently in house and include a series of blend stocks and co-processed fuels with AMS biogenic quantification. These samples have also been ^{13}C values. These samples, in addition to other previously supplied fuels and feedstock, will be analyzed for ^{13}C within each chemical class, utilizing sample processing and quality control techniques developed in the initial phase of the project, and an interlaboratory comparison will be conducted. The availability and acquisition of a larger number and greater variety of samples would allow calculation of the variability and precision estimates to establish, with a high level of

statistical significance, the capability and limitations of the method. Statistical analysis of the data will also allow the quantification of individual sources of uncertainty, pointing to where ^{13}C data would be compared to AMS percent biocarbon measurements of blend stocks.

This initial work will ^{13}C values using compound-specific datasets and GC-C-IRMS. This work will also allow for an interlaboratory comparison of sample handling and processing methods (e.g., direct-injection EA-IRMS) to evaluate the use of this capability in different settings/laboratories.

4.0 Conclusions

This project demonstrated progress towards using chemical separations in combination with stable isotope analysis to track the distribution of biogenic carbon across co-processed fuel streams, by compound, chemical class, or BP range, while obtaining a biogenic carbon balance for representative refinery conditions. Additional work with fuel fractions includes further refining the methods for analyzing ^{13}C values from fractions to allow for the evaluation of biogenic carbon. Furthermore, the biogenic compositions of blended and co-processed fuel samples were not always known for the samples presented in this report, and additional work is necessary to quantify the biogenic carbon balance in fuel fractions of blended and co-processed fuels for samples and blend stocks with known origin. To achieve accurate quantification, it will be essential to analyze samples representing individual processes (i.e., feedstocks and products) for which AMS data have been acquired.

This project consisted of six tasks with the goal of exploring the ^{13}C values of fuels and fuel fractions to broaden the capability of stable carbon isotope analyses for quantifying and tracking biogenic carbon in blended and co-processed transportation fuels. Having analyzed 49 samples and their fractions, we find that the analysis of ^{13}C via IRMS has the potential to provide percent biocarbon at low blend ratios at the precision and accuracy of AMS. To attain consistency across labs and within our own, we identified fuel-like standards to serve as reference materials. These were discussed in Sections 2.2 and 5.2. These sections also describe the use of direct-injection EA-IRMS as a feasible approach to introducing higher-volatility liquid samples into the IRMS. The use of ^{13}C values from fuels and feedstocks can at times be challenging due to the small range of ^{13}C values between feedstocks, blendstocks, and products, which can lead to less-precise percent biocarbon estimates, as was discussed in Section 2.3. However, this work suggests that there is potential to broaden the use of ^{13}C analyses via IRMS. By incorporating new sample processing methods and through the analysis of the ^{13}C signature of fuel fractions and specific compounds, the range of ^{13}C values between feedstocks, blendstocks, and products can be expanded and thereby provide the percent biocarbon with improved accuracy and precision. Proof-of-concept for using separations was discussed in Section 2.4. Section 2.5 discussed the results from a small interlaboratory comparison of IRMS results from LANL and PNNL, as well as a comparison of IRMS results to AMS results from ASTM D6866, Method B (ASTM 2020). Results from PNNL and LANL for the same samples are precise and statistically similar for blended fuels, even when the ^{13}C values between the blended end-member fuels were <1.7‰. The pMC values calculated from ^{13}C values via IRMS are statistically similar and within 10% of the pMC values provided by ^{14}C measurements using AMS (ASTM-D6866, Method B; ASTM 2020). This analytical method will benefit from interlaboratory comparison.

Successful quantification of low levels of renewable feedstock incorporation in co-processed fuels by the IRMS methods demonstrated here could help incentivize the increased incorporation of renewable feedstocks into transportation fuels in a seamless manner that also readily enables scaling. As additional data are accrued, the accuracy and precision of these techniques will be better understood, allowing refiners to adopt this approach for quantifying blended or co-processed biogenic components in their final products. Additionally, it is expected that these methods will gain acceptance with federal and state regulators, allowing petroleum refiners to make better use of tax incentives, leading to increased willingness to co-process more renewable feedstock, with guaranteed quality of infrastructure-compatible fuels, concomitantly stimulating production and availability of renewable feedstocks.

5.0 Experimental

5.1 Chemicals - Fuel Samples and Feedstocks

Samples were obtained via the CRC and the AVFL-38 Panel Members. These comprised samples of fossil-derived transportation fuels, gasoline, and diesel, produced in accordance with industry standards, and a wide variety of biogenic feedstocks from various sources.

The samples were provided to CanmetENERGY in two groups, labeled Batch 1 and Batch 2. Batch 1 consisted of 23 neat samples sourced from refiners R1, R2, and R3. Batch 2 comprised 24 blended samples selected from Batch 1. Details about the samples and the analyses conducted are provided in Table 5 (Batch 1) and Table 6 (Batch 2).

Table 5. Batch 1 samples and the analyses conducted on them. Refiners are listed as R1, R2, and R3.

No	Origin	Sample info	SOAP	GC×GC	GC-VUV
1	R1	R100	Yes	Yes	-
2	R1	MP-30, D-535	Yes	Yes	Yes
3	R1	MP-30, D-140	Yes	Yes	Yes
4	R1	Renewable Naphtha	Yes	Yes	Yes
5	R1	CARBOB, 1005	Yes	Yes	Yes
6	R1	EPA, 1007	Yes	Yes	-
7	R2	Renewable HEFA - Mixture of FOG	Yes	Yes	Yes
8	R2	R100 Soy/DCO, Renewable Diesel Mix	Yes	Yes	-
9	R2	Renewable Biodiesel from Soy Feedstock	Yes	Yes	-
10	R2	Renewable Diesel from Sugar Mixture	Yes	Yes	Yes
11	R2	Renewable SAK - Mixture of Sugars	Yes	Yes	Yes
12	R2	Petroleum #2 Diesel	Yes	Yes	-
13	R3	Neste Propel HPR	Yes	Yes	-
14	R3	#2 HDS Feed Surge Drum, Distillates with S compounds	Yes	Yes	-
15	R3	#2 ULSD w/ 5V% biofuel HPR	Yes	Yes	-
16	R3	#2 ULSD w/ 15V% biofuel HPR	Yes	Yes	-
17	R3	#2 ULSD w/ 25V% biofuel HPR	Yes	Yes	-
18	R3	#2 ULSD w/ 50V% biofuel HPR	Yes	Yes	-
19	R3	#3 HDS Feed Surge Drum, Distillates with S compounds	Yes	Yes	-
20	R3	#3 HDS Product	Yes	Yes	-
21	R3	#2 HDS Product	Yes	Yes	-
22	R3	ULSD#2 Tank 37 Final	Yes	Yes	-
23	R3	ULSD#2 Tank 30 Final	Yes	Yes	-

Abbreviations: CARBOB = California Air Resources blendstock for oxygenate blending; DCO = distillers corn oil; EPA = U.S. Environmental Protection Agency; FOG = fats, oils, greases; GC = gas chromatography; GC×GC = two-dimensional gas chromatography; HDS = hydrodesulfurization; HEFA = hydroprocessed esters and fatty acids; HPR = high performance renewable; MP = ; R1, R2, R3 = refiner 1, 2, 3; R100 = 100% renewable fuel; SAK = synthetic aromatic kerosene; SOAP = saturate, olefin, aromatic, and polar fractions; ULSD = ultra-low sulfur diesel; V% = volume percent; VUV = vacuum ultraviolet spectroscopy.

Table 6. Batch 2 samples and the analyses conducted on them.

No	PNNL ID	Sample Information*	SOAP	GC×GC
1	1	1% R3 HDS #3 Product in R2 Pet. #2 Diesel	Yes	Yes
2	2	5% R3 HDS #3 Product in R2 Pet. #2 Diesel	Yes	Yes
3	3	2.5% R3 HDS #3 Product in R2 Pet. #2 Diesel	Yes	Yes
4	4	7.5% R3 HDS #3 Product in R2 Pet. #2 Diesel	Yes	Yes
5	5	10% R3 HDS #3 Product in R2 Pet. #2 Diesel	Yes	Yes
6	6	50% R3 HDS #3 Product in R2 Pet. #2 Diesel	Yes	Yes
7	7	100% R2 Pet. #2 Diesel for R3 HDS #3 Product blends	Yes	Yes
8	0	100% R3 HDS #3 Product	Yes	Yes
9	8	1% R2 Renewable HEFA - Mixture of FOG in Pet. #2 Diesel	Yes	Yes
10	9	5% R2 Renewable HEFA - Mixture of FOG in Pet. #2 Diesel	Yes	Yes
11	10	2.5% R2 Renewable HEFA - Mixture of FOG in Pet. #2 Diesel	Yes	Yes
12	11	7.5% R2 Renewable HEFA - Mixture of FOG in Pet. #2 Diesel	Yes	Yes
13	12	10% R2 Renewable HEFA - Mixture of FOG in Pet. #2 Diesel	Yes	Yes
14	13	50% R2 Renewable HEFA - Mixture of FOG in Pet. #2 Diesel	Yes	Yes
15	14	100% R2 Pet. #2 Diesel for Renewable HEFA - Mixture of FOG blends	Yes	Yes
16	101	100% R2 Renewable HEFA - Mixture of FOG blends	Yes	Yes
17	21	1% R2 Renewable Diesel from Sugar Mixture in Pet. #2 Diesel	Yes	Yes
18	22	5% R2 Renewable Diesel from Sugar Mixture in Pet. #2 Diesel	Yes	Yes
19	23	2.5% R2 Renewable Diesel from Sugar Mixture in Pet. #2 Diesel	Yes	Yes
20	24	14% R2 Renewable Diesel from Sugar Mixture in Pet. #2 Diesel	Yes	Yes
21	25	60% R2 Renewable Diesel from Sugar Mixture in Pet. #2 Diesel	Yes	Yes
22	26	100% R2 Renewable Diesel from Sugar Mixture	Yes	Yes
23	27	100% R2 Pet. #2 Diesel for Renewable Diesel from Sugar Mixture	Yes	Yes
24	15	1% R1 MP30-D535 in R2 Pet. #2 Diesel	Yes	-
25	16	5% R1 MP30-D535 in R2 Pet. #2 Diesel	Yes	-
26	17	2.5% R1 MP30-D535 in R2 Pet. #2 Diesel	Yes	-
27	18	7.5% R1 MP30-D535 in R2 Pet. #2 Diesel	Yes	-
28	19	10% R1 MP30-D535 in R2 Pet. #2 Diesel	Yes	-
29	20	50% R1 MP30-D535 in R2 Pet. #2 Diesel	Yes	-
30	99	100% R1 MP30-D535	Yes	-
31	98	100% R2 Pet. #2 Diesel for R1 MP30-D535	Yes	-

* Percentages are listed as weight percent of the bio-blendstock in the identified fossil-derived blendstock.

Abbreviations: FOG = fats, oils, greases; GC×GC = two-dimensional gas chromatography; HDS = hydrodesulfurization; HEFA = hydroprocessed esters and fatty acids; Pet. = petroleum; PNNL = Pacific Northwest National Laboratory; R1, R2, R3 = refiner 1, 2, 3; SAK = synthetic aromatic kerosene; SOAP = saturate, olefin, aromatic, and polar fractions.

5.2 Standards Development

Agreed- ^{13}C matrix-matched standards are vital for determining the accuracy and precision of liquid fuels and fractions and to assist in cross-validating bulk IRMS data between PNNL and LANL. For this project, we utilized ^{13}C standards provided by the

University of Indiana and the United States Geological Survey (USGS) and developed a set of in-house standards to correct/normalize the ^{13}C values of samples, both bulk material and fractions (Table 7; https://hcnisotopes.earth.indiana.edu/reference-materials/). ^{13}C values ^{13}C values of the unknowns, which adjust the unknown, raw ^{13}C values to a common scale. The analytical methodology utilized for this project was applied to the in-house standards and are described in the subsections below. In addition, PNNL leveraged its own existing, in-house glutamic acid (calibrated to USGS40 and USGS41) standards to confirm values obtained from other standards.

Table 7. Table of Standards. List of accepted and developed fuel-like standards for bulk and ^{13}C analyses. In-house glutamic acid standards were used to normalize solid samples (e.g., animal-based feedstocks), as PNNL did not have a representative standard and prioritized liquid fuel samples. PNNL Low and Medium have standard deviations that have been estimated from runs over a 2.5-year period.

Standard	^{13}C (‰ VPDB)	Standard type
PNNL heptamethylnonane	25.77 ± 0.06	In-house, this project
PNNL hexadecane	31.35 ± 0.05	In-house, this project
PNNL ethanol	11.69 ± 0.08	In-house, this project
PNNL Low	11.09 ± 0.10	In-house glutamic acid
PNNL Medium	16.73 ± 0.20	In-house glutamic acid
Methanol	46.77 ± 0.04	University of Indiana
USGS #B hexadecane	10.55 ± 0.04	University of Indiana, USGS
USGS #3 hexadecane	34.50 ± 0.05	University of Indiana, USGS
USGS #2 hexadecane	26.15 ± 0.02	University of Indiana, USGS
n-alkane mix B5 (*n* = 15 n-alkanes)	various	University of Indiana, USGS

Abbreviations: $^{13}C = ((R_{sample} / R_{standard}) - 1)) \times 1000$, in per mil (‰) where R = $^{13}C/^{12}C$ ratio; PNNL = Pacific Northwest National Laboratory; USGS = United States Geological Survey; VPDB = Vienna Peedee Belemnite.

5.3 Sample Preparation for Various Analyses

^{13}C analysis to evaluate the utility of stable carbon isotopes for determining percent biocarbon in blended samples composed of fossil fuel and either biofuel or co- ^{13}C values between the fossil carbon and biocarbon end-members (*n* = 27, 4 blend sets). Samples were blended while cold using weight percent (wt%) in 20 mL subsamples, refrigerated, and aliquoted into 2 mL GC vials. Aliquots were then sent to LANL for method comparison (direct-injection EA-IRMS versus argon cold welding EA-IRMS) and CanmetENERGY for fraction separation. Blending targeted 1%, 2.5%, 5%, 7.5%, 10%, and 50% biofuel and co-processed fuel component mixed with fossil diesel. Fuel components used to form blended samples were sent to CanmetENERGY, where ^{13} ^{13}C analysis to determine percent biocarbon in an unknown blended sample (*n* = 5) when the end-

members were known. The “percent carbon from biogenic end-member fuel” was then calculated using the percent carbon from elemental analysis (see Section 5.4).

5.4 Sample Composition Analyses

Samples were analyzed using an Elementar Vario Macro Cube. Combustion and reduction tubes were packed accordingly to analyze percent carbon, nitrogen, sulfur, and hydrogen. The combustion tube was heated to 1150 °C, and the reduction tube to 650 °C. Helium was used as the carrier gas. Typical sample sizes ranged from 10–30 µL.

Samples were analyzed for density and viscosity using an Anton Paar SVM 3001 Cold Properties Viscometer. Approximately 3 mL of sample were loaded into the instrument cell for measurement. A preset mode of ultrafast was chosen to measure with ultrafast precision and a repetition value of 2. The sample was analyzed at 20 °C. Viscometer calibration was checked at 20 °C using a certified N26 viscosity reference standard purchased from Cannon Instrument Company. The weight percent was converted to percent biocarbon using percent carbon data for each fuel. The percent carbon was determined using elemental analysis (Table A.2, Appendix A).

5.5 Gas Chromatography

Diesel samples were analyzed by a one-dimensional gas chromatographic system with a GC-VUV detector. The GC-VUV system consisted of an Agilent 7890 gas chromatograph (Agilent Technologies, Inc, CA, USA) equipped with a VGA-101 VUV detector (VUV Analytics, Inc., TX, USA). The procedure and system setup followed the guidelines provided in the ASTM D8071 standard documents, ensuring standardized and reliable results. By adhering to this standard, the analysis achieved high-resolution separation and accurate quantification of paraffins, iso-paraffins, olefins, naphthenes, and aromatics in the light naphtha samples.

5.6 Two-Dimensional Gas Chromatography

The samples were analyzed using GC×GC-FID, and all hydrocarbon quantifications provided in this study were based on the FID response. The FID response is linear over a wide range of concentrations and proportional to the mass flow rate of carbon. The GC×GC-FID analysis was conducted in both “normal” and “reversed” column configuration setups.

The “normal” GC×GC-FID instrument equipped with a “normal” column combination set was used to study the volatility behavior of the samples. The primary column was a DB-5 column (29.9 m × 0.32 mm × 0.25 µm), and the secondary column was a BPX-50 column (1.21 m × 0.1 mm × 0.1 µm). The modulation period was set at 6 seconds for all experiments. A 0.1 µL sample was injected at 300 °C at a 50:1 split ratio. The carrier gas was helium (grade 5.3, Messer, Edmonton, AB). The separations were started at 40 °C, reaching 330 °C at 3 °C/min, with a hold time of 1 min at the beginning and end of the run. The secondary oven and modulator were kept at 10 °C and 40 °C above the main oven temperature, respectively.

The “reversed” column GC×GC-FID instrument was equipped with a “reversed” column combination. The primary column was a DB-17 MS column (59.15 m × 0.25 mm × 0.25 µm), and the secondary column was a RTX-5 column (1.41 m × 0.18 mm × 0.2 µm). The modulation period was set to 5 seconds for all experiments. A 0.1 µL sample was injected at 340 °C with a 50:1 split ratio. The carrier gas was helium (grade 5.3, Messer, Edmonton, AB). The separations

began at 40 °C and reached 320 °C at a rate of 3 °C/min, with a hold time of 1 minute at both the start and end of the run. The secondary oven and modulator were maintained at 15 °C and 45 °C above the main oven temperature, respectively.

5.7 Solid-Phase Extraction Method

Solid-phase extraction (SPE) is a technique that uses the selective partitioning of sample components between solid and liquid phases. This method is both time efficient and environmentally friendly, utilizing less solvent compared to other open column chromatography separation techniques. In this study, SPE analysis was applied to separate samples into SOAP fractions. The SPE process is depicted in Figure 19. Samples pass through a cartridge filled with a silica-based stationary phase, utilizing various solvents or solvent mixtures. The setup includes two 14 mL SPE cartridges (or columns): the first contains 5 g of silica, and the second is loaded with 10% silver nitrate in silica, arranged sequentially. Initially, 14 mL of pentane is used through the cartridges to extract saturates. Subsequently, the lower cartridge, containing silver nitrate/silica, is detached and run with 20 mL of dichloromethane to isolate olefins. The upper silica column is then processed again with 20 mL of dichloromethane to extract aromatics. Finally, 20 mL of methanol is used to recover any polar compounds.

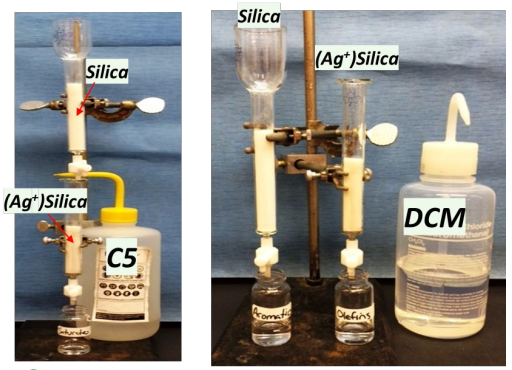

Figure 19. Hydrocarbon class separation (saturates, olefins, aromatics, polars) by solid-phase extraction. The resulting fractions have a 1:1000 solvent dilution.

5.8 ^{13}C Analytical Methods

Bulk ^{13}C Analytical Methods: ^{13}C via continuous flow EA (Costech, Valencia CA) IRMS and a connected interface (Conflo IV) that acted to dilute samples before introduction into the IRMS instrument and supply reference gas (CO_2) before and after each sample analysis (Thermo Scientific Delta V Plus IRMS, Bremen). Solid samples and oils were weighed (ca. 0.1 to 0.2 mg) into tin capsules and added to a carousel for automated runs. Liquid samples (ca. 0.2 µL) were manually introduced into the EA-IRMS instrument using a syringe. Samples were measured in two to five replicates.

^{13}C include a subset of bulk fuel samples analyzed at PNNL with the intention to compare methodologies between LANL and PNNL. Fuel samples were drawn into a syringe (0.2 to 0.4 µL) and volumetrically dispensed (targeting ca. 250 µg of liquid fuel sample) in smooth-sided tin capsules in an argon environment and analyzed via EA-IRMS using a Thermo Delta V IRMS instrument (Geeza et al. 2020; Li et al. 2020a). Samples were

warmed before weighing and packing into tin capsules to prevent microaggregation and isotope fractionation.

^{13}C via EA-IRMS in triplicate. Fractions samples were diluted within a solvent at a 1:1000 ratio. To separate sample fractions from the solvents, liquids were pipetted into smooth-sided tin capsules, and the solvent was evaporated, leaving the sample fraction within the tin capsule.

Samples were introduced to the Costech EA-IRMS instrument for combustion under pulsed O_2 (1020 °C at PNNL, 1050 °C at LANL). The resulting gas was carried in a helium gas flow to a reduction reactor to reduce any N_2O to N_2 (reduced copper filings under CO_2, 650 °C) and passed through a magnesium perchlorate trap to remove H_2O. Then, CO_2 and N_2 were separated using a GC column packed with molecular sieves (45 °C) before sample dilution and introduction into the IRMS instrument. Before each analytical run, the analytical system (EA-IRMS) was checked for leaks, the background signal (i.e., blank check) was determined on IRMS Faraday detectors (mV), and the instrument precision and signal linearity were determined using an internal CO_2 reference gas.

External standards were interspersed throughout an analytical run (beginning, every 6 to 9 samples, and at the end of a run).

Compound-Specific ^{13}C Analytical Methods: ^{13}C values of individual compounds and groups of compounds from fuel fractions were analyzed via GC-C-IRMS (Thermo Trace GC, Thermo Scientific Delta Q IRMS, Bremen). A volume of 4 to 8 µL of fuel fractions and standards dissolved in solvent were automatically injected into a GC system to separate compounds under a helium flow/carrier gas. Compounds were then passed through a micro combustion reactor packed with nickel and platinum wires at 940 °C. To aid combustion, 1% O_2 was added to the helium carrier gas stream prior to reactor introduction. The gas flow was then passed through a water removal column (Nafion membrane) before introduction into the IRMS instrument ^{13}C analysis. Run parameters are outlined in Table 8.

Analytical runs included unknown samples interspersed between standards (at the beginning and end of a run and every 3 to 6 unknowns). In addition to the external n-alkane reference, an internal CO_2 reference gas was pulsed into the IRMS instrument at the beginning and end of each analysis. System blanks were determined before and after each analytical run session, and the internal linearity was determined prior to beginning the series of analytical runs. Samples were run with 0 to 2 replicates.

Chromatographic peaks of saturates in GC-C-IRMS analysis were identified by reference to the isotopically characterized Arndt Schimmelmann Laboratory (Indiana University) Type B n-alkane mix based on the elution time and order. This standard mixture contains a range of n-alkanes at different relative concentrations. We used an analysis of the differences between the measured ^{13}C values for peaks in the standard to test whether a linearity correction needed to be applied and determined by way of 95% confidence intervals that the ^{13}C values changed insignificantly with the ^{13}C values of samples were corrected ^{13}C values of all saturate peaks for every Type B n-alkane mix standard.

^{13}C values for analytical replicates presented as the average ± 1 standard deviation. The internal precision of the IRMS was ca. ±0.05‰ around runs.

Table 8. Table of GC parameters for the GC-C-IRMS sample analysis.

Parameter	Value
Column Type	Rtx-1, 60 meters
Inlet Temperature	340 °C
Split Flow	10 mL/min
Split Ratio	5
Helium Carrier Gas Flow	2 mL/min
Flow Mode	Constant Flow
GC Column Initial Temperature	35 °C
Initial Hold Time	8 min
Ramp 1 Rate	5 °C/min
Ramp 1 Temp	320 °C
Ramp 1 Hold Time	30 min
End Temperature	35 °C

Abbreviations: °C = degree(s) Celsius; C = combustion; GC = gas chromatography; IRMS = isotope ratio mass spectrometry; min = minute(s); mL = milliliter(s).

5.9 Accelerator Mass Spectrometry Method

Select samples with a volume of 1 mL were sent to Beta Analytic (Miami, Florida) for ^{14}C counting via AMS. The method used for determining the biobased content using ^{14}C is the accepted ASTM D6866-24, Method B analytical method (ASTM 2024). Samples were combusted, and the resulting CO_2 was then purified before transformation into graphite and the introduction of the graphite into the particle accelerator according to Beta Analytic operating procedures. ^{14}C data were used to calculate the pMC and percent biocarbon relative to international standards. Method details are supplied on the Beta Analytic website.

5.10 Data Analysis Methods

Linear and nonlinear models were fitted to available data for the ^{13}C values from sets of blended fuels. Models were fitted to evaluate the linear response of the ^{13}C values, particularly at low blend ratios (0% to 10% biofuel added to fossil fuel). These data were compared with the linear response from biocarbon oils (Li et al., 2020a). Comparisons of the retention time and the peak intensity of CO_2 resulting from the combusted fraction compounds via GC-C-IRMS were considered using GC traces from related fuel sets. Statistical methods are detailed in Appendix D. Further analysis focused on the features extracted from the GC traces was conducted using principal component analysis (PCA), with traces and results shown in Figure D.14 and Figure D.15. The features found through the peak analysis, clustering, and PCA show that replicates remain very close, indicating good sample processing, and that it is easy to find features that clearly distinguish the samples available. This can be relevant for finding specific compound signatures and help quantify the similarity between samples.

6.0 References

ASTM. 2014. Standard Test Method for Determination of Individual Components in Spark Ignition Engine Fuels by 100 Metre Capillary High Resolution Gas Chromatography. ASTM International *ASTM D6729*.

ASTM. 2016. Standard Test Method for Boiling Range Distribution of Petroleum Fractions by Gas Chromatography. ASTM International *ASTM D2887*.

ASTM. 2020. Standard Test Methods for Determining the Biobased Content of Solid, Liquid, and Gaseous Samples Using Radiocarbon Analysis. ASTM International *ASTM D6866*.

ASTM. 2024. Standard Test Methods for Determining the Biobased Content of Solid, Liquid, and Gaseous Samples Using Radiocarbon Analysis. ASTM International *ASTM D6866-24, 4.2 Method B*.

DOE. n.d. "Co-Optimization of Fuels & Engines." U.S. Department of Energy. Accessed August 11, 2025. https://www.energy.gov/eere/bioenergy/co-optimization-fuels-engines.

EIA. 2023. *Annual Energy Outlook 2023*. U.S. Energy Information Administration AEO2023.

Geeza, T. J., Z.-H. Li, O. V. Maltsev, and J. E. Lee. 2020. "Cold-Weld Sealing in Argon Atmosphere for High Precision Carbon Isotope Analysis of Co-Processed Biofuels Using a Continuous-Flow Isotope Ratio Mass Spectrometer." *Energy & Fuels 34* (9): 11134–11142. https://doi.org/10.1021/acs.energyfuels.0c02114.

Haverly, M. R., S. R. Fenwick, F. P. K. Patterson, and D. A. Slade. 2019. "Biobased Carbon Content Quantification Through AMS Radiocarbon Analysis of Liquid Fuels." *Fuel 237*: 1108–1111. https://doi.org/10.1016/j.fuel.2018.10.081.

Kohn, M. J. 2010. "Carbon Isotope Compositions of Terrestrial C3 Plants as Indicators of (Paleo)ecology and (Paleo)climate." *PNAS 107* (46): 19691–19695. https://doi.org/10.1073/pnas.1004933107.

Li, Z.-H., K. Magrini-Bair, H. Wang, O. V. Maltsev, T. J. Geeza, C. I. Mora, and J. E. Lee. 2020a. "Tracking Renewable Carbon in Bio-oil/Crude Co-processing with VGO Through $^{13}C/^{12}C$ Ratio Analysis." *Fuel 275*: 117770. https://doi.org/10.1016/j.fuel.2020.117770.

Li, Z.-H., H. Wang, K. A. Magrini, J. E. Lee, T. Geeza, O. V. Maltsev, and J. P. Helper. 2020b. "Quantitative Determination of Biomass-Derived Renewable Carbon in Fuels from Coprocessing of Bio-oils in Refinery Using a Stable Carbon Isotopic Approach." *ACS Sustainable Chemistry & Engineering 8* (47): 17565–17572. https://doi.org/10.1021/acssuschemeng.0c07323.

Montgomery, D. C., E. A. Peck, and G. G. Vining. 2021. *Introduction to Linear Regression Analysis*. John Wiley & Sons.

Mook, W. G. 2000. *Environmental Isotopes in the Hydrological Cycle – Principles and Applications*. Paris: UNESCO.

Mueller, C. J., W. J. Cannella, T. Bays, T. J. Bruno, K. DeFabio, H. D. Dettman, R. M. Gieleciak, M. L. Huber, C.-B. Kweon, S. S. McConnell, W. J. Pitz, and M. A. Ratcliff. 2016. "Diesel

Surrogate Fuels for Engine Testing and Chemical-Kinetic Modeling: Compositions and Properties." *Energy & Fuels 30* (2): 1445–1461. https://doi.org/10.1021/acs.energyfuels.5b02879.

Schoell, M. 1984. "Stable Isotopes in Petroleum Research." In *Advances in Petroleum Geochemistry*, edited by J. Brooks and D. Welte, 215–245. Academic Press.

Sofer, Z. 1984. "Stable Carbon Isotope Compositions of Crude Oils: Application to Source Depositional Environments and Petroleum Alteration." *The American Association of Petroleum Geologists Bulletin*, 68 (1): 31–49. https://doi.org/10.1306/AD460963-16F7-11D7-8645000102C1865D.

Vieth, A., and H, Wilkes. 2010. "Stable Isotopes in Understanding Origin and Degradation Processes of Petroleum." In *Handbook of Hydrocarbon and Lipid Microbiology*, edited by K. N. Timmis. Berlin: Springer. https://doi.org/10.1007/978-3-540-77587-4_5.

Yan, C., Z. Li, S. Li, Z. Wang, L. Xing, Y. Liu, W. Mou, and K. Wang. 2019. "Determination of ^{13}C of Trace Hydrocarbons in Natural Gas Using Syringe Solid Phase Extraction (SSPE) Coupled with Gas Chromatography/Isotope Ratio Mass Spectrometry (GC/IRMS)." *Geofluids* 2019 (1): 6352378. https://doi.org/10.1155/2019/6352378.

Appendix A – Sample Identification and Information

Table A.1. Sample listing. Origins include refiners R1, R2, and R3; a landfill gas refiner (LG); and a canola diesel refiner (CD).

Origin	Sample
R3	Biofuel HPR
R3	#2 HDS Feed Surge Drum, Distillates with Sulfur Compounds
R3	#2 ULSD w/ 5V% Biofuel HPR
R3	#2 ULSD w/ 15V% Biofuel HPR
R3	#2 ULSD w/ 25V% Biofuel HPR
R3	#2 ULSD w/ 50V% Biofuel HPR
R3	#3 HDS Feed Surge Drum, Distillates with Sulfur Compounds
R3	#3 HDS Product
R3	#2 HDS Product
R3	ULSD#2 Tank 37 Final
R3	ULSD#2 Tank 30 Final
R3	Tallow-based biofeed
R2	Renewable HEFA - Mixture of FOG
R2	R100 Soy/DCO, Renewable Diesel Mix
R2	Renewable Biodiesel from Soy Feedstock
R2	Renewable Diesel from Sugar Mixture
R2	Renewable SAK - Mixture of Sugars
R2	Petroleum #2 Diesel
R2	Soy biodiesel
R2	Soy oil
R2	Sugar Feedstock
R2	Choice pork
R2	White grease
R2	Filtered tallow-based biofeed
R2	Poultry fat
R2	Soy oil
R2	DCO feedstock
LG	A no F
LG	2F
LG	5F
LG	10F
LG	50F
LG	100F
LG	CRU AP
LG	CRU 2% P
LG	CRU 5% P
LG	CRU 10% P
LG	CRU 50% P

Origin	Sample
CD	Canola biodiesel
CD	Canola
CD	Canola bleached
CD	Canola refined
R1	R100
R1	MP-30, D-535
R1	MP-30, D-140
R1	Renewable Naphtha
R1	CARBOB, 1005
R1	EPA, 1007
R1	Soy oil

Abbreviations: CARBOB = California Air Resources blendstock for oxygenate blending; CRU = circulating riser unit; DCO = distillers corn oil; EPA = U.S. Environmental Protection Agency; FOG = fats, oils, greases; HDS = hydrodesulfurization; HEFA = hydroprocessed esters and fatty acids; HPR = high performance renewable; R1, R2, R3 = refiner 1, 2, 3; R100 = 100% renewable fuel; SAK = synthetic aromatic kerosene; ULSD = ultra-low sulfur diesel; V% = volume percent.

Table A.2. Sample property analysis results.

Sample ID	Reason	C [%]	H [%]	N [%]	S [%]	Mean viscosity (cSt 20 °C)	Mean density (g/cm^3)	API-D
R3 Biofuel HPR	Blend curve biofuel end-member	84.525	16.132	0.305	n/a	5.0638 ± 0.02	0.7847 ± 0.00004	0.7884
R3 #2 HDS product	Blend curve fossil fuel end-member	86.665	15.02	0.06	n/a	7.3491± 0.00	0.8515 ± 0.00001	0.855
R2 Pet. #2 Diesel	Blend curve fossil fuel end-member	86.775	13.512	0.18	0.084	n/a	n/a	n/a
R2 R100 Soy	Blend curve biofuel end-member	84.98	15.949	0.405	0.059	n/a	n/a	n/a
R2 Renewable HEFA & FOG	Blend curve biofuel end-member	84.365	16.256	0.395	0.026	n/a	n/a	n/a
R2 Renewable Diesel from Sugar	Blend curve biofuel end-member	84.565	11.081	0.265	0.109	n/a	n/a	n/a
R3 #3 HDS Product	Blend curve biofuel end-member	85.515	14.645	0.34	0.035	n/a	n/a	n/a
R1 MP30 D-535	Blend curve biofuel end-member	72.215	14.566	0.2	0.162	n/a	n/a	n/a

Sample ID	Reason	C [%]	H [%]	N [%]	S [%]	Mean viscosity (cSt 20 °C)	Mean density (g/cm^3)	API-D
R3 #3 Fossil Feed Stock Surge	Fossil feedstock for co-proceed fuels	85.225	14.803	0.265	0.307	n/a	n/a	n/a
R3 Tallow-based biofeed	Biofeedstock for co-proceed fuels	76.375	12.727	0.075	0.083	n/a	n/a	n/a
R3 #3 HDS Product	Co-processed product	85.515	14.645	0.34	0.035	n/a	n/a	n/a
R3 Tank 37 Final	Co-processed product	85.715	15.146	0.325	0.073	n/a	n/a	n/a
R3 Tank 30 Final	Co-processed product	85.1	15.18	0.2	0.051	n/a	n/a	n/a
R1 Soybean oil	Biofeedstock	77.06	12.563	0.225	0.071	n/a	n/a	n/a
R1 Renewable Naphtha	Biofuel for co-processed fuels	63.205	13.079	0.37	0.123	n/a	n/a	n/a
R1 MP30 D-140	Co-processed product	83.775	11.615	0.34	0.355	n/a	n/a	n/a
R1 MP30 D-535	Co-processed product	72.215	14.566	0.2	0.162	n/a	n/a	n/a
R1 CARBOB 1005	Petroleum + co-processed product	77.237	12.709	0.273	0.478	n/a	n/a	n/a

Abbreviations: API-D = American Petroleum Institute density measurement at 15 °C; CARBOB = California Air Resources blendstock for oxygenate blending; cSt = centistoke(s); FOG = fats, oils, greases; g/cm^3 = gram(s) per cubic centimeter; HDS = hydrodesulfurization; HEFA = hydroprocessed esters and fatty acids; HPR = high performance renewable; MP = ; Pet. = petroleum; R1, R2, R3 = refiner 1, 2, 3; R100 = 100% renewable fuel.

Table A.3. ^{13}C values of bulk samples.

Sample ID	^{13}C (‰ VPDB)	± (‰)	# of Replicates
R3 5% Biofuel HPR	28.98	0.03	3
R3 15% Biofuel HPR	28.40	0.08	2
R3 25% Biofuel HPR	28.18	0.08	3
R3 50% Biofuel HPR	26.91	0.04	3
R3 #3 HDS Product	27.61	0.06	3
R3 ULSD#2 Tank 30 Final	28.49	0.07	3
R3 Tank 37 final	29.06	0.04	3
R3 #2 HDS Product	29.11	0.07	3
R3 #3 HDS Feedsurge	28.26	0.38	4
R3 #2 HDS Feedsurge	29.29	0.13	3

Sample ID	^{13}C (‰ VPDB)	± (‰)	# of Replicates
R3 100% Biofuel HPR (98.5% renewable)	24.10	0.08	3
R3 Tallow-based biofeed	23.64	0.05	
R1 MP-30 D-140	25.29	0.36	3
R1 MP-30 D535	26.66	0.02	2
R1 CARBOB 1005	25.45	0.23	3
R1 EPA 1007	23.53	0.05	3
R1 R100	30.81	0.10	3
R1 Renewable Naphtha	32.66	0.20	3
R1 Soy oil	30.76	0.07	2
R2 Soy oil	31.43	0.11	
R2 Pet. No. 2	29.14	0.01	3
R2 Renewable HEFA-FOG	21.55	0.16	3
R2 R100 Soy DCO	31.62	0.51	3
R2 DCO feedstock	16.13	0.16	
R2 Renewable Diesel from Sugar Mixture	10.62	0.02	2
R2 Renewable SAK - Mixture of Sugars	10.14	0.01	2
R2 Sugar Feedstock	10.35	0.22	2
R2 Choice Pork	14.11	0.01	
R2 White Grease	15.01	0.05	
R2 Filtered Tallow-based biofeed	17.58	0.03	
R2 Poultry Fat	18.89	0.03	
R2 Soy Biodiesel/MPC Renewable Biodiesel from Soy	31.72	0.24	3
R2 Soy Oil	31.82	0.17	3
CD Canola Biodiesel	29.54	0.05	3
CD Canola	28.35	0.07	3
CD Canola Bleached	28.70	0.51	3
CD Canola Refined	28.32	0.10	3
LG A no F	29.91	0.50	3
LG 2F	30.25	0.16	2
LG 5F	30.35	0.37	3
LG 10F	31.11	0.26	3
LG 50F	37.25	0.03	2
LG 100F	43.79	0.20	3
LG CRU AP	29.19	0.06	3
LG CRU 2%	29.31	0.10	2
LG CRU 5% P	29.58	0.04	2
LG CRU 10% P	29.98	0.25	3
LG CRU 50% P	33.95	0.41	3

Sample ID	^{13}C (‰ VPDB)	± (‰)	# of Replicates

Abbreviations: $^{13}C = ((R_{sample} / R_{standard}) - 1)) \times 1000$, in per mil (‰) where R = $^{13}C/^{12}C$ ratio; CARBOB = California Air Resources blendstock for oxygenate blending; CD = canola diesel refiner; CRU = circulating riser unit; DCO = distillers corn oil; EPA = U.S. Environmental Protection Agency; FOG = fats, oils, greases; HDS = hydrodesulfurization; HEFA = hydroprocessed esters and fatty acids; HPR = high performance renewable; LG = landfill gas refiner; R1, R2, R3 = refiner 1, 2, 3; SAK = synthetic aromatic kerosene; ULSD = ultra-low sulfur diesel; VPDB = Vienna Peedee Belemnite.

Table A.4. pMC and percent biocarbon from AMS and IRMS.

Sample Identification			AMS: ^{14}C data			R ^{13}C data				
Origin	Sample ID	Description, nominal % biofeed	pMC	± pMC	% BioC	^{13}C (‰ VPDB)	stdev (±)	Reps	pMC	% BioC
LG	A no F	Fossil feed	<0.44	-	0	29.91	0.50	3	0.04	0
LG	2% F	2% biofeed	0.74	0.04	1	30.25	0.16	2	1.03	1
LG	5% F	5% biofeed	2.07	0.05	2	30.35	0.37	3	1.32	1
LG	10% F	10% biofeed	3.08	0.05	3	31.11	0.26	3	3.51	4
LG	50% F	50% biofeed	16.05	0.08	16	37.25	0.03	2	21.37	21
LG	100% F	100% biofeed	40.42	0.15	40	43.79	0.20	3	40.40	40
LG	CRU A P	Product with 0% biofeed	<0.44	-	0	29.19	0.06	3	0.38	0
LG	CRU 2% P	Product with 2% biofeed	0.95	0.04	1	29.31	0.10	2	0.68	1
LG	CRU 5% P	Product with 5% biofeed	1.38	0.04	1	29.58	0.04	2	1.34	1
LG	CRU 10% P	Product with 10% biofeed	2.44	0.05	2	29.98	0.25	3	2.33	2
LG	CRU 50% P	Product with 50% biofeed	11.97	0.08	12	33.95	0.41	3	12.00	12

Abbreviations: AMS = accelerator mass spectrometry; BioC = biocarbon; CRU = circulating riser unit; $^{13}C = ((R_{sample} / R_{standard}) - 1)) \times 1000$, in per mil (‰) where R = $^{13}C/^{12}C$ ratio; IRMS = isotope ratio mass spectrometry; LG = landfill gas refiner; pMC = percent modern carbon; stdev = standard deviation; VPDB = Vienna Peedee Belemnite.

Table A.5. pMC and percent biocarbon from AMS and IRMS. Two sets of samples were not appropriate for calculating the percent biocarbon fro ^{13}C values because the exact relationship between samples was unknown and would have meant applying a number of assumptions.

		AMS Data			IRMS Data				
Origin	Sample ID	pMC (%)	± pMC (%)	BioC (%)	^{13}C (‰ VPDB)	^{13}C (±)	Reps	pMC (%)	% BioC
R2, R3	Blind Blend % sample	<0.44	0.00	0	29.31	0.02	3	0.49	0
R2, R3	50.12% R3 HDS #3 Product	8.72	0.07	9	28.48	0.05	3	8.83	9
R2, R3	10.69% R3 HDS #3 Product	1.68	0.05	2	29.15	0.03	4	1.88	2
R2, R3	5.35% R3 HDS #3 Product 2 of 2	0.80	0.04	1	29.25	0.07	4	0.94	1
R2, R3	5.35% R3 HDS #3 Product 1 of 2	0.99	0.04	1	29.25	0.07	4	0.94	1
R2, R3	1.04% R3 HDS #3 Product	<0.44	0.00	0	29.35	0.08	4	0.18	0
R2	R2 Pet. #2 Diesel	<0.44	0.00	0	29.38	0.03	3	0	0
R3	R3 HDS #3 Product	17.62	0.09	18	27.68	0.03	3	17.62	18
R3	ULSD#2 Tank 30 Final	13.38	0.08	13	28.49	0.07	3	-	-
R3	ULSD#2 Tank 37 Final	1.20	0.04	1	29.06	0.04	3	-	-
R3	#3 HDS Feed Surge Drum	12.92	0.08	13	28.26	0.38	4	-	-
R3	Tallow-based biofeed (#3 HDS biofeed)	100.31	0.28	100	23.64	0.05	3	-	-
R1	R100	100.57	0.30	100	30.81	0.10	3	-	-
R1	CARBOB, 1005	0.44	0.00	0	25.45	0.23	3	-	-
R1	MP30 D140	0.44	0.00	0	25.29	0.36	3	-	-
R1	MP30 D535	1.16%	0.04%	1%	26.66	0.02	2	-	-
R1	Renewable Naphtha	94.14%	0.28%	94%	32.66	0.20	3	-	-
R1	Renewable Soybean Oil	101.05%	0.30%	100%	30.76	0.07	2	-	-

Origin	Sample ID	AMS Data			IRMS Data				
		pMC (%)	± pMC (%)	BioC (%)	^{13}C (‰ VPDB)	^{13}C (±)	Reps	pMC (%)	% BioC

Abbreviations: AMS = accelerator mass spectrometry; BioC = biocarbon; CARBOB = California Air Resources blendstock for oxygenate blending; $^{13}C = ((R_{sample} / R_{standard}) - 1)) \times 1000$, in per mil (‰) where R = $^{13}C/^{12}C$ ratio; HDS = hydrodesulfurization; IRMS = isotope ratio mass spectrometry; Pet. = petroleum; pMC = percent modern carbon; R1, R2, R3 = refiner 1, 2, 3; R100 = 100% renewable fuel; ULSD = ultra-low sulfur diesel; VPDB = Vienna Peedee Belemnite.

Table A.6. Correct ^{13}C values of n-alkanes from saturate fuel fractions from fuel feedstocks and co-processed fuel products.

C# Peak	Fuel identification	^{13}C (‰ VPDB)	Retention Time (seconds)
9	ULSD#2 Tank 30 Final	36.22	807.6
10	ULSD#2 Tank 30 Final	29.75	1056.3
11	ULSD#2 Tank 30 Final	31.94	1263
12	ULSD#2 Tank 30 Final	29.44	1446.1
13	ULSD#2 Tank 30 Final	27.82	1613.9
14	ULSD#2 Tank 30 Final	27.28	1770.4
15	ULSD#2 Tank 30 Final	29.93	1917.4
16	ULSD#2 Tank 30 Final	25.99	2057
17	ULSD#2 Tank 30 Final	27.95	2188.6
18	ULSD#2 Tank 30 Final	25.76	2315.5
19	ULSD#2 Tank 30 Final	26.96	2433.8
20	ULSD#2 Tank 30 Final	27.88	2547.9
10	ULSD#2 Tank 37 Final	27.95	1055.9
11	ULSD#2 Tank 37 Final	35.69	1262.6
12	ULSD#2 Tank 37 Final	24.53	1445.7
13	ULSD#2 Tank 37 Final	37.33	1613.3
14	ULSD#2 Tank 37 Final	29.12	1769.8
15	ULSD#2 Tank 37 Final	30.80	1916.9
16	ULSD#2 Tank 37 Final	27.61	2056.1
17	ULSD#2 Tank 37 Final	31.05	2188
18	ULSD#2 Tank 37 Final	29.60	2313.6
19	ULSD#2 Tank 37 Final	29.99	2433.2
20	ULSD#2 Tank 37 Final	28.99	2547.5
21	ULSD#2 Tank 37 Final	32.33	2656.8
22	ULSD#2 Tank 37 Final	32.97	2761.5
	#3 HDS Product	28.39	251.6
12	#3 HDS Product	26.94	1446.1
13	#3 HDS Product	29.01	1613.5
14	#3 HDS Product	28.43	1769.8
15	#3 HDS Product	28.93	1916.9

C# Peak	Fuel identification	^{13}C (‰ VPDB)	Retention Time (seconds)
16	#3 HDS Product	26.06	2056.6
17	#3 HDS Product	28.39	2188.2
18	#3 HDS Product	25.39	2314.9
19	#3 HDS Product	29.19	2433.2
20	#3 HDS Product	29.74	2547.5
	Tallow-based biofeed	29.85	921.3
13	Tallow-based biofeed	25.72	1614.3
14	Tallow-based biofeed	27.52	1770.4
15	Tallow-based biofeed	32.97	1917.6
16	Tallow-based biofeed	24.42	2056.8
17	Tallow-based biofeed	28.66	2188.6
18	Tallow-based biofeed	24.15	2314.5
33	Tallow-based biofeed	33.08	3188.5
34	Tallow-based biofeed	22.64	3339
35	Tallow-based biofeed	20.31	3570.6
36	Tallow-based biofeed	35.83	3675.5
37	Tallow-based biofeed	31.88	3717.3
38	Tallow-based biofeed	26.91	4110
39	Tallow-based biofeed	25.59	4172.1
41	Tallow-based biofeed	25.05	4303.1
42	Tallow-based biofeed	23.26	4384.4
43	Tallow-based biofeed	26.24	4577.9
	#3 HDS Feed Surge Drum	25.25	290.7
12	#3 HDS Feed Surge Drum	34.87	1446.9
13	#3 HDS Feed Surge Drum	35.47	1614.7
14	#3 HDS Feed Surge Drum	27.81	1771.3
15	#3 HDS Feed Surge Drum	30.95	1918.4
16	#3 HDS Feed Surge Drum	29.37	2057.6
17	#3 HDS Feed Surge Drum	28.08	2189.7
18	#3 HDS Feed Surge Drum	25.74	2315.7
19	#3 HDS Feed Surge Drum	30.95	2434.9
20	#3 HDS Feed Surge Drum	30.06	2549.2

Abbreviations: $^{13}C = ((R_{sample} / R_{standard}) - 1)) \times 1000$, in per mil (‰) where $R = {}^{13}C/{}^{12}C$ ratio; HDS = hydrodesulfurization; ULSD = ultra-low sulfur diesel; VPDB = Vienna Peedee Belemnite

Table A.7. ^{13}C values of grouped iso/cyclo-paraffins from saturate fuel fractions from fuel feedstocks and co-processed fuel products.

C# Peak	Fuel identification	^{13}C (‰ VPDB)	Retention Time (seconds)
9.5	ULSD#2 Tank 30 Final	25.38	968.3
10.25	ULSD#2 Tank 30 Final	30.02	1105.8
10.5	ULSD#2 Tank 30 Final	30.67	1192.6
11.25	ULSD#2 Tank 30 Final	37.59	1326.1
11.5	ULSD#2 Tank 30 Final	31.06	1381.9
12.5	ULSD#2 Tank 30 Final	47.96	1569.2
13.5	ULSD#2 Tank 30 Final	20.25	1734.3
14.5	ULSD#2 Tank 30 Final	33.88	1863.7
15.5	ULSD#2 Tank 30 Final	31.03	1991.4
16.5	ULSD#2 Tank 30 Final	27.57	2121.8
17.5	ULSD#2 Tank 30 Final	31.46	2267.9
18.5	ULSD#2 Tank 30 Final	36.67	2390.1
?	ULSD#2 Tank 37 Final	13.04	383.1
?	ULSD#2 Tank 37 Final	9.49	897.2
9.5	ULSD#2 Tank 37 Final	36.79	989.2
10.25	ULSD#2 Tank 37 Final	25.60	1105.6
10.5	ULSD#2 Tank 37 Final	43.02	1191.9
11.25	ULSD#2 Tank 37 Final	20.12	1325.9
11.5	ULSD#2 Tank 37 Final	26.26	1381.3
12.25	ULSD#2 Tank 37 Final	15.36	1517.8
12.5	ULSD#2 Tank 37 Final	25.00	1553.9
13.5	ULSD#2 Tank 37 Final	26.12	1733.9
14.5	ULSD#2 Tank 37 Final	33.93	1862.8
15.5	ULSD#2 Tank 37 Final	29.33	1990.7
16.5	ULSD#2 Tank 37 Final	32.26	2121.1
17.5	ULSD#2 Tank 37 Final	33.56	2267.4
18.5	ULSD#2 Tank 37 Final	13.03	2389.7
19.5	ULSD#2 Tank 37 Final	32.56	2480.6
?	ULSD#2 Tank 37 Final	26.89	2862
?	ULSD#2 Tank 37 Final	29.55	2958.8
?	ULSD#2 Tank 37 Final	37.36	3038.2
?	#3 HDS Product	28.59	251.6
13.5	#3 HDS Product	26.85	1733.9
14.5	#3 HDS Product	28.29	1863.4
15.5	#3 HDS Product	26.99	1990.9
16.5	#3 HDS Product	27.69	2121.1
17.5	#3 HDS Product	27.04	2267.4
18.5	#3 HDS Product	23.20	2389.5
?	Tallow-based biofeed	30.05	921.3

C# Peak	Fuel identification	^{13}C (‰ VPDB)	Retention Time (seconds)
13.5	Tallow-based biofeed	11.25	1734.7
14.5	Tallow-based biofeed	28.80	1863.9
15.5	Tallow-based biofeed	29.47	1991.6
16.5	Tallow-based biofeed	28.89	2150.6
17.5	Tallow-based biofeed	36.77	2268.1
18.5	Tallow-based biofeed	18.10	2512.2
?	#3 HDS Feed Surge Drum	25.45	290.7
13.5	#3 HDS Feed Surge Drum	33.10	1735.1
14.5	#3 HDS Feed Surge Drum	29.06	1864.7
15.5	#3 HDS Feed Surge Drum	29.37	1992.4
16.5	#3 HDS Feed Surge Drum	28.34	2122.6
17.5	#3 HDS Feed Surge Drum	29.71	2268.9
18.5	#3 HDS Feed Surge Drum	33.74	2391

Abbreviations: $^{13}C = ((R_{sample} / R_{standard}) - 1)) \times 1000$, in per mil (‰) where R = $^{13}C/^{12}C$ ratio; HDS = hydrodesulfurization; ULSD = ultra-low sulfur diesel; VPDB = Vienna Peedee Belemnite.

Table A.8. ^{13}C values of n-alkanes from saturate fuel fractions from blends of co-processed fuel (R3 #3 HDS Product) and fossil fuel (R2 Pet. #2 Diesel).

Fraction Sample ID	C# Peak	^{13}C (‰ VPDB)	Retention Time (seconds)
R3 100%	10	29.34	1044
R3 100%	11	27.49	1263
R3 100%	12	26.49	1455
R3 100%	13	27.93	1604
R3 100%	14	29.25	1600
R3 100%	15	29.15	1770
R3 100%	16	27.68	1910
R3 100%	17	29.93	2187
R3 100%	18	30.48	2300
R3 100%	19	30.56	2423
R3 10%	10	28.20	1044
R3 10%	11	26.55	1263
R3 10%	12	27.95	1455
R3 10%	13	30.65	1604
R3 10%	14	30.70	1455
R3 10%	15	31.12	1770
R3 10%	16	30.69	1910
R3 10%	17	31.31	2187
R3 10%	18	29.08	2300

Fraction Sample ID	C# Peak	^{13}C (‰ VPDB)	Retention Time (seconds)
R3 10%	19	30.92	2423

Abbreviations: $^{13}C = ((R_{sample} / R_{standard}) - 1)) \times 1000$, in per mil (‰) where R = $^{13}C/^{12}C$ ratio; R2, R3 = refiner 2, 3; VPDB = Vienna Peedee Belemnite.

Appendix B – Sample Relationships

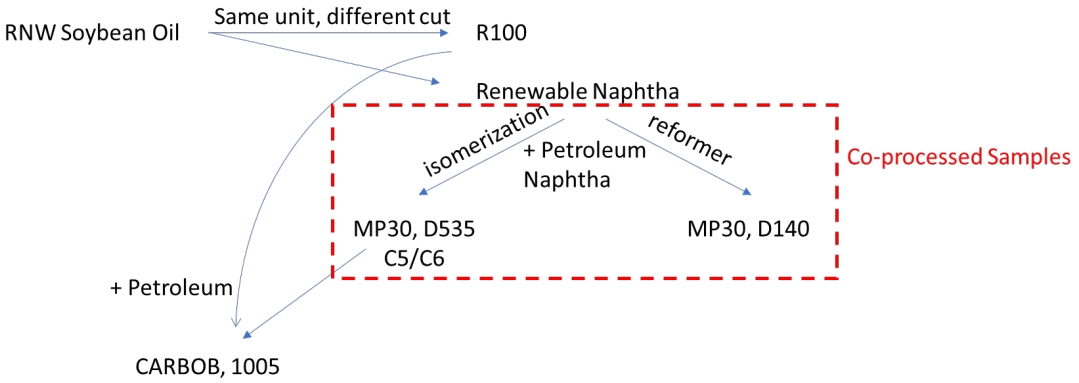

Samples	Samples for Separation
7	6

Figure B.1. Sample relationships for R1 samples. Abbreviations: CARB = California Air Resources Board; CARBOB = California Air Resources blendstock for oxygenate blending; EPA = U.S. Environmental Protection Agency; R1 = refiner 1; R100 = 100% renewable fuel; RNW = renewable.

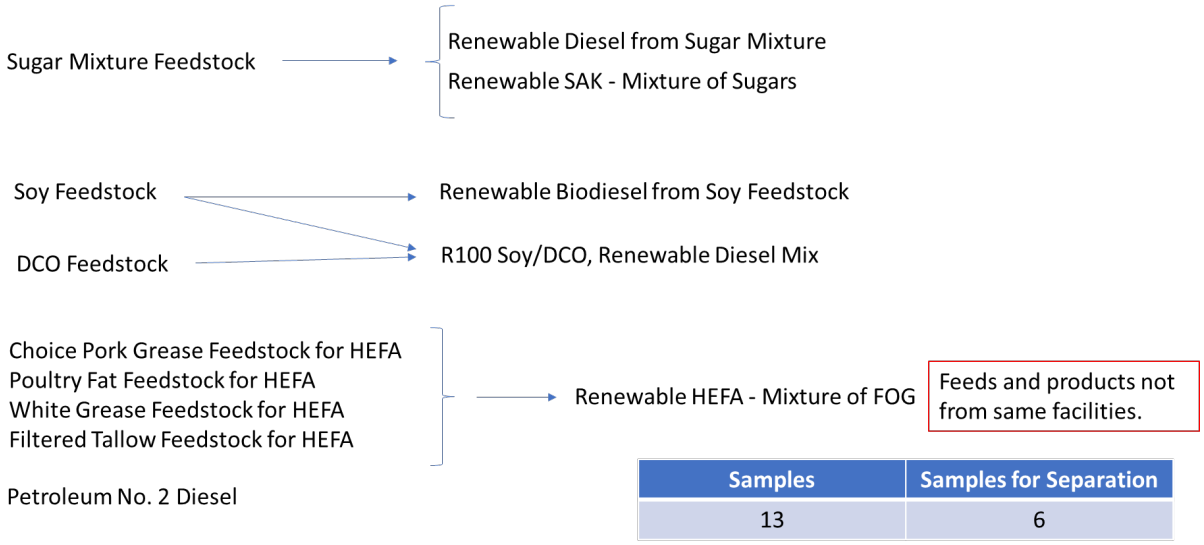

Samples	Samples for Separation
13	6

Figure B.2. Sample relationships for R2 samples. Abbreviations: DCO = distillers corn oil; HEFA = hydroprocessed esters and fatty acids; R2 = refiner 2; R100 = 100% renewable fuel; SAK = synthetic aromatic kerosene.

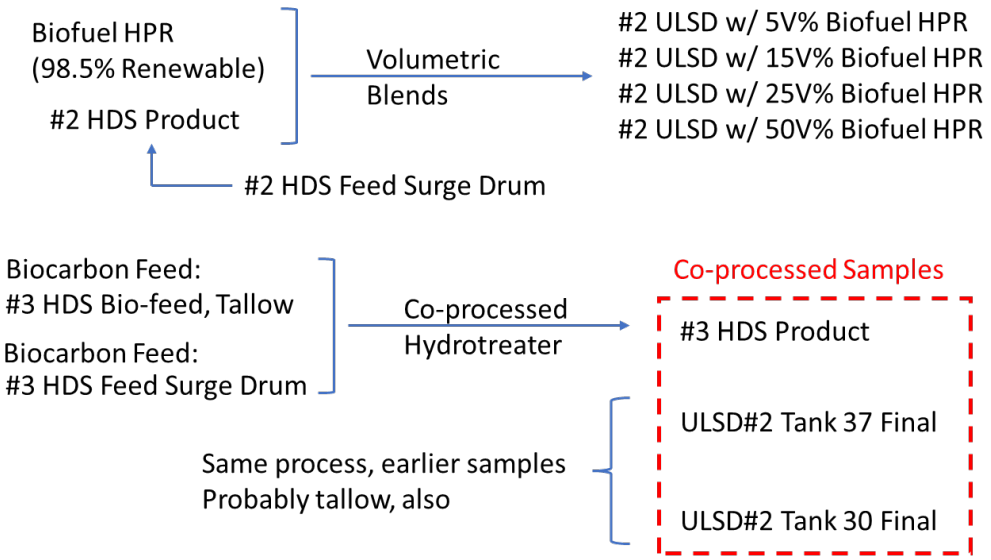

Samples	Samples for Separation
11	10

Figure B.3. Sample relationships for R3 samples. Abbreviations: HDS = hydrodesulfurization; HPR = high performance renewable; R3 = refiner 3; ULSD = ultra-low sulfur diesel; V% = volume percent.

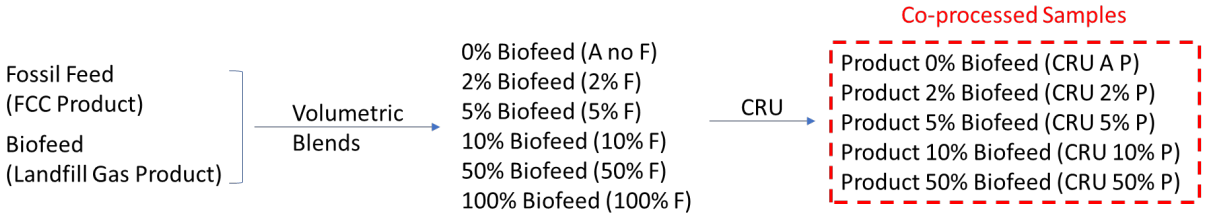

Samples	Samples for Separation
11	0

Figure B.4. Sample relationships for LG samples. Abbreviations: CRU = circulating riser unit; FCC = fluid catalytic cracking; LG = landfill gas refiner.

Appendix C – Blend Line Relationships

Blend Line: Co-processed HDS BP#3 Product

$$\widehat{\delta^{13}} = \beta_0 + \beta_1 Mass\%\ bioC + \beta_2 (Mass\%\ bioC)^2$$

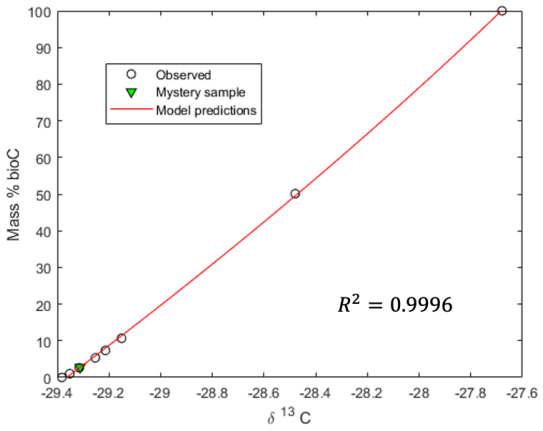

	Estimate	Std. Error	t-value	p-value
β_0	-29.3634	0.0068	-4334.77	<0.001
β_1	0.0189	6.2672e-04	30.09	<0.001
β_2	-2.0395e-05	6.3327e-06	-3.22	0.0235

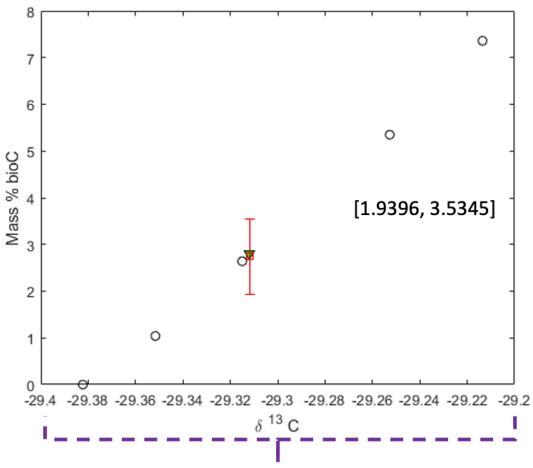

0 to 10% Biocarbon = 0.17 ‰ range

Mystery blend bio component (wt%): 2.13%
Range with 95% confidence intervals: 1.94 to 3.53%

Figure C.1. Blend curve for R3 biocarbon-derived fuel (co-processed) and R2 fossil fuel. The blind-blend sample is denoted as the mystery sample or mystery blend in the figure. Abbreviations: $^{13}C = ((R_{sample} / R_{standard}) - 1)) \times 1000$, in per mil (‰) where R = $^{13}C/^{12}C$ ratio; HDS = hydrodesulfurization; R2, R3 = refiner 2, 3; wt% = weight percent.

Blend Line: Renewable HEFA-FOG

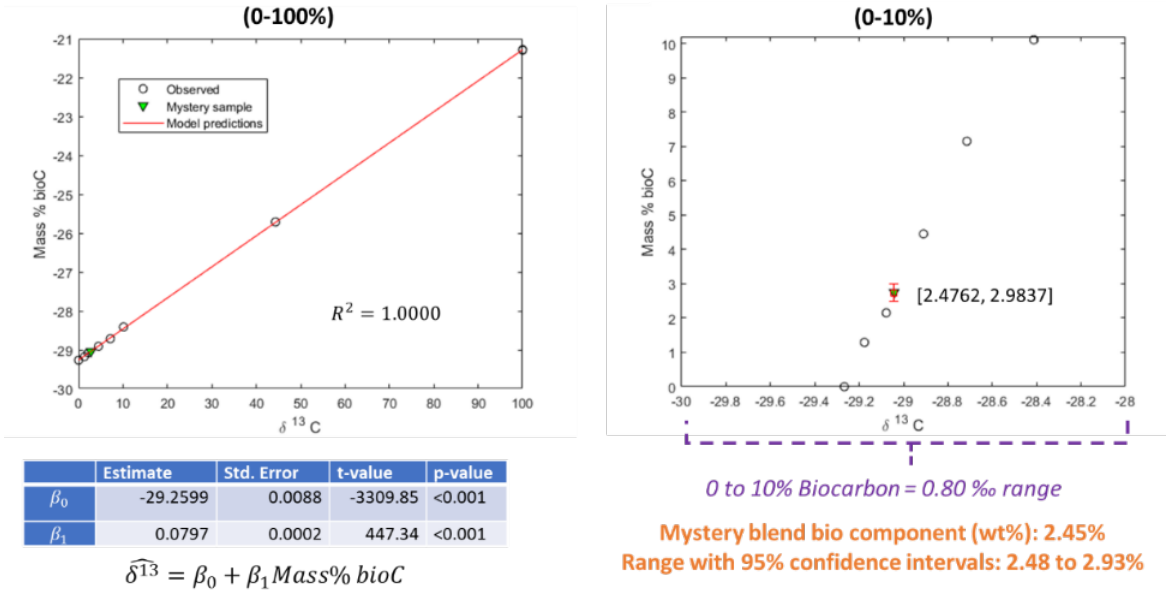

	Estimate	Std. Error	t-value	p-value
β_0	-29.2599	0.0088	-3309.85	<0.001
β_1	0.0797	0.0002	447.34	<0.001

$$\widehat{\delta^{13}} = \beta_0 + \beta_1 Mass\%\ bioC$$

Figure C.2. Blend curve for R2 biofuel and R2 fossil fuel. The blind-blend sample is denoted as mystery sample or mystery blend in the figure. Abbreviations: $^{13}C = ((R_{sample} / R_{standard}) - 1)) \times 1000$, in per mil (‰) where R = $^{13}C/^{12}C$ ratio; FOG = fats, oils, greases; HEFA = hydroprocessed esters and fatty acids; R2 = refiner 2; wt% = weight percent.

Blend Line: Renewable Sugar Mixture

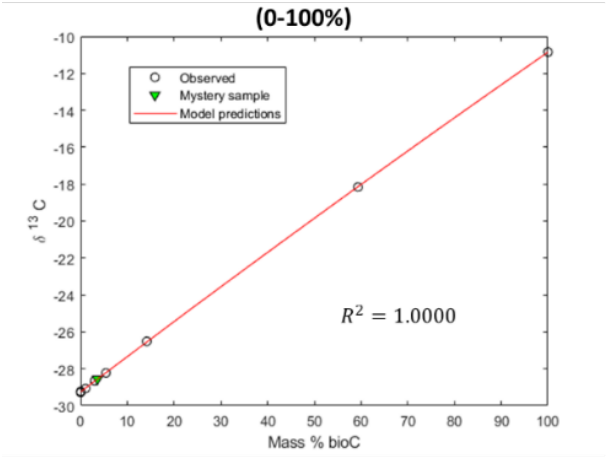

	Estimate	Std. Error	t-value	p-value
β_0	-29.2501	0.0129	-2269.14	<0.001
β_1	0.1920	0.0012	156.51	<0.001
β_2	-7.9649e-05	1.2738e-05	-6.25	0.001

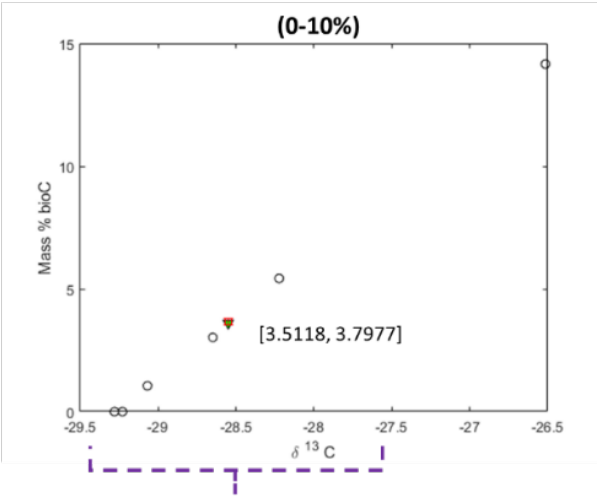

0 to 10% Biocarbon = 1.84 ‰ range

Mystery blend bio component (wt%): 3.59%
Range with 95% confidence intervals: 3.51 to 3.80%

Figure C.3. Blend curve for R2 biofuel and R2 fossil fuel. The blind-blend sample is denoted as mystery sample, or mystery blend in the figure. Abbreviations: $^{13}C = ((R_{sample} / R_{standard}) - 1)) \times 1000$, in per mil (‰) where R = $^{13}C/^{12}C$ ratio; R2 = refiner 2; wt% = weight percent.

Appendix D – Statistical Analyses

The statistical ^{13}C (per mil notation describing $^{13}C/^{12}C$) values as an analytical method to determine the biogenic carbon content of transportation fuels (i.e., gasoline and diesel fuel components) containing a biogenic fraction, along with the estimation of confidence or prediction intervals and an analysis of the model adequacy and goodness of fit. Some calibration models allowing the estimation of the ^{13}C were also calculated.

Some notable results include the presence of curvature in some models in the form of a quadratic term of the percent biocarbon. In models with no significant curvature, a statistically significant offset distinguishing the results by the analytical method was found. In general, the 95% confidence or prediction intervals are reasonably narrow and reflect the variability observed in the data.

Approach

This report contains results from the analysis of fuel samples analyzed using isotope ratio mass spectrometry (IRMS) and accelerator mass spectrometry (AMS). Samples with a biocarbon ^{13}C values for each analyzed sample. The objective is to build models relating the ^{13}C value to the biocarbon content using experimental data from available samples.

^{13}C values as a function of the biocarbon content. During model building, tests were carried out to check for the significance of the effect of the analytical method, as well as testing for curvature.

The models fit the data well and can be used to develop calibration curves. Calibration curves are useful to estimate the biocarbon content of new samples.

Results for hydrodesulfurization (HDS) BP#3 data

^{13}C to biocarbon present is shown in Equation (D.1). Figure D.1 shows plots of the model performance and model parameter estimates. Related statistics are shown in Table D.1.

$$\widehat{\delta^{13}} = \beta_0 + \beta_1 Mass\%\ bioC + \beta_2 (Mass\%\ bioC)^2 \quad (D.1)$$

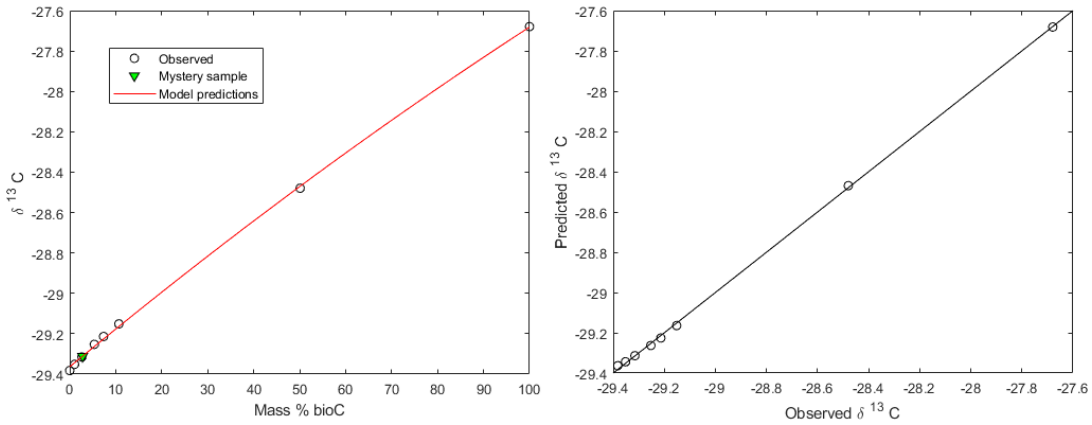

Figure D.1. (left panel) Plot of the R3 ^{13}C values (*y*-axis) versus the mass percent biocarbon (*x*-axis) and (right panel) a parity plot showing the model performance, where the solid black line at 45° ($y = x$) represents perfect prediction. R^2 for the model is 0.9996. The blind-blend sample is denoted as "Mystery sample" in the legend. Abbreviations: $^{13}C = ((R_{sample} / R_{standard}) - 1)) \times 1000$, in per mil (‰) where R = $^{13}C/^{12}C$ ratio; HDS = hydrodesulfurization; R3 = refiner 3.

Table D.1. Model parameter estimates and related statistics for the model in Equation (D.1).

Parameter	Estimate	Std. Error	t-value	p-value
$\boldsymbol{\beta_0}$	29.3634	0.0068	4334.77	<0.001
$\boldsymbol{\beta_1}$	0.0189	6.2672×10^{-4}	30.09	<0.001
$\boldsymbol{\beta_2}$	2.0395×10^{-5}	6.3327×10^{-6}	3.22	0.0235

The model has significant curvature (p-value for the quadratic term < 0.05) and fits the data well. A blind-blend sample, not used for model fitting, follows the trend of available data closely, indicating that the model is useful for predicting samples within the fitted range and composition.

A model fitted to only the low-carbon region (0–10 wt%) also contains significant curvature but, as expected, fits the data in the low-carbon region better the 0 wt% to 100 wt% data plotted in Figure D.1. If the region of interest includes only samples with a biocarbon content smaller than 10%, a model fitted to the data in the region of interest is recommended. A comparison of the performance for the model fitted to the available data to a model fitted using only data in the 0–10 wt% carbon range is shown in Figure D.2. The model parameter estimates and related statistics for the model fitted to data in the low-carbon region are shown in Table D.2.

Table D.2. Model parameter estimates and related statistics for the model in Equation (D.1) but using only data for samples with biocarbon in the 0–10 wt% range.

Parameter	Estimate	Std. Error	t-value	p-value
$\boldsymbol{\beta_0}$	29.3806	0.0015	1.98×10^{4}	<0.001
$\boldsymbol{\beta_1}$	0.0262	0.0007	35.76	<0.001
$\boldsymbol{\beta_2}$	4.4483×10^{-4}	6.7123×10^{-5}	6.63	0.007

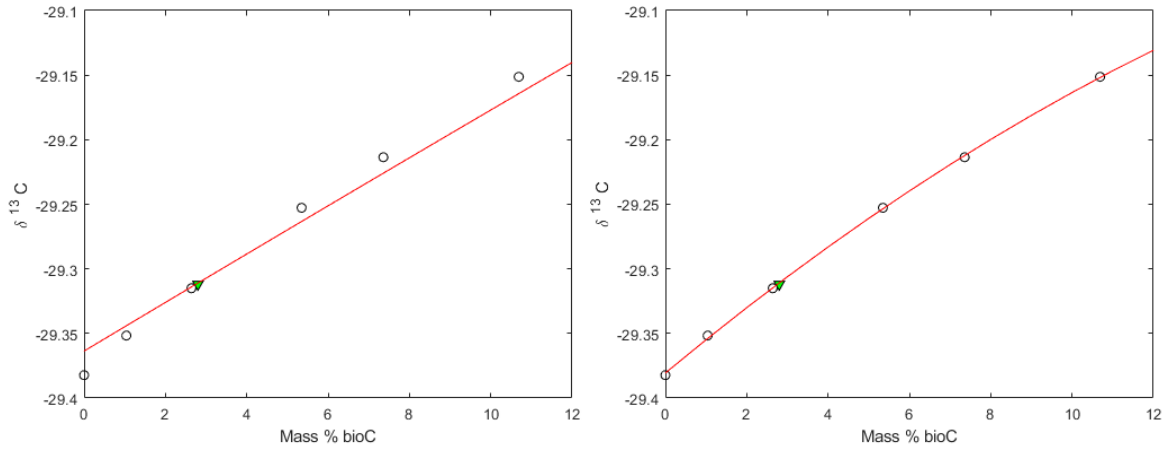

Figure D.2. Comparison of the model performance for the R3 HDS BP#3 data for the low-carbon region. The plot on the left shows the performance of the model using the entire dataset, and the right panel shows the model fitted using only data with low weight percent biocarbon. Abbreviations: $^{13}C = ((R_{sample} / R_{standard}) - 1)) \times 1000$, in per mil (‰) where R = $^{13}C/^{12}C$ ratio; HDS = hydrodesulfurization; R3 = refiner 3.

It is of interest to obtain model predictions for samples not included in the data used to fit the model. This includes predictions of the ^{13}C values and the use of a calibration model to predict the weight percent of biocarbon ^{13}C value is known or can be accurately estimated.

It is also of interest to develop calibration models to estimate the biocarbon content of samples ^{13}C value is known. An inverse estimator model was fitted to the data to develop a calibration model for the samples shown (Montgomery et al. 2021). The same procedure used to estimate the models predicting the ^{13}C value as a function of the carbon balance shown in this work was used to fit the inverse estimator. The results from fitting calibration models for blind-blend samples are shown in the corresponding portions of this report.

Figure D.3 shows the ^{13}C model predictions for a blind-blend sample using the model with parameters shown in Table D.1. Figure D.3 shows a relatively wide prediction interval. **Prediction intervals are wider than confidence intervals because they reflect the added uncertainty about future, unknown samples**. Figure D.4 shows a calibration interval for the blind-blend sample using a model fitted to the entire dataset available. The calibration interval is also relatively wide.

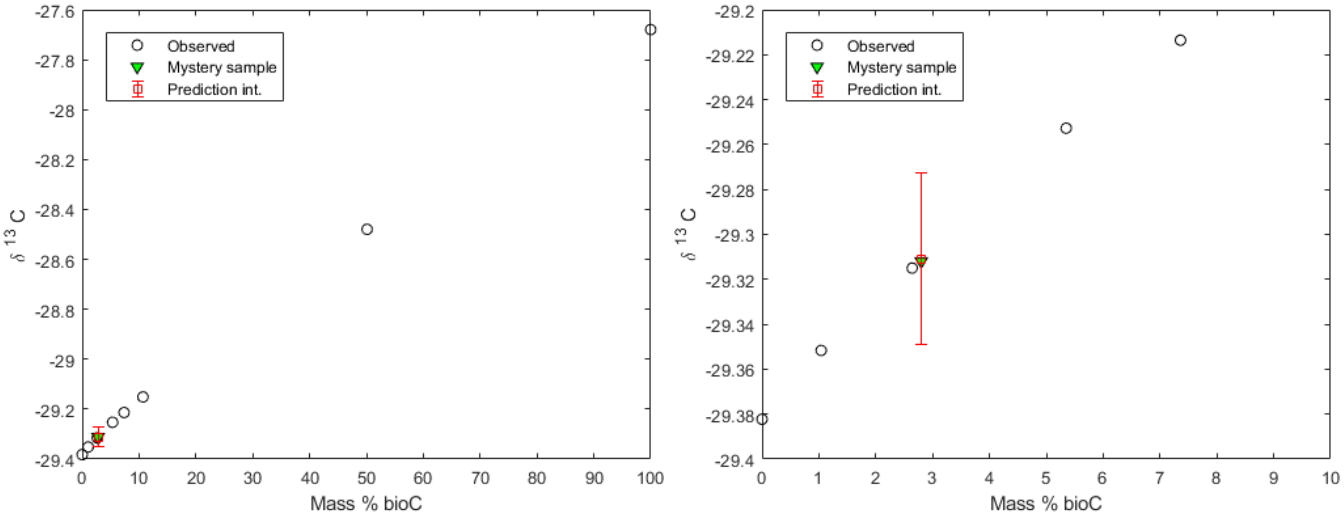

Figure D.3. Plot of the 95% prediction interval for the R3 HDS BP#3 sample. The plot on the left shows how the blind-blend sample fits among the dataset used to fit the model. The panel on the right shows a close-up of the low-carbon region. Within the legend, "Mystery sample" refers to the blind-blend sample. Abbreviations: $^{13}C = ((R_{sample} / R_{standard}) - 1)) \times 1000$, in per mil (‰) where R = $^{13}C/^{12}C$ ratio; HDS = hydrodesulfurization; R3 = refiner 3.

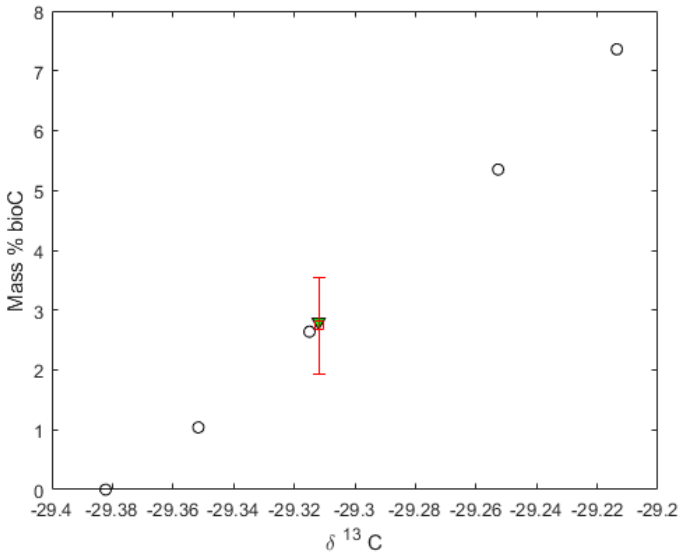

Figure D.4. Calibration interval for the blind-blend sample using a model fitted to all the data available. The interval is [1.9396, 3.5345] wt% biocarbon. The blind-blend sample has a measured biocarbon content of 2.89% for predictions based on 0–10 wt% biocarbon fuel. Abbreviations ^{13}C = per mil notation describing $^{13}C/^{12}C$; wt% = weight percent.

Analysis of the renewable hydroprocessed esters and fatty acids (HEFA) fats, oils, greases (FOG) data

Figure D.5 shows the data and the performance of a model fitted to the available data. The model fitted, shown in Equation (D.2), is similar to the model fitted to the refiner 3 (R3) HDS

BP#3 data, but, in this case, no significant curvature was detected. The parameter estimates and related statistics for the model in Equation (D.2) are shown in Table D.3.

$$\widehat{\delta^{13}} = \beta_0 + \beta_1 Mass\%\ bioC \qquad (D.2)$$

Table D.3. Model parameter estimates and related statistics for the model in Equation (D.2) for the HEFA-FOG samples. Abbreviations: FOG = fats, oils, greases; HEFA = hydroprocessed esters and fatty acids.

Parameter	Estimate	Std. Error	t-value	p-value
β_0	29.2599	0.0088	3309.85	<0.001
β_1	0.0797	0.0002	447.34	<0.001

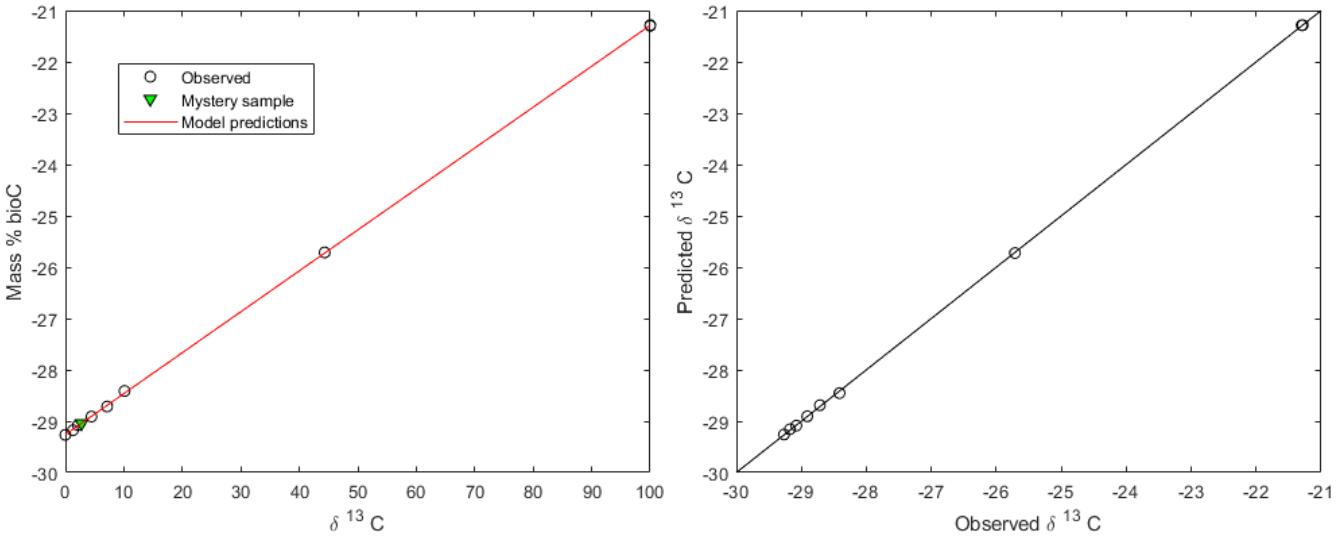

Figure D.5. (left panel) Plot of the HEFA-FOG data showing the mass percent biocarbon (*y*-axis) versus the ^{13}C values (*x*-axis) and (right panel) a parity plot showing the model performance, where the solid black line at 45° (*y* = *x*) represents perfect prediction. The R^2 for the model is 1.0000. Within the legend, "Mystery sample" refers to the blind-blend sample. Abbreviations: $^{13}C = ((R_{sample} / R_{standard}) - 1)) \times 1000$, in per mil (‰) where R = $^{13}C/^{12}C$ ratio; FOG = fats, oils, greases; HEFA = hydroprocessed esters and fatty acids.

Figure D.5 shows that the model fits the data very well and that the blind-blend sample aligns closely with the projections of the proposed model. A model fitted to the low-carbon region resulted in parameter estimates similar to those shown in Table D.3. Figure D.6 shows a 95% prediction interval for the blind-blend sample. The 95% prediction interval is relatively narrow, reflecting how well the model fits the data.

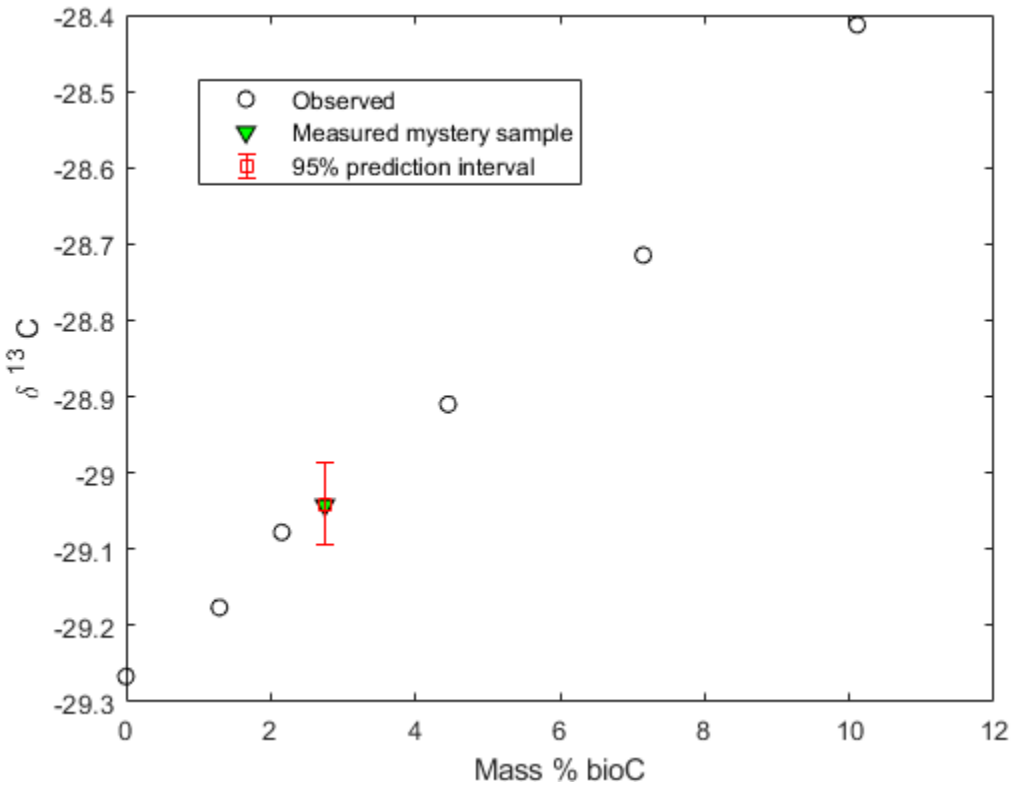

Figure D.6. Plot of the 95% prediction interval for the HEFA-FOG blind-blend sample. The interval is relatively small, reflecting how well the model fits the data. Within the legend, "Measured mystery sample" refers to the blind-blend sample. Abbreviations: $^{13}C = ((R_{sample} / R_{standard}) - 1)) \times 1000$, in per mil (‰) where R = $^{13}C/^{12}C$ ratio; FOG = fats, oils, greases; HEFA = hydroprocessed esters and fatty acids.

Figure D.7 displays the calculated calibration interval for the HEFA-FOG blind-blend sample, with an estimated range of [2.4762, 2.9837] wt% biocarbon.

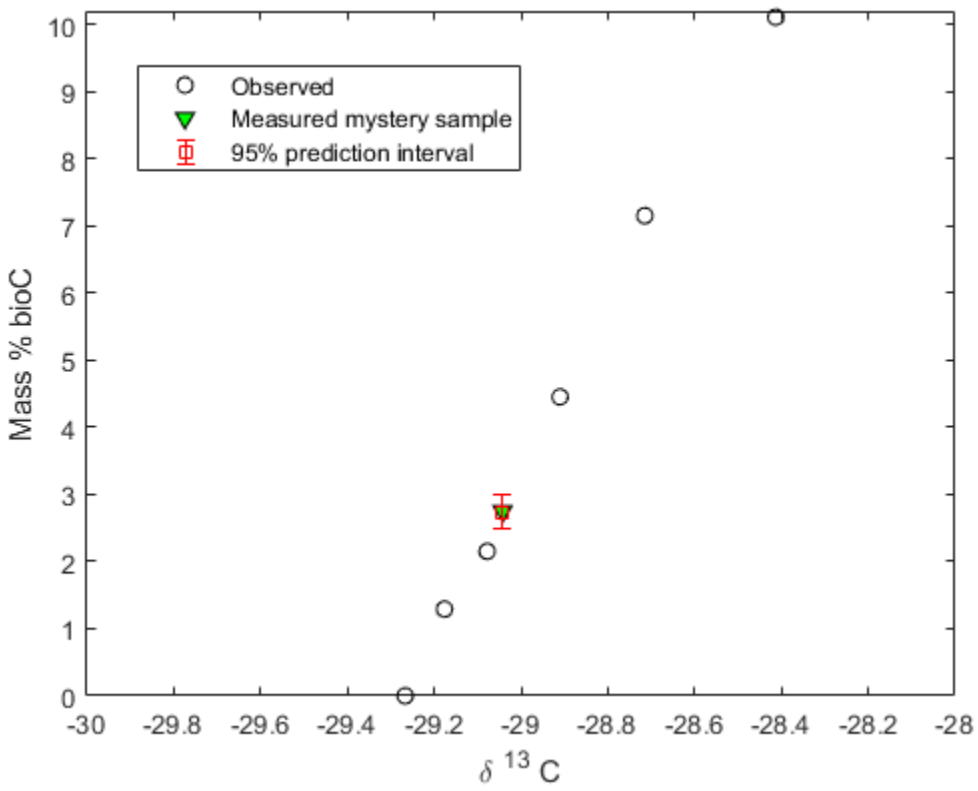

Figure D.7. Ninety-five percent calibration interval for the HEFA-FOG blind-blend sample using a model fitted to all the data available. The calibration interval is [2.4762, 2.9837]. Abbreviations: $^{13}C = ((R_{sample} / R_{standard}) - 1)) \times 1000$, in per mil (‰) where R = $^{13}C/^{12}C$ ratio; FOG = fats, oils, greases; HEFA = hydroprocessed esters and fatty acids.

Analysis of renewable sugar mix data

A quadratic model was fitted to the available renewable sugar mix data. The model fitted is analogous to the one shown in Equation (D.1). The model parameter estimates and related statistics are shown in Table D.4, and the model performance is shown in Figure D.8.

Table D.4. Model parameter estimates and related statistics for the quadratic renewable sugar mix data model.

Parameter	Estimate	Std. Error	t-value	p-value
$\boldsymbol{\beta_0}$	29.2501	0.0129	2269.14	<0.001
$\boldsymbol{\beta_1}$	0.1920	0.0012	156.51	<0.001
$\boldsymbol{\beta_2}$	7.9649×10^{5}	1.2738×10^{5}	6.25	0.001

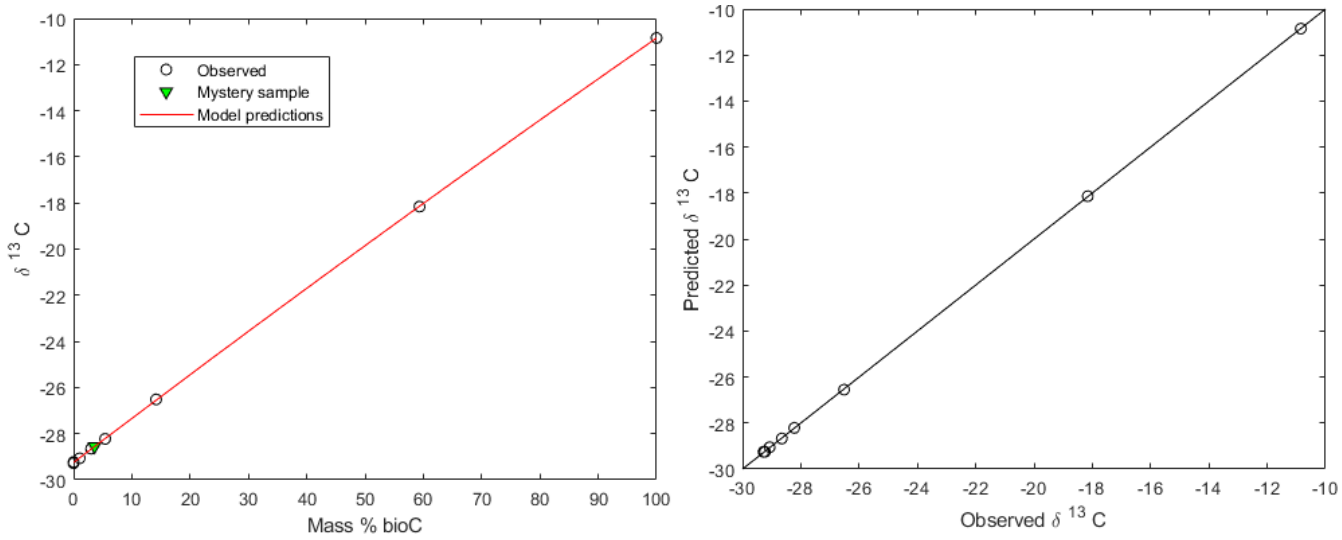

Figure D.8. (left panel) Plot of the ^{13}C values (*y*-axis) versus the mass percent biocarbon (*x*-axis) and (right panel) a parity plot showing the model performance, where the solid black line at 45° ($y = x$) represents perfect prediction. R^2 for the model is 1.0000. Within the legend, "Mystery sample" refers to the blind-blend sample. Abbreviation: $^{13}C = ((R_{sample} / R_{standard}) - 1)) \times 1000$, in per mil (‰) where R = $^{13}C/^{12}C$ ratio.

It is of interest to fit a model to the low-carbon portion of the data. This model does not show significant curvature and was used to compute 95% prediction and calibration intervals for a blind-blend sample, which are shown in Figure D.9. The model has the form shown in Equation (D.2). The model parameter estimates and related statistics are shown in Table D.5.

Table D.5. Model parameter estimates and related statistics for the linear renewable sugar mix model fitted to the low-carbon portion of the data.

Parameter	Estimate	Std. Error	t-value	p-value
$\boldsymbol{\beta_0}$	29.2579	0.0127	2299.30	<0.001
$\boldsymbol{\beta_1}$	0.1936	0.0020	96.24	<0.001

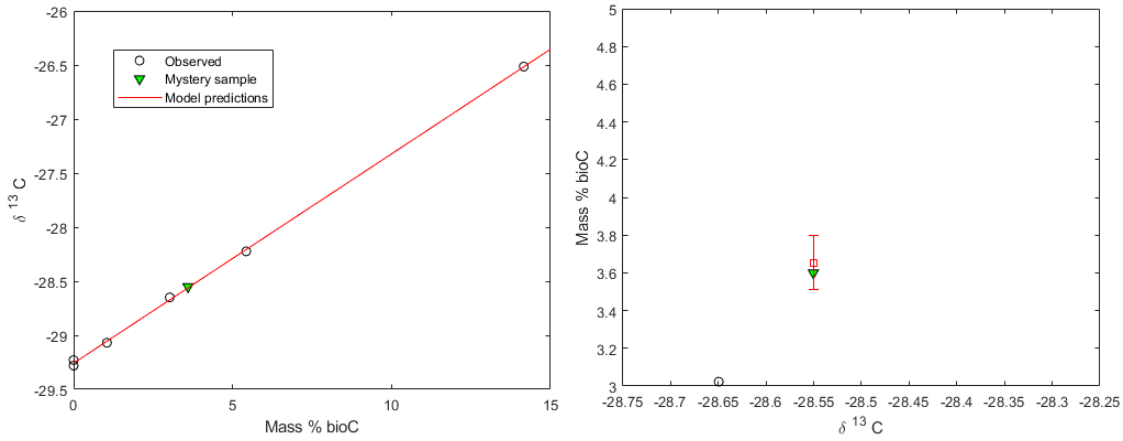

Figure D.9. (left panel) Plot of the ^{13}C values (*y*-axis) versus the mass percent biocarbon (*x*-axis) and (right panel) a 95% calibration interval for the blind-blend sample (denoted as mystery sample). R^2 for the linear model in the left panel is 0.9996. The calibration interval shown in the right panel is [3.5118, 3.7977]. Abbreviation: $^{13}C = ((R_{sample} / R_{standard}) - 1)) \times 1000$, in per mil (‰) where $R = {}^{13}C/{}^{12}C$ ratio.

Analysis of Refiner 1 (R1) MP30-D535 data

The same process applied to other samples shown in this document was applied to the P66 MP30-D535 data. A linear model (no significant curvature) was fitted to the data, and the parameter estimates and related statistics are shown in Table D.6. The model performance is shown in the plots in Figure D.10.

Table D.6. Model parameter estimates and related statistics for the P66 MP30-D535 data. No significant curvature is present for this dataset.

Parameter	Estimate	Std. Error	t-value	p-value
$\boldsymbol{\beta_0}$	29.2892	0.0336	870.81	<0.001
$\boldsymbol{\beta_1}$	0.0313	0.0009	36.26	<0.001

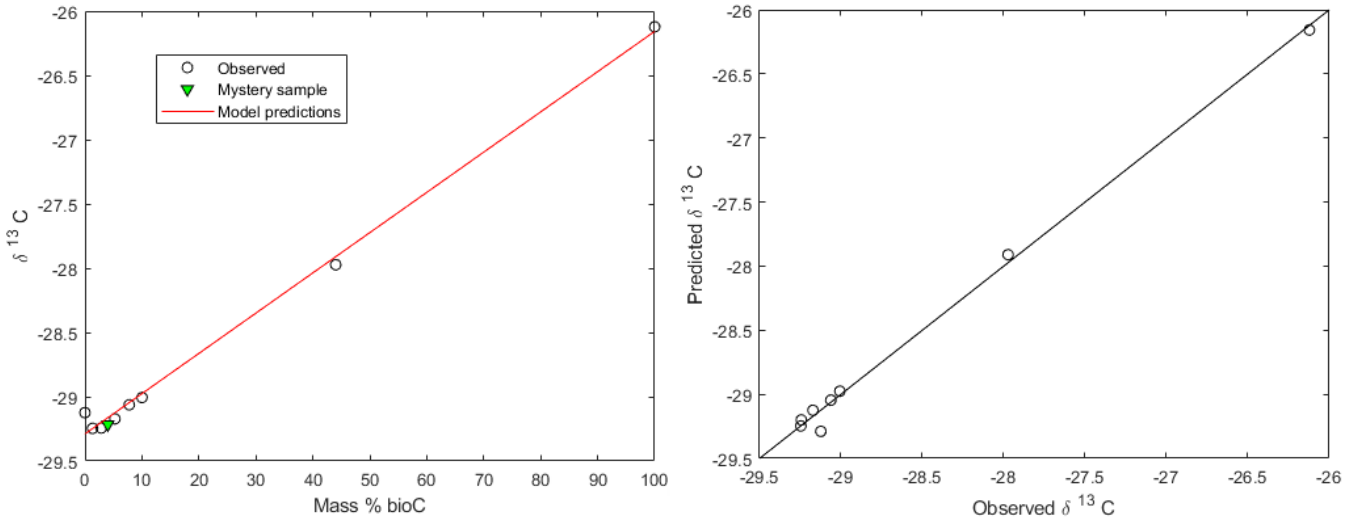

Figure D.10. (left panel) Plot of the R1 MP30- ^{13}C values (*y*-axis) versus the mass percent biocarbon (*x*-axis) and (right panel) a parity plot showing the model performance, where the solid black line at 45° (*y* = *x*) represents perfect prediction. R^2 for the model is 0.9955. Abbreviations: $^{13}C = ((R_{sample} / R_{standard}) - 1)) \times 1000$, in per mil (‰) where R = $^{13}C/^{12}C$ ratio; R1 = Refiner 1.

Even though R^2 for the model shown in Figure D.10 is high, the plot in the left panel shows that the point with 0 wt% biocarbon is off the trend from the rest. It was thought that an accident in the handling or reading of the sample may have been responsible. To be thorough, models were fitted with and without this outlying observation and also to the full range and low-carbon range of the data. Even using a dataset without the outlying observation, the 95% prediction and calibration intervals are relatively wide, possibly too wide to be useful. The width of the intervals reflects the relatively large variability of the data, which stands out from the other datasets in this work. For completeness, the 95% prediction and calibration intervals for the blind-blend sample in this dataset are shown in Figure D.11.

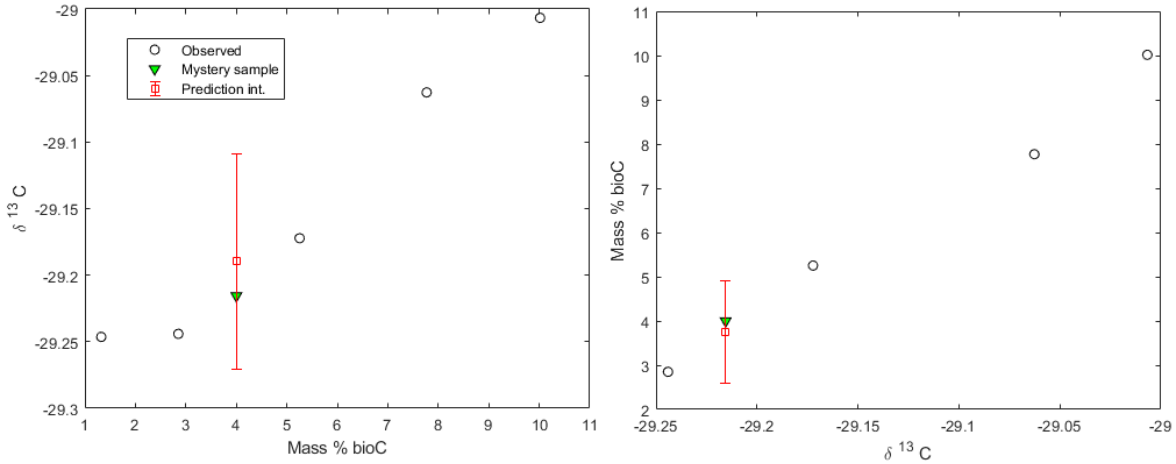

Figure D.11. (left panel) Plot of the 95% prediction interval for the blind-blend sample using a reduced R1 MP30-D535 dataset (outlying observation and higher-carbon range not used) and (right panel) the corresponding 95% calibration interval. The calibration interval is [2.6030, 4.9064], which is probably too wide to be of practical

use. Within the legend, “Mystery sample” refers to the blind-blend sample. Abbreviations: $^{13}C = ((R_{sample} / R_{standard}) - 1)) \times 1000$, in per mil (‰) where R = $^{13}C/^{12}C$ ratio; R1 = refiner 1.

Analysis of chromatogram data from gas chromatography (GC)–combustion (C) IRMS runs

Chromatograms of fuel samples were obtained and analyzed to identify features useful for grouping and distinguishing samples. An example GC-C-IRMS chromatogram for a selected saturate fraction sample is shown in Figure D.12.

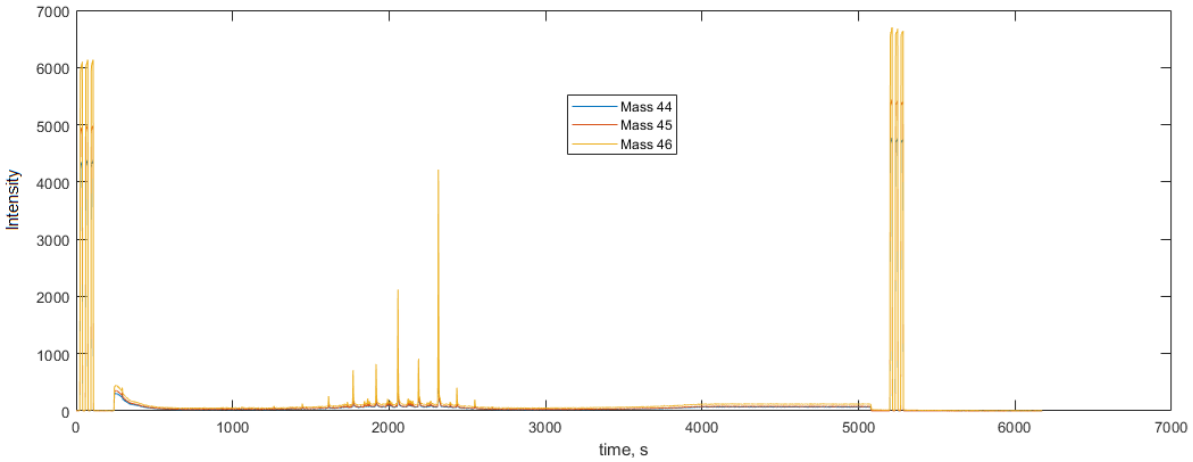

Figure D.12. Chromatogram of the SAT20 sample. The plot shows chromatograms for Masses 44, 45 and 46. Peaks eluting as groups of three at ~0 seconds and 5200 seconds represent injections of n-hexadecane used as a reference. Abbreviation: s = second.

Figure D.13 shows chromatograms from multiple saturate samples (SAT) overlaid on each other, including replicates that have underwent baseline adjustment and standardization. Saturate samples were those provided by CanmetENERGY after separating saturates from aromatics using solid-phase extraction. Figure D.13 clearly shows multiple peaks common to many of the available samples, as well as unique peak locations and intensities that belong to one or a few.

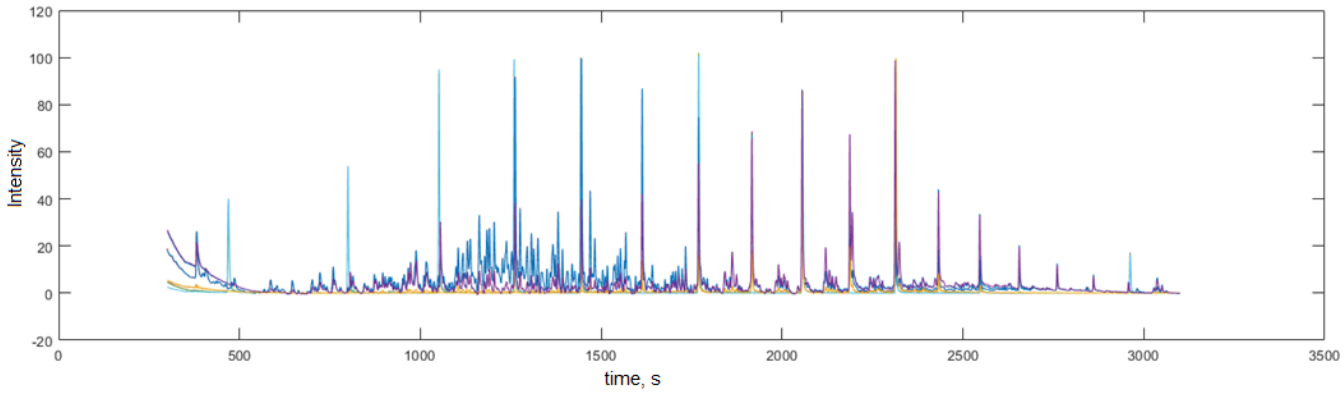

Figure D.13. Processed chromatograms for 11 saturate samples. Original data were baseline-corrected, aligned, and standardized for intensities. Abbreviation: s = second.

After processing the available Mass 44 data, 67 features were extracted and employed as inputs for principal component analysis (PCA). A plot of the features using the first two principal components is shown in Figure D.14. Figure D.14 shows that replicates cluster together in the space defined by the first two principal components. The plot also shows that it is relatively easy to distinguish among available samples.

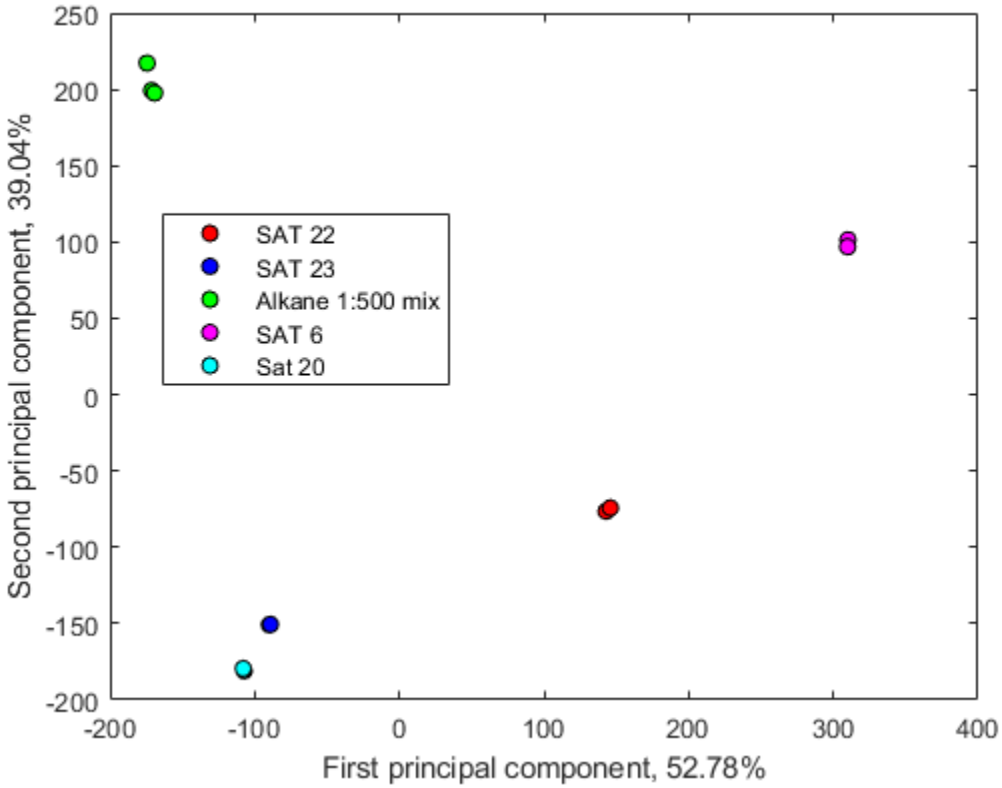

Figure D.14. Plot using the first two principal components of data extracted from 11 SAT chromatograms. The first two principal components account for around 92% of the total variance in the dataset. Abbreviation: SAT = saturate sample.

An analysis similar to that for the saturates data was applied to chromatograms from aromatic samples (ARO). PCA was applied only to chromatograms after performing the same processing steps as for the saturate data. This leaves out the long-term underlying curves present in the data, which were separated for further analysis. Figure D.15 shows a plot of the first two principal components for the aromatic data.

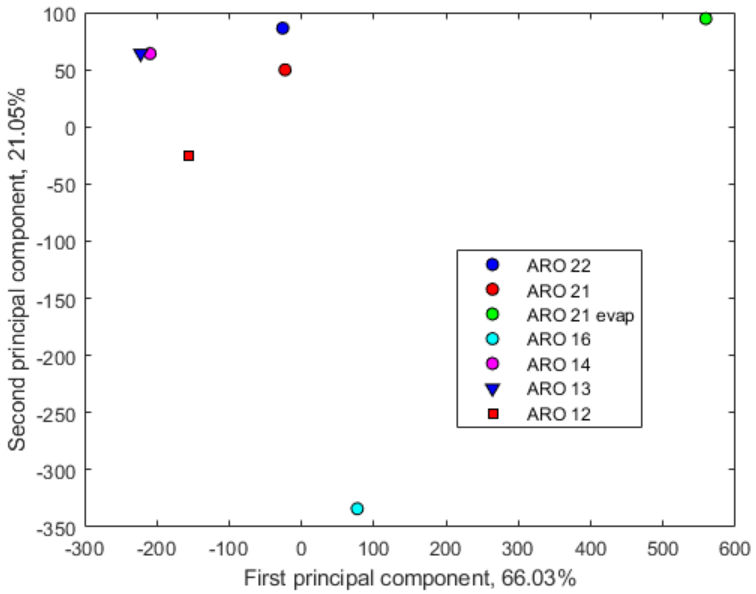

Figure D.15. Plot using the first two principal components of data extracted from 7 ARO chromatograms. The first two principal components account for around 87% of the total variance in the dataset. Abbreviation: ARO = aromatic sample.

The plot in Figure D.15 shows two of the samples clearly apart from the majority, indicating that they are easily distinguishable.

PNNL-37699
LA-UR-20444

Pacific Northwest National Laboratory

902 Battelle Boulevard
P.O. Box 999
Richland, WA 99354

1-888-375-PNNL (7665)

www.pnnl.gov